UNIVERSITY OF NAIROBI

DEPARTMENT OF MECHANICAL AND MANUFACTURING ENGINEERING

PROJECT TITLE:

"PERFORMANCE OF A PARABOLIC TROUGH COLLECTOR AIR HEATER"

BY:

WILSON KABINGU KARIUKI

REGISTRATION NUMBER: F56/72521/2012

PROJECT SUPREVISORS:

DR. A.A. AGANDA

PROF. J.A. NYANG'AYA

A PROJECT REPORT FOR THE PARTIAL FULFILLMENT OF MASTER OF SCIENCE DEGREE IN ENERGY MANAGEMENT OF THE UNIVERSITY OF NAIROBI

AUGUST, 2014

Declaration

A. Student's Declaration

I declare that this project is my original work and it has not been submitted to any other college or University for academic credit.

Signed _____ Date_____

Wilson Kabingu Kariuki **F56/72521/2012**

B. Supervisors Declaration

1. I confirm that the above student carried out this project work under my supervision for the entire period of the project.

   Signed _____ Date_____

   Dr. A.A. Aganda Project Supervisor

2. I confirm that the above student carried out this project work under my supervision for the entire period of the project.

   Signed _____ Date_____

   Prof. J.A. Nyang'aya Project Supervisor

Dedication

To my wife Jane, my son Vince and my mother, Zipporah for their continuous encouragement during the entire study at the University of Nairobi.

Abstract

A low cost parabolic trough concentrator (PTC) was built at the Mechanical Engineering workshop of the University of Nairobi. The PTC was built to heat air to temperatures of 100^0C and above which cannot be attained by direct sunlight or by flat plate collectors.

The trough was made of a standard galvanized sheet with two hard board end pieces. Aluminum foil was used as the reflective material and was glued on the inside of the trough on the galvanized sheet. The stand was made of 50.8 X 50.8 X 3mm square tubes. The receiver pipe was made of 1 inch (25.4mm) diameter galvanized water pipe. A manual tracking system was used to track the sun. The trough when assembled had a width of 1.077m, a length of 2.44m and a depth of 0.3m and a focal length of 0.25m. When the PTC was assembled with the stand, it had an overall height of 1.176m as shown in Drawing No. 007/PTC/2013 in Appendix 2.

The PTC was tested between 1100hrs and 1500hrs standard time at the Mechanical Engineering workshop of the University of Nairobi. This was because it is during these hours that there is maximum solar radiation during a typical day. The minimum and the maximum air mass flow rates tested were 0.0006kg/s and 0.0078kg/s respectively. The results showed that the outlet air temperature followed closely the variation in solar radiation. The same was true with actual useful energy as it is a function of outlet air temperature. When the sky is clear, it was found that solar radiation values are fairly steady with little intermittence. During cloudy days, the solar radiation was found not to be steady but changes as the cloud cover appears and can get as low as $150W/m^2$.

Temperature rise was found to be higher with smaller air mass flow rates and reduces as the mass flow rates increases. However the useful energy obtained from the PTC was found to be lower with lower mass flow rates and higher with higher mass flow rates. This was also true with overall efficiency. The maximum outlet air temperature obtained from tests was 182^0C with the least flow rate of 0.0006kg/s while the maximum overall efficiency was 27.7% with the maximum air flow rate tested of 0.0078kg/s. Data obtained from testing one trough was used to theoretically approximate the performance when two troughs were connected in series. It

was found that while outlet temperature, heat losses and useful energy increased, the overall efficiency and the receiver efficiency reduced.

Covering the collector with glass led to a significant increase in outlet air temperature and thus the actual useful energy. This increase was between 0.035^0C per W/m^2 with a mass flow rate of 0.0006kg/s to 0.019^0C per W/m^2 with a mass flow rate of 0.0078kg/s.

This study showed that a PTC has the ability to heat air to 100^0C and above which has the potential to increase the drying rate of biomass. The PTC has the potential to be used for generating drying air in industries such as sugar industry for drying of bagasse, local authorities for drying of municipal solid waste and in tea industry.

Acknowledgements

I wish to extend my sincere gratitude to the following, first to the Almighty God for giving me the opportunity to study at the University of Nairobi without which this project would not have been possible. I wish to express my sincere appreciation to my project supervisors Dr. Alex Aganda and Prof J.A. Nyang'aya, for their great guidance and encouragement during the study. I learnt a lot during the interaction with them.

I am greatly indebted to my boss Eng. George Kibiru for allowing me to take off days to do the research and also for encouraging me. I wish to thank the Mechanical Engineering technicians led by Mr. James Kimani, Mr. Peter Kogi, Mr. John Kahiro and Mr. Kenneth Njoroge for their guidance during the fabrication and testing of the Parabolic Trough Concentrator. I would wish to thank Mr. D.N. Kariithi from the Meteorology Department, Chiromo Campus for providing me with the Henni Solarimeter and Mr. Joseph Akello for helping me with an air flow meter.

Lastly but not least am thankful to my family, my wife Jane, and my son Vince for their understanding and support during my studies at the University.

Table of contents

List of abbreviations

α	Absorptivity of receiver pipe
T_a	Ambient temperature (^oC)
A_{ap}	Aperture area (m^2)
W	Aperture width (m)
I_b	Beam radiation (W/m^2)
C	Concentration ratio
F'	Collector efficiency factor
d	Depth (m)
T_{dp}	Dew point temperature
I_d	Diffuse radiation (W/m^2)
η	Efficiency
ε	Emissivity
f	Focal length (m), friction factor.
Gr	Grashof Number
F_R	Heat removal factor
h_f	Heat transfer coefficient inside absorber tube ($W/m^{2\,0}C$)
A_i	Inner tube area (m^2)
D_i	Internal tube diameter (m)
ν	Kinematic viscosity (m^2/s)
$\dot{m}$	Mass flow rate (kg/s)
$T_{m,f}$	Mean film temperature
Nu	Nusselt number
A_o	Outer tube area (m^2)
D_o	Outside tube diameter (m)
U_l	Overall heat loss coefficient ($W/m^{2\,0}C$)
Pr	Prandtl Number
PTC	Parabolic trough concentrator
Ra	Rayleigh Number
ρ	Reflectance of the reflective surface
θ	Rim angle
σ	Stefan Boltzmann's constant (=5.67 X 10-8 $W/m^2\,K^4$)
T_i	Temperature of the fluid entering the collector (^oC)

T_o Temperature of the fluid leaving the collector (^oC)

T_r Temperature of the surface of the receiver (^0C)

k Thermal conductivity

β Thermal expansion coefficient (K^{-1})

List of figures

List of Tables

CHAPTER 1

INTRODUCTION

1.0 Background

The world's energy is largely based on fossil fuels. The primary sources of these fuels are limited and therefore their prices are increasing steadily. Furthermore the fossil fuels are responsible for green house effect resulting into negative environmental impact [**1**]. Therefore there is need for alternative and renewable energy sources to make compatible the future energy demand and a sustainable economic growth.

Many countries are now increasingly integrating renewable energy in their energy mix in order to mitigate the negative impacts of fossil fuels. In Kenya the total installed power capacity was 1,712MW as of June 2012 [**2**]. This installed power capacity was made up of 812MW of hydro, 646MW of thermal, 205.8MW of geothermal, 5.1MW of wind, 26MW from cogeneration and 18MW of isolated grid. Power from isolated grid is obtained from dispatch of diesel power plants. It is clear that currently, renewable energy i.e. hydro, geothermal, wind and cogeneration, contribute 62% of the country's energy mix.

Although there is no solar energy that is fed to the national grid, the government through the Ministry of Energy and Petroleum has been connecting public institutions e.g. schools, dispensaries and police posts for away from the grid with solar PV systems. Kenya has great potential for the use of solar energy throughout the year because of its strategic location near the equator. The total area capable of delivering on average 6kWh/m^2 per day is 106,000km^2 which represents 18% of the area of the country [**4**].

Solar drying has been used since pre-historic times and has been used mainly in food drying. For example, open sun drying has been used to dry food and to evaporate sea water to yield salt [**5**]. Open sun drying is however characterized by low temperatures of 35^{0}C and below [**6**, **7**]. Again, large surface areas are required and there is lack of ability to control the drying process [**8**]. For example harvested rice contains a moisture content of between 20-25% and needs to be dried down to 12-14% moisture content [**9**]. It was found that for the best energy

use, rice should be dried in two stages. The first stage is to use a fluidized bed drier at a temperature of 100^0C to 110^0C and the second stage is to use an indirect type solar drier where the maximum air temperature required is 50^0C. An air collector installed before the drying chamber is used to heat the air.

Food drying is sensitive to drying temperature because of the need to maintain quality. For example, the international standard maximum temperature for drying of maize grain and wheat for human consumption is 60^0C, while for seed grains the drying temperatures should not exceed 42^0C. Solar driers that are used to deliver these temperatures have a flat plate collector that heat the air and are installed before the drying chamber.

A parabolic trough collector (PTC) can heat air to higher temperatures than a flat plate collector. It can thus be installed before the drying chamber of a solar drier to replace the flat plate collector. A PTC is composed of a parabolic trough shaped concentrator that reflects direct solar radiation on to a receiver tube [**1**]. Since the collector area is bigger than the outer area of the receiver pipe, the heat transfer fluid is heated to higher temperatures not achievable by flat plate collectors.

PTC's have normally been installed for power generation where very high temperatures are required. This requires high precision in manufacturing with mirror reflecting surfaces and very large in size. PTCs can also be suitable for generating dry air at temperatures in the range of 100-130^0C, more suitable for drying of biomass, but without expensive materials and high precision in construction required for high temperatures.

Biomass such as bagasse and municipal solid waste are excellent organic fuels for boilers that can substitute other types of energy providing fuels in industry. The use of concentrated solar energy such as PTC for generating drying air for biomass drying will save energy in industry. The energy saved will be the one required to evaporate the moisture content in biomass. The moisture content in bagasse for instance is about 50%. Drying of biomass would also increase its calorific value thereby improving the boiler efficiency.

A PTC will be built and its performance while heating air investigated. The effect of solar variability on the PTC will be investigated. The effect of mass flow rates and collector length on temperature rise, useful energy, overall efficiency, receiver efficiency and theoretical efficiency will be noted. The effect of glass cover on the collector performance will also be noted. Finally an analysis on the application of the PTC on biomass drying will be carried out.

The results of this study will give insight into the performance and therefore the application of PTC in drying of biomass. This is because the data on the performance of the PTC while generating hot air at 100^0C and above for drying of biomass is limited especially for local conditions.

1.1 Problem statement

In Kenya, power generation using fossil fuels account for 38% of the installed capacity [**2**]. This has led to high cost of electricity as the cost of fossil fuels keeps increasing. Wind contributes 0.3% of the installed capacity while solar energy doesn't contribute power to the installed capacity. To reduce the cost of electricity, there is need to increase solar energy integration as it is abundant and reduce use of fossil fuels. This is because Kenya is endowed with abundant solar radiation because of its geographic position along the Equator.

Biomass such as bagasse and municipal solid waste has a potential for the generation of power and industrial process heat. Currently, Mumias Sugar Company generates 36MW through cogeneration of which it sells 26MW to the National grid and consumes the rest. This process has bagasse being fed to boilers with a moisture content of about 50% thus making the process less efficient. There is no power that is generated by municipal solid waste in Kenya. Biomass would require faster drying as quality considerations are not important. Thus there is need to promote drying of biomass using concentrated solar energy so as to increase the rate of drying. This would increase the efficiency of boilers while generating power from the dried biomass.

There is limited information on the performance of PTC in Kenya when generating drying air. Thus one cannot be able to size accurately a drying system which would incorporate a PTC using the local climatic conditions. Thus there is need to construct a PTC using locally available

materials and perform tests so as to ascertain its performance and potential for drying of biomass.

1.2 Objectives

The overall objective of this study is to design, construct and test the PTC when heating air to 100^0C to 130^0C. The specific objectives are;

1. Design and fabricate a PTC.
2. Evaluate the performance of the collector when generating drying air.

CHAPTER 2

LITERATURE REVIEW

2.0 Introduction

This chapter briefly reviews the various methods of solar drying. The different types of solar driers and collectors are described and a brief outline of biomass drying is presented.

2.1 Solar drying

Drying is basically a phenomenon of the removal of liquid by evaporation from a solid. One application of solar energy is in drying. It is an alternative option to the conventional drying mainly due to unlimited and renewable source of solar radiation. This eliminates the use of fossil fuels and reduces environmental impact due to the consumption of non-renewables.

During solar drying, heat is transferred by convection from the surrounding air and by absorption of direct and diffuse radiation at the surface of the product. The conducted heat is partly conducted to the interior increasing the temperature of the product and partly used for effecting migration of water and vapor from the interior to the surface [**10**]. The remaining energy is used for evaporation of the water at the surface or lost to the ambient via convection or radiation. Finally the evaporated water is removed from the surrounding of the crop by natural convection supported by the wind.

There are two methods of solar drying, the open sun drying and the sun drying using driers. These drying methods are reviewed in the following sections.

2.1.1 Open sun drying

Open sun drying has been practiced by man from ancient times for drying agricultural based foods and non-food products [**5**]. It involves spreading the product on a safe place on the ground where it receives direct sunlight during the major part of the day and also natural air circulation. Shown in Figure 2.1 is the working principle of open sun drying;

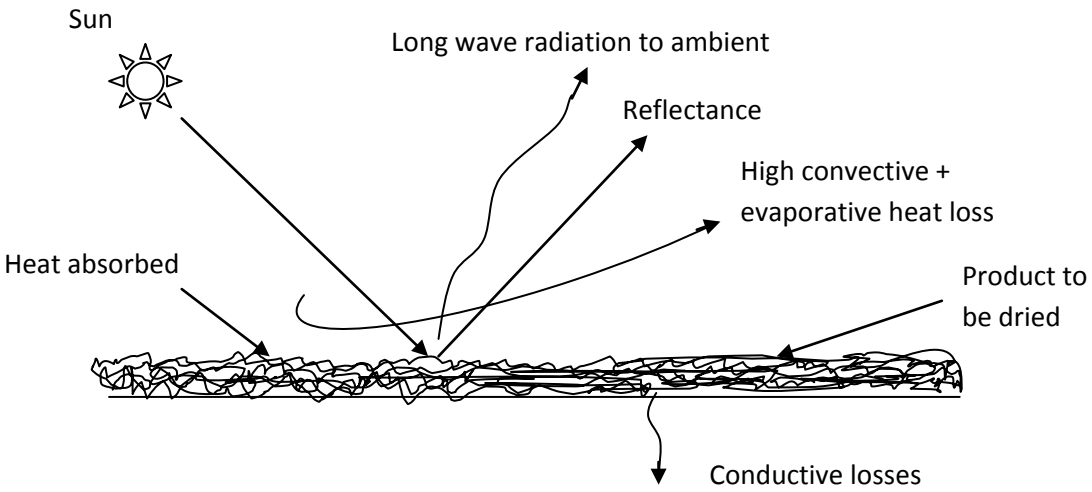

Figure 2.1: Open sun drying

From Figure 2.1 some energy from the sun is reflected and the remaining is absorbed by the surface of the product. This depends on the color of the product. The absorbed radiation is converted into thermal energy. This makes the temperature of the material being dried begin to rise. Under ambient conditions, the process of drying continues until the vapor pressure of the moisture held by the product equals to that of the atmosphere. At this point, the rate of desorption from the product to the environment and absorption from the environment are in equilibrium. The product moisture content at this condition is known as the equilibrium moisture content [**10**].

In addition, there are energy losses such as the long wavelength radiation loss from the surface of the product, convective heat losses due to the blowing wind through moist air over the crop surface and also conductive losses.

The main advantages of open sun drying are low capital, low operating costs and the fact that little expertise is required. This is because the process is independent of any other source of energy except sunlight. The disadvantages of open sun drying in the case of food drying are contamination, theft or damage by rain, dust, birds, rats and insects. Also, since the open sun drying depends on uncontrolled factors, production of uniform and standard quality of food is not guaranteed [**7**]. Finally, it encourages mould growth and may result in high final moisture content [**10**].

There are no quality considerations when drying biomass since it will finally be burnt. When open sun drying is used for biomass drying, the rate of drying is likely to be low since the drying temperatures are low (30^0C- 35^0C) [**6, 7**].

2.1.2 Sun drying using driers

In this method of drying, solar driers supply the product with more heat than is available under ambient conditions, increasing sufficiently the vapor pressure of the moisture held within the product [**5**]. This enhances moisture migration from within the product and decreases significantly the relative humidity of the drying air. The moisture carrying capability is increased and ensures sufficiently low equilibrium moisture content. The rate of drying can also be increased.

Hot air is supplied mostly by flat plate collectors. A typical flat plate collector is shown in Figure 2.2;

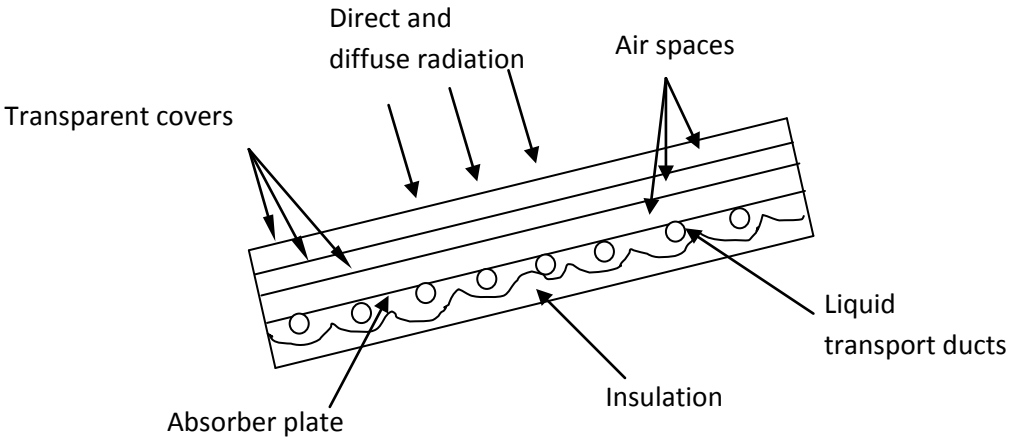

Figure 2.2 Flat plate collector

Flat plate collectors are designed for applications requiring energy delivery at moderate temperatures up to 100^0C [**5**]. The important parts of a typical flat plate collector as shown in Figure 2.2 are; the black solar energy-absorbing surface with means for transferring the absorbed energy to the fluid, glass cover transparent to solar radiation over the solar absorber surface to reduce the radiation and convective losses to the atmosphere, and back insulation to reduce heat loss by conduction. Flat plate collectors are almost always mounted in a

stationary position facing the sun. They are easy to construct and install. However for biomass drying, higher temperatures, from 110^0C are required.

2.2 Types of solar driers

There are two types of solar energy driers; passive and active solar energy driers. Three distinct subclasses of either passive or active solar energy driers are direct type solar driers, indirect type solar driers and hybrid solar driers.

Indirect type solar driers and hybrid solar driers use solar collectors to heat air before getting to the drying chamber. They absorb the incoming solar radiation, convert it into heat and transfer this heat into heat [**5**].

The various types of solar driers are briefly reviewed in the following section.

2.2.1 Passive solar driers

In passive solar driers, air is heated and circulated naturally by buoyancy force or as a result of wind pressure or in combination of both [**11**]. They can be either direct, indirect or mixed mode. The difference in specific weight between the drying air and the ambient air promotes a vertical air flow. They are cheap and simple to build. However their rate of drying is lower than solar driers having air circulated by forced convection [**7**].

2.2.1.1 Direct type passive solar energy drier

The features of a typical direct-type passive solar drier are illustrated in Figure 2.3. The moisture in the crop is taken away by the air entering into the cabinet from below and escaping at the top exit. Of the total solar impinging on the glass cover in the cabinet drier, a part is reflected back to the atmosphere and the remainder transmitted through the glass cover to the inside of the cabinet. A small part of the transmitted radiation is then reflected back from the crop surface and the rest is absorbed by the crop. This causes its temperature to increase and therefore emit long wavelength radiation which isn't allowed to escape back to the atmosphere due to the glass cover. The overall phenomenon causes the temperature above the crop inside the cabinet to be higher. The glass cover in the cabinet dryer thus serves in reducing direct

convective losses to the ambient. It also plays an important role in increasing the crop and cabinet temperature. These driers are simple to construct and are mainly used to dry foods.

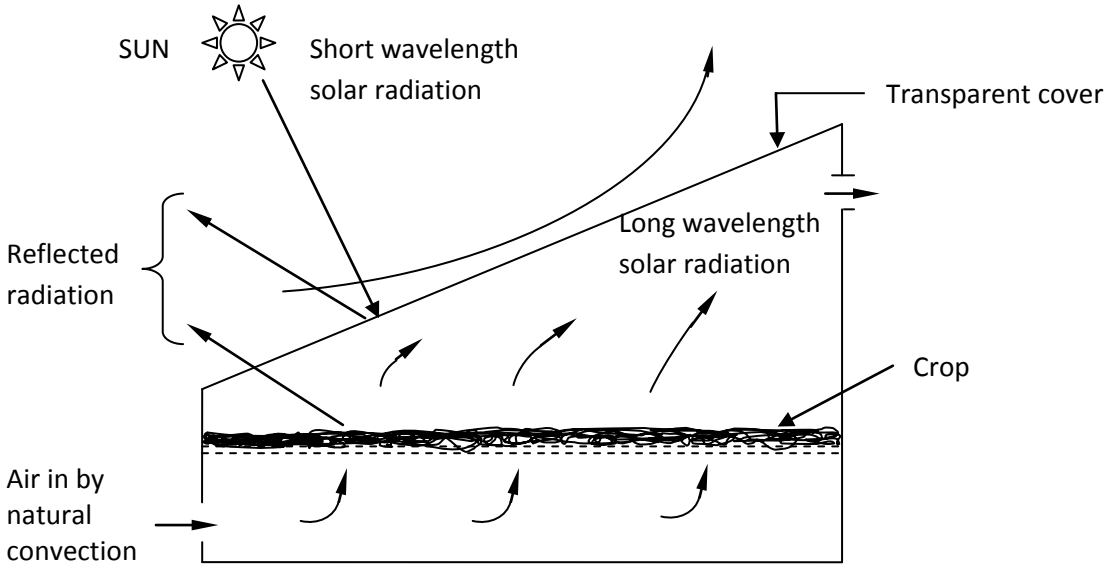

Figure 1.3: Direct type passive solar energy drier

The temperatures achieved by this type of drier have been reported to be in the range of 50^0C to 100^0C [**7, 10, 11, 12**]

2.2.1.2 Indirect type passive solar energy drier

Figure 2.4 shows the working principle of an indirect type passive solar energy drier. These driers differ from direct passive driers in the mode of heat transfer and vapor removal. The drying material is located in trays or shelves inside an opaque drying cabinet and a solar collector, normally flat plate is used for heating of the entering air into the cabinet.

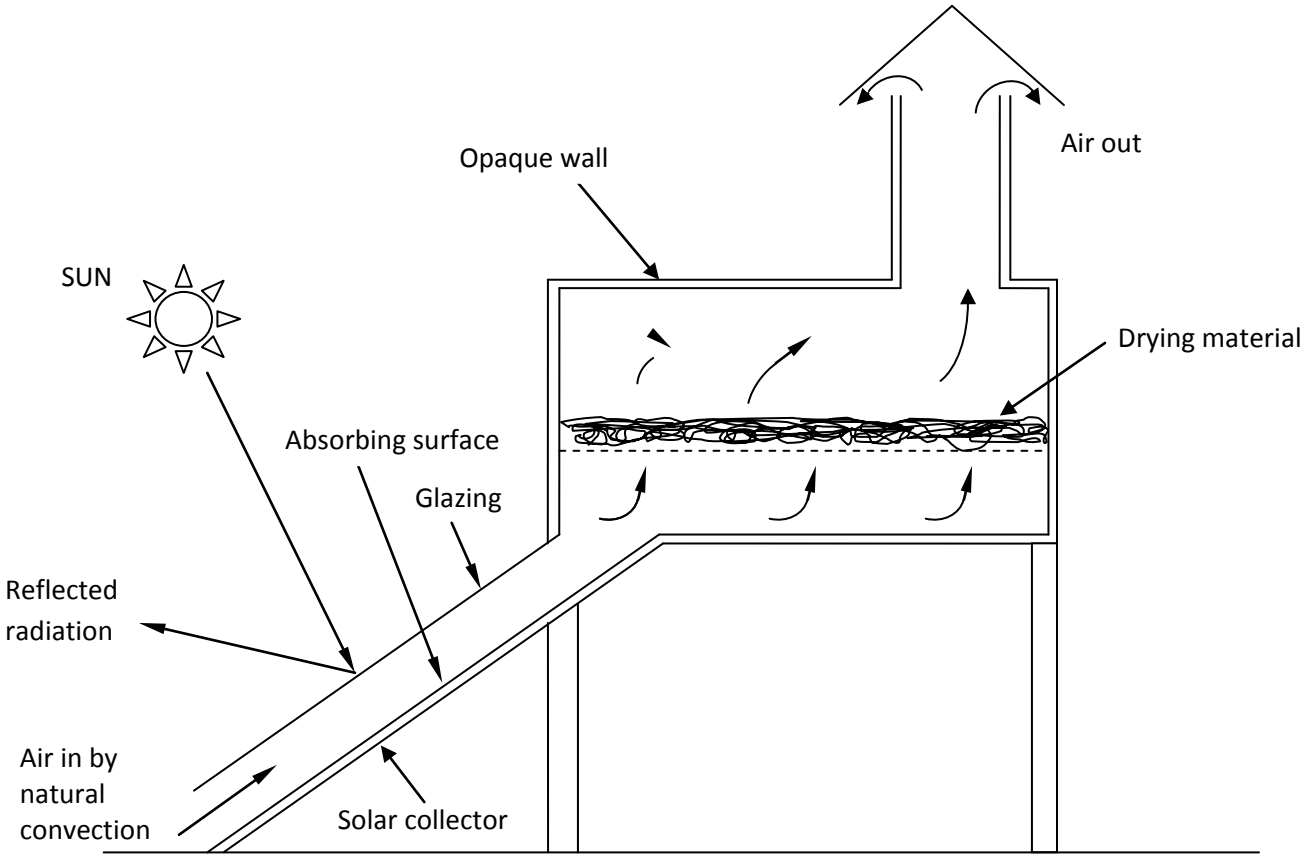

Figure 2.4: Indirect type passive energy drier

The heated air is allowed to flow through/over the wet crop that provides the heat for moisture evaporation by convective heat transfer between the hot air and the wet crop. Drying takes place due to the difference in moisture concentration between the drying air and the air in the vicinity of crop surface.

The temperatures achieved by this type of solar drier are lower than that of cabinet driers. An indirect solar drier was used in an experiment by Sankat C.K. [**7**] in drying salted fish fillets. The average temperature attained was 43.1^0C.

2.2.1.3 Mixed mode passive solar energy driers

Figure 2.5 shows a mixed mode passive solar energy drier. These driers which are also called hybrid solar dryers combine the features of the direct and indirect type solar energy dryers. Thus the combined action of incident direct solar radiation on the product to be dried and air

pre-heated in a solar collector heater produces the necessary heat required for the drying process [**11**].

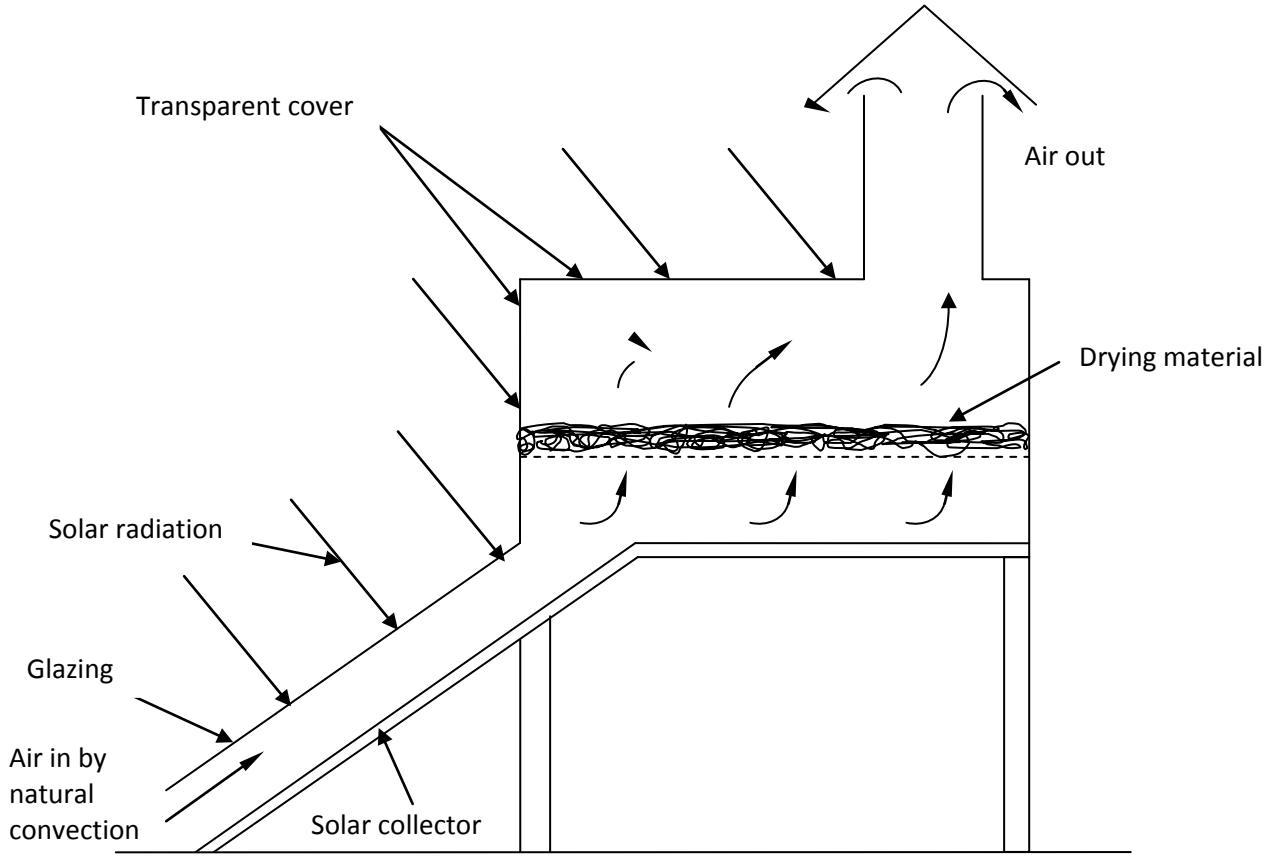

Figure 2.5: Mixed mode passive solar energy drier

2.2.2 Active solar energy driers

These driers are designed incorporating external means of pushing air into the drying chamber - mostly by fans. Optimum air flow can be provided in the drier throughout the drying process to control temperature and moisture in wide ranges independent of weather conditions. Hence the capacity and reliability of the passive solar energy driers are increased considerably compared to natural convection driers. The use of forced convection can reduce drying time by up to three times and decrease the required collector area by 50% [**10**].

Active solar energy driers can be direct, indirect or mixed mode. Their design and construction is similar to passive solar energy drier system presented in **Section 2.3.1** except that they have a fan on the air inlet side. This fan pushes the heated air through the shelves in the drying chamber.

2.3 Selected case studies of solar drying

2.3.1 Drying of parsley leaves

Akpinar et al [**6**] investigated the drying behavior of parsley leaves using open air drying and compared the rate of drying with a convective type drier with forced convection mode. Open sun drying was done in September of 2004 in Elazig, an area of the eastern part of Anatolia, Turkey. The drier had a fixed air flow rate of 1m/s. The drying temperatures used with the convective driers were 56, 67, 85 and 93^0C. Parsley leaves were to be dried from a moisture content of 5.25g water/g of dry matter (80%) to 0.1g water/g dry matter (10%). The drying time was between 1030hrs to 1700hrs.

It was found that it took 6 ½ hours to dry the leaves using open sun drying and 4 hours when using the forced convection drier with a temperature of 56^0C and 1 hour when the drying temperature was 93^0C. This study thus showed that using a forced convection and at higher temperatures, the drying time decreases, and this results into increased drying rate.

It was found that the drying rate in the convective drier operating at forced convection mode was higher than the natural open-air sun drying mode. Parsley leaves can be dried with a temperature of up to 170^0C to preserve its medicinal value. Thus a PTC can be used to generate hot air for drying of parsley leaves.

2.3.2 Drying of salted shark fillets

Sankat et al [**7**] investigated the drying of salted shark fillets using open air sun drying and two natural convection solar driers of similar design but employing direct and indirect drying. The study was done in Trinidad. The direct solar dryer was essentially a wooden cabinet (0.72m x 1.88m x 0.31m) sloping at 10° to the horizontal to maximize the collection of incident solar radiation. The drier was built to hold three (3) trays, each wooden and framed with wire mesh. Vents (0.17m x 0.035m) at the front and rear of the cabinet allowed for entry of air into the dryer, and on heating, to rise by natural convection and exit through the outlet. The internal parts of the cabinet were painted with black paint. The air speed inside the dryer was less than 0.5m/s.

Fillets were dried between the hours of 9am and 4pm (7hrs) each day during early April, which is the hot, dry period of the year in Trinidad and Tobago. At hourly intervals during the drying process, the trays were taken out of each dryer and quickly weighed. The fillets were dried from a moisture content of 1.95g water/g dry mass or 65.3% wet basis to the recommended 0.69g water/g dry mass or 40% wet basis. It was found out that ambient temperature and the temperatures in the direct and indirect dryers averaged 32.4°C, 43.8°C and 43.1°C respectively for the period between 9am to 4pm over the 5 days of drying.

Of the three drying treatments, slabs dried in the open air dried the fastest while drying was slowest in the indirect dryer. In order to achieve the recommended moisture content in open-sun dried and solar dried samples, slabs had to be exposed to the sun for 13hours in the case of open sun-drying, 14hours when using a direct solar dryer and 16hours when using an indirect solar dryer. Sun-dried slabs were of acceptable quality but somewhat inconsistent in color. Slabs dried in the direct solar dryer had a pleasing and even color and texture. Although drying time was increased in the indirect dryer, slabs were soft and pliable and with an appealing color.

Therefore drying using open sun drying is seen to take a very long time, 7 hours or more. This may be necessary for food because of quality considerations, but it is not suitable for say biomass drying.

2.3.3 Drying of potato slices

Bhuiyan et al [**12**] investigated the drying of potato slices using a combined solar and mechanical cabinet drier. The cabinet solar drier was tested in three modes, natural convection, forced convection and using an electric heater to heat the drying air. In the forced convection mode, two cases were investigated, with one fan and two fans. The velocity of air in one fan operational system was 0.35m/s and 0.7m/s with two fans operational system. When the drier was operating in the solar mode, the highest temperature was achieved in the natural convection mode at 50^0C and the least temperature with 2 fans operational system at 45^0C. These temperatures were attained at 12.00pm when the ambient temperature was 30^0C.

Low temperatures were reached in this study with a maximum of 50^0C when radiation was maximum. The rate of drying is expected to be similarly low.

2.3.4 Drying of bagasse pulp

Zeinab et al [**13**] studied solar drying of bagasse pulp using a direct type solar drier. Bagasse pulp was dried using two methods, one using natural air convection and the other using forced air. The set up consisted of a wood tray of 0.4m X 0.4m X0.1m which had its base and walls painted black. A reflector of play-wood of 0.38 x 0.38 m was covered with highly reflecting Aluminum foil to increase the input solar energy. The arrangement is shown in Figure 2.6. The reflector acting as a lid was hanging at one end of the tray, with a wooden lever for adjusting the tilting angle of the reflector.

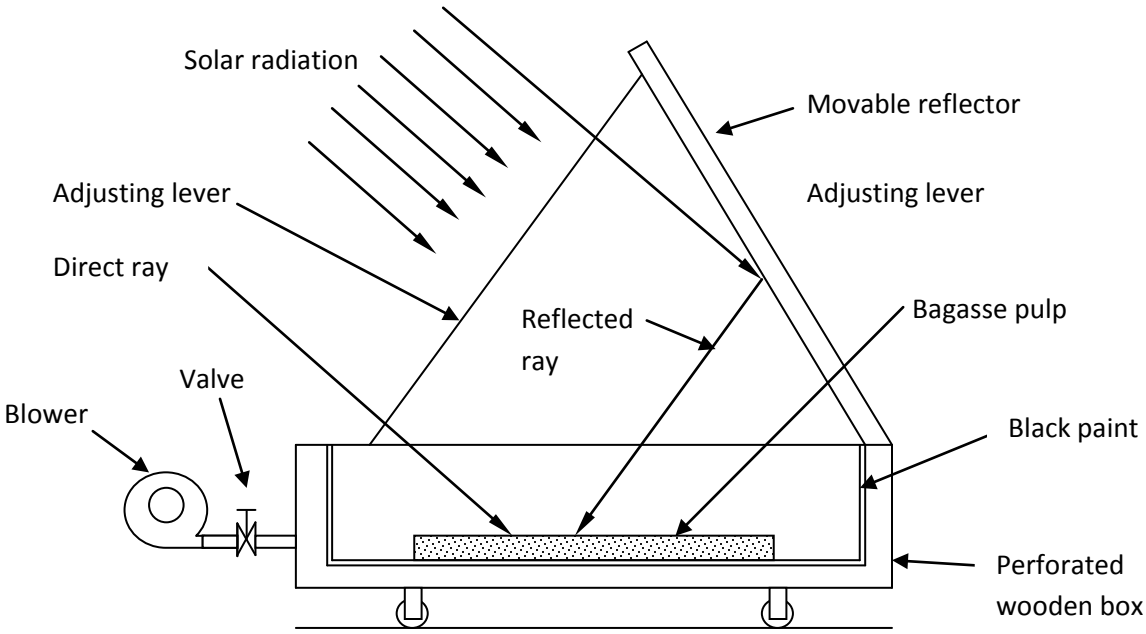

Figure 2.6: Schematic of the experimental set-up [13]

The maximum temperature measured during drying was 52^0C using natural convection and 44^0C using forced convection with the air mass flow rate being 0.1kg/s. The moisture content of the bagasse pulp was reduced from 43% to 10% in 8 hours using natural convection and to 6% in 8 hours using forced convection.

Low temperatures were reached in this study with the maximum being 52^0C. The drying time of bagasse is found to be long i.e. 8 hours. Higher temperatures are suitable for drying of bagasse and can be attained by using a PTC.

2.4 Solar collectors

Solar collectors play the part of primary energy source for a solar dryer. Essentially it has functions of energy conversion and energy transfer [**8**]. As an energy converter the collector converts the direct and diffuse radiation coming from the sun into heat. As an energy transferring device, it transfers the radiation energy transferred into heat in the absorber to the working fluid of the collector. This working fluid may be air, water, oil etc.

A brief review of various types of typical solar collectors is presented here.

2.3.1 Compound parabolic collectors

The compound parabolic collectors (CPC) are non-imaging concentrators. They are designed in such a way that they have two sections of a parabola facing each other [**14**]. Shown in Figure 2.7 is a CPC with a flat absorber and Figure 6.8 shows a CPC with a tubular receiver. The angle between the axis of the CPC and the line connecting the focus of one of the parabola with the opposite edge of the aperture is called the acceptance half angle. If the reflector is perfect, any radiation entering the aperture at angles between $\pm\boldsymbol{\theta_c}$will be reflected to a receiver at the base of the concentrator by specularly reflecting parabolic reflectors.

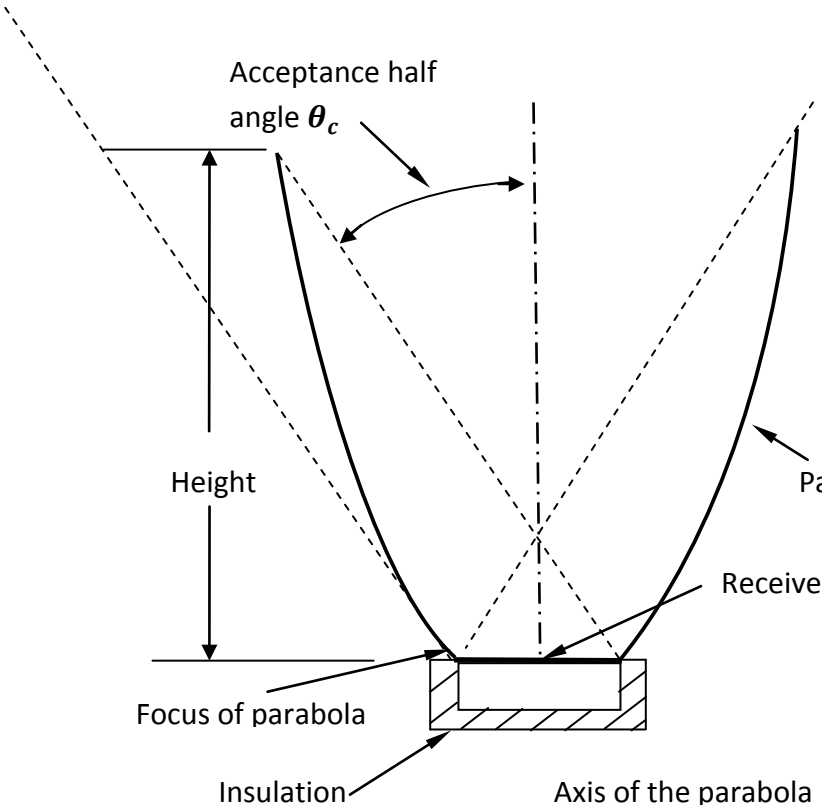

Figure 2.7: Compound parabolic collectors with flat receiver

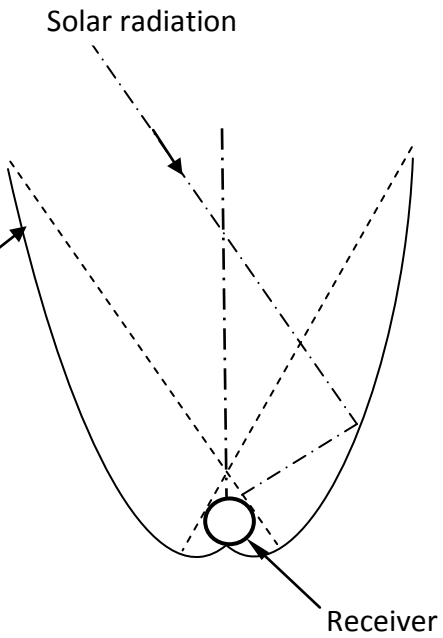

Figure 2.8: Compound parabolic collectors with a tubular receiver

An ideal compound parabolic collector has an acceptance half angle $\theta_c$of 12^0. A mathematical model for computing the thermal performance of an air heater with a truncated compound parabolic concentrator having a flat one-sided absorber was carried out by Rene Tchinda [**15**]. It was found that the CPC could achieve a temperature of 45^0C, 50^0C and 70^0C with an air mass flow rate of 0.0013, 0.0065 and 0.0013kg/s respectively on a 2m long receiver.

This collector is not suitable for drying of biomass because the temperatures achieved are low. Furthermore, its fabrication is more complex and requires higher accuracy during fabrication than that of a parabolic trough concentrator.

2.3.2 Linear Fresnel reflector

This collector technology relies on an array of linear mirror strips which concentrate light onto a fixed receiver mounted onto a linear tower. A typical Linear Fresnel reflector (LFR) field is shown in Figure 2.9; [**5**];

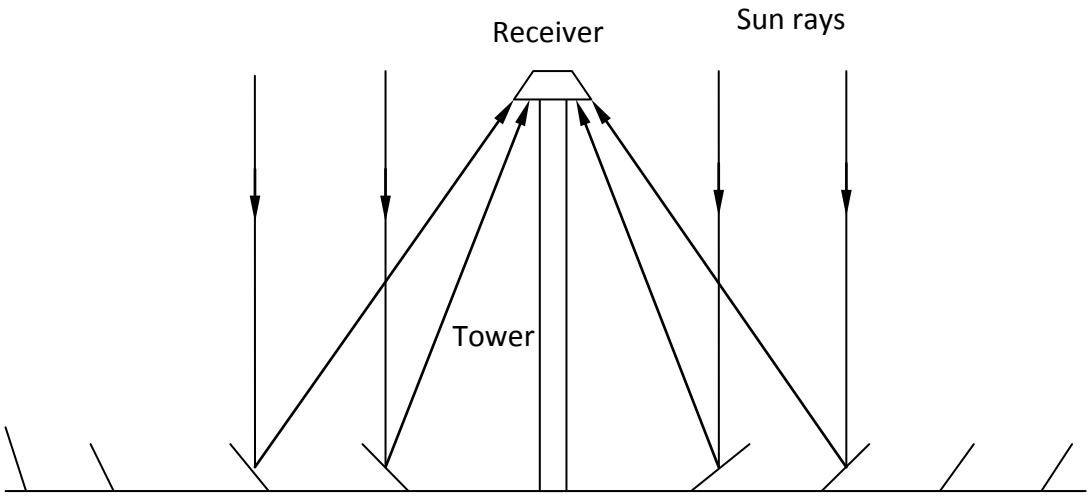

Figure 2.9: Downward facing receiver illuminated from a linear Fresnel reflector field

The system can be imagined as a broken-up parabolic trough collector, but unlike the parabolic troughs, it doesn't have to be a parabolic shape. They cover a wide area and are expensive to build. These solar collectors are mainly used for power generation. For example, a Fresnel solar power plant known as PE 1 was built in Germany by Biosol N. in 2009 [**17**]. The solar thermal power plant has a capacity to generate 1.4 mega watts. The plant comprises of a solar boiler with mirror surface of approximately 18,000m^2. The steam is generated by concentrating sunlight directly on a linear receiver, which is 7.4m above the ground. An absorber tube is positioned in the focal line of the mirror field where water is heated to 270^{0}C.

A LFR field can be useful for drying of biomass. However a heat exchanger will have to be installed so as to transfer heat from steam generated to air. Furthermore, its construction is more complex and expensive.

2.3.3 Heliostat field collector

This technology is similar to LFR only that the solar energy concentration and collection is done by a field of individually sun tracking mirrors (heliostats) with altazimuth mounts that reflect the incident sunshine to a receiver (boiler) at the top of a centrally located tower [**9**]. This is shown in Figure 2.10;

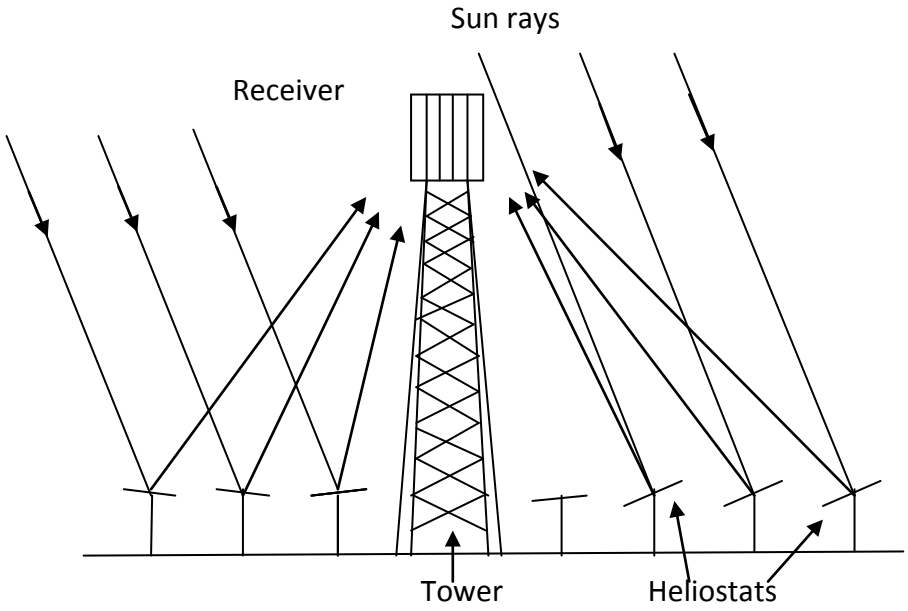

Figure 2.10: Heliostat field collector

Heliostat field collector systems are usually used to generate steam for generation of electricity or for use in industry. Because of their ability to track the sun, they can attain high temperatures of more than 1500^0C.

Heliostat field collector can be suitable for drying of biomass. However a heat exchanger will have to be installed so as to transfer heat from steam generated to air. Furthermore, its construction is more complex and is costly.

2.4.4 Parabolic dish reflector

A parabolic dish reflector is a point-focus collector that tracks the sun in two axes, concentrating solar energy onto a receiver located at the focal point of the dish. An illustration of a typical parabolic dish reflector is shown in Figure 2.11;

The receiver absorbs the radiant solar energy, converting it into thermal energy in a circulating fluid. The thermal energy can then either be converted into electricity using an engine-generator coupled directly to the receiver, or it can be transported through pipes to a central power-conversion system. Parabolic-dish systems can achieve temperatures in excess of 1500 ^{0}C [**9**]. A parabolic dish reflector is used for producing steam.

For it to be suitable for drying biomass a heat exchanger is needed to transfer heat from steam to generate hot air. It will however be complex to make flexible ducts to transport steam to the heat exchanger installed on the ground. Sometimes biomass drying may be done directly by steam. The steam must however be much superheated with large temperature difference from saturation.

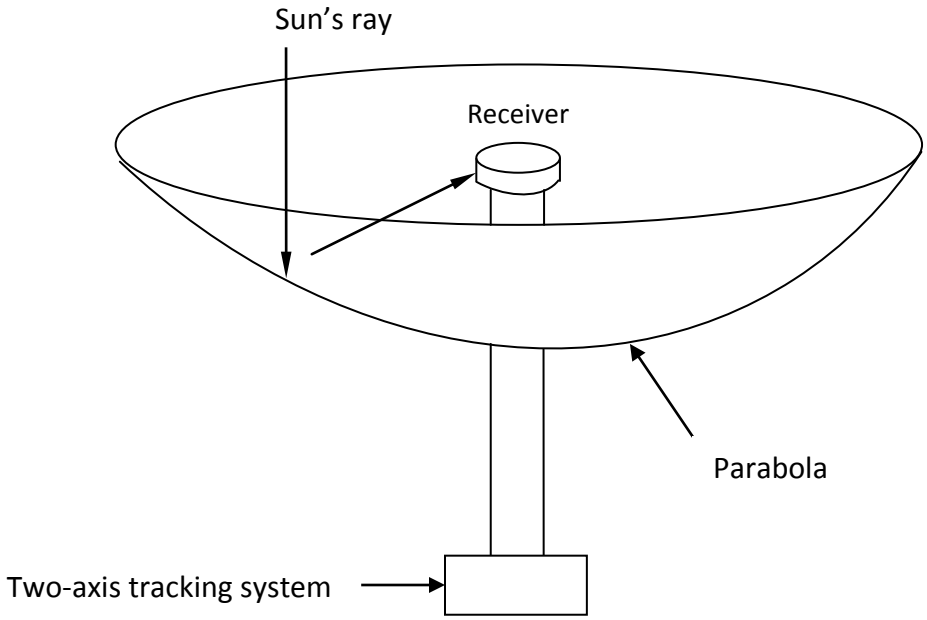

Figure 2.11: Parabolic dish collector

2.4.5 Parabolic trough concentrators

An illustration of a typical parabolic trough concentrator (PTC) is shown in Figure 2.12. PTCs are made by bending a sheet of reflective material into a parabolic shape. A metal tube, covered by glass tube to reduce heat losses is placed along the focal line of the receiver. When the parabola is pointed towards the sun, parallel rays incident on the reflector are concentrated onto the receiver tube.

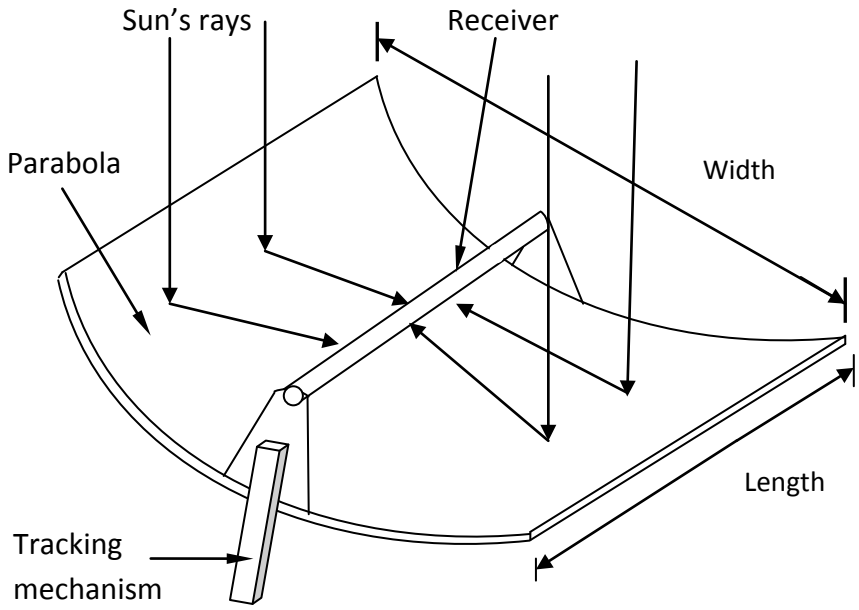

Figure2.12: Schematic of a parabolic trough collector

A tracking mechanism is necessary to enable parabolic trough collector to follow the sun with a certain degree of accuracy. It must also track during periods of irregular cloud cover.

There have been several promising developments going on in the field of PTC and their applications. Troughs used for commercial purposes are fabricated with high accuracy and are normally big in size e.g. for power generation. For example Figure 2.13 shows a row of parabolic trough concentrator installed in Shiraz power plant [**17**]. The troughs have an aperture width of 3.4m, focal length of 0.88m, length of 25m and a receiver of 0.77m diameter. The reflecting mirror type used is silvered low-iron float glass. The collector tracks the sun automatically using sensors with a hydraulic drive system. The PTC heats oil flowing in the receiver tube at a rate of $9m^3$/hr and is required to attain a temperature of 150^0C.

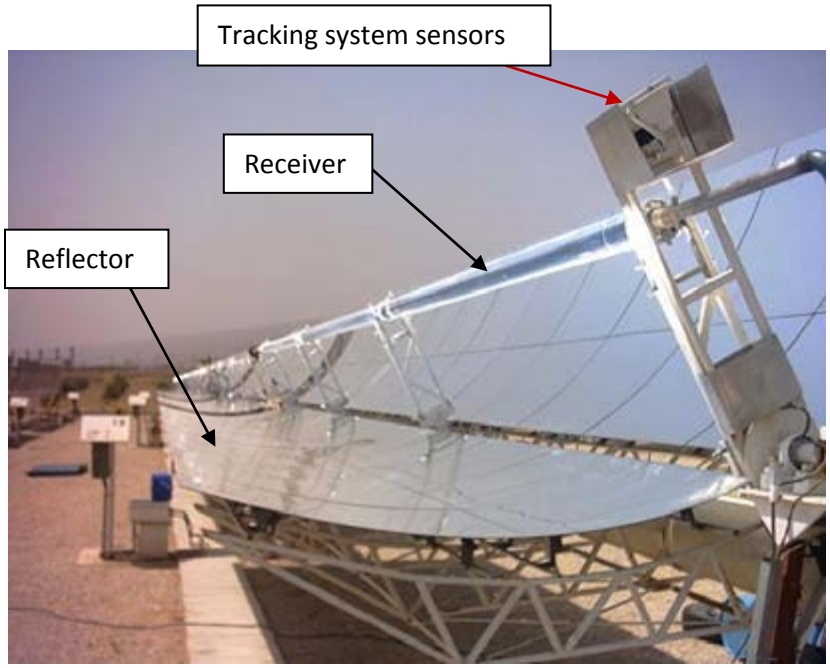

Figure 2.13: Parabolic trough concentrator installed for a power plant [17].

These high temperatures results in high heat losses. The heat loss is minimized by surrounding the receiver pipe with an evacuated glass envelope. The vacuum between the pipe and the glass envelope cuts out convective losses, and conduction is reduced by using materials of low thermal conductivity.

To ensure that the receiver pipe absorbs solar radiation efficiently, it is painted with a selective coating which has low emissivity. The receiver emits infrared radiation, which represents the 'losses' very poorly, thus efficiently retaining most of the heat.

However, such large installations are very expensive and the construction that involves mirror lining, high concentration ratios as well as developing and maintaining vacuum requires high skills.

The biggest installation of PTC is in the Southern California power plants known as the Solar Electricity Generating Systems. The plant has a total generation capacity of 354MW. The collectors used have an aperture width between 2.55-5.76m, focal length between 0.94-1.71m, length per collector of between 50.2-99m receiver diameters of between 40-70mm and peak optical efficiency of between 71-80%. These are large and expensive and require high accuracy in their manufacture.

Manikandan et al [**3**] performed a thermal analysis of a PTC with four heat transfer fluids, water, therminor, palm oil and castor oil. The PTC had a collector length of 3m, width of 2.5m and a rim angle of 65^0. The PTC was experimented at the institute of Energy Studies, Anna University, Chennai, India. The tracking system was semi automatic. The receiver pipe was made of stainless steel and had an absorptivity of 0.9. The inlet fluid temperatures ranged from 30^0C to 80^0C. The concentration ratios used were 12, 22 and 32.

It was found that the PTC achieved the highest efficiency of 69% when water was the heat transfer fluid. When palm oil, therminol and castor oil were used, the PTC efficiency was 58%, 56% and 54.5% respectively. It was also found out that the efficiency of a PTC decreases for various mass flow rates and heat transfer fluids, as the inlet fluid temperatures increases. The collector efficiency for a mass flow rate of 0.05kg/s was 65% when the inlet fluid temperature was 30^0C and 60% when the inlet fluid temperature was 80^0C. The useful energy was found to increase as solar radiation was increased with constant inlet fluid temperature. When the solar radiation (I) was 600W/m^2 for instance, the useful energy obtained from the PTC was 2500W while when I was 800W/m^2 the useful energy was 3400W. Finally, it was found that the useful energy from the PTC increases as the concentration ratio increases. For a concentration ratio of 12 the useful energy was 2500W while for concentration ratio of 32, the useful energy was 8000W.

Yassen [**18**] did an experimental and theoretical study of a PTC. The experiments were performed in winter and summer in Tikrit, Iraq. The PTC had a length of 1.9m, width of 1m, rim angle of 90^0 and a focal length of 0.25m. The receiver pipe was of galvanized steel and had an internal diameter of 0.026m, an external diameter of 0.03m and an absorptivity of 0.9. The heat transfer fluid used was water. The experiments were conducted from 0800hrs to 1600hrs (8hrs). The highest thermal efficiency achieved by the PTC was 63% when the mass flow rate was 40kg/hr. The solar radiation was not constant during the days of experimentations. It varied from 250-350W/m^2 at 0800hrs, and then it increased to a maximum at noon at 960w/m^2 and finally started falling until it got to 400-450W/m^2 at 1600hrs.

The PTC used by Yassen T.A. is similar to that used in the current study in terms of the width and the focal length. However the PTC performance will be slightly different as Kenya does not experience winter. Again basing on Kenya's geographical location which is in the equator, the solar radiation during the day will be high between 1000hrs to 1500hrs assuming there is no cloud covers.

2.5 Potential PTC application on biomass driers

Various types of driers are in use nowadays. They are used to dry tea, coffee, bagasse and so on. They derive the heat from fossil fuels, steam flue gases and electricity. Drying using solar driers have not been adopted because they have not been built for long term use. With the rising cost of fossil fuels and the negative impact of using fossil fuels there is need to adopt renewable energy sources for generating the heat required for drying. A PTC is can be able to generate hot air above 100^0C.

A brief review of driers that can incorporate a PTC air heater is presented below.

2.5.1 Cyclone driers

For a long time, cyclones have been used as gas cleaners. They find applications in tea, coffee, and construction etc. Not only does a cyclone collect dust, it provides a good contact between solid and gas phases.

Correa et al [**21**] studied the use of a cyclone in drying sugarcane bagasse. They compared earlier work done by drying bagasse using a cyclonic chamber. The cyclone and drying chamber used are shown below.

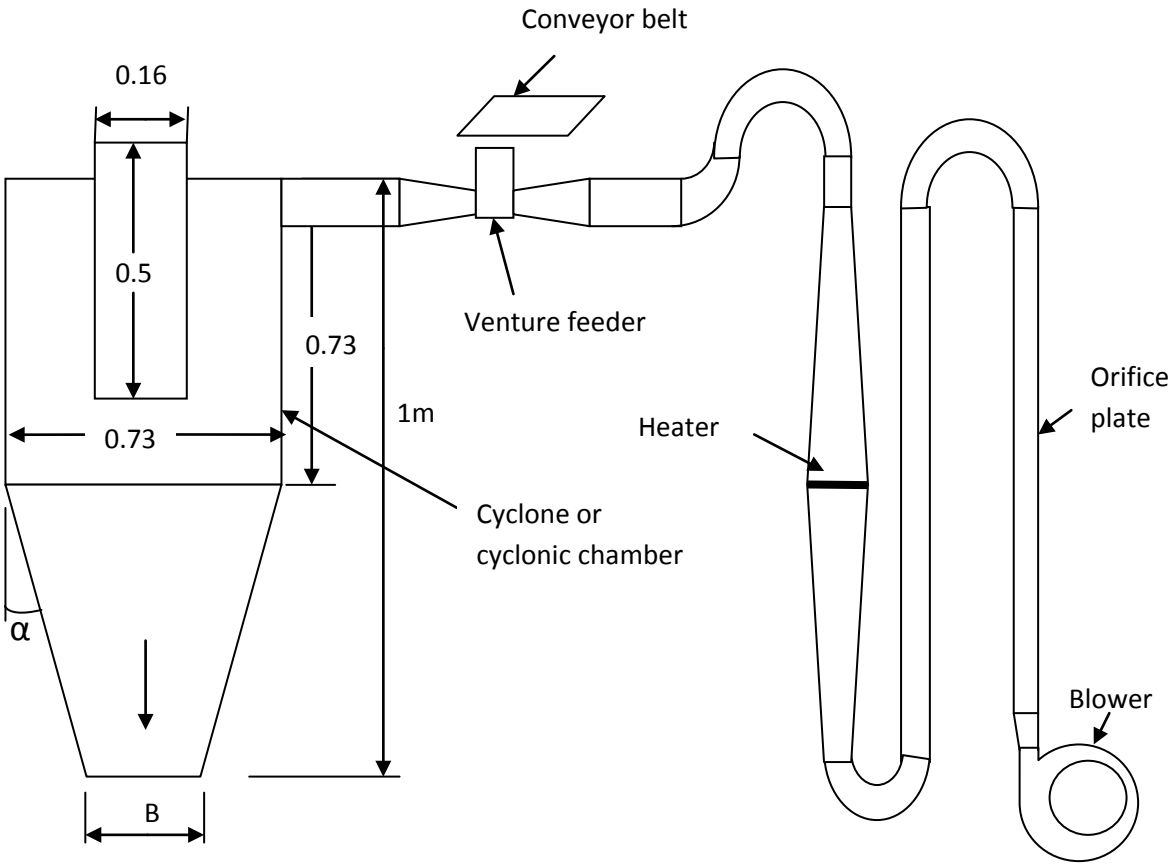

Figure 2.14: Cyclone device and drier system

Hot air with a temperature between 35^0C and 211^0C was used as the drying agent. An electric heater with a controllable temperature was used to heat the air. The ratio of solid mass flow rate to gas mass flow rate was from 0.02 to 0.07. The different dimensions between the cyclone and the cyclonic chamber are the particulate outlet **B** and the conical part angle **α**. **B** is equal to 0.65m for the cyclonic chamber and 0.10m for the cyclone used and reported by their work. The conical part modification led to an improved drier. It was responsible for large average particle residence time and large moisture reduction.

The drier can be modified so that a PTC generates hot air thus replacing the electric heater. The blower would be used to push air through the receiver pipe.

2.5.2 Flash driers

They are also called pneumatic driers. In these driers, the feed stock is suspended in an upward flow of the drying medium usually flue gas. They are cost effective only at larger scale use. They require small particle sizes of 10-500 microns. Figure 2.15 shows a schematic flash drier.

The capital and operating costs are high. They are also prone to corrosion wearing and erosion due to the many moving parts.

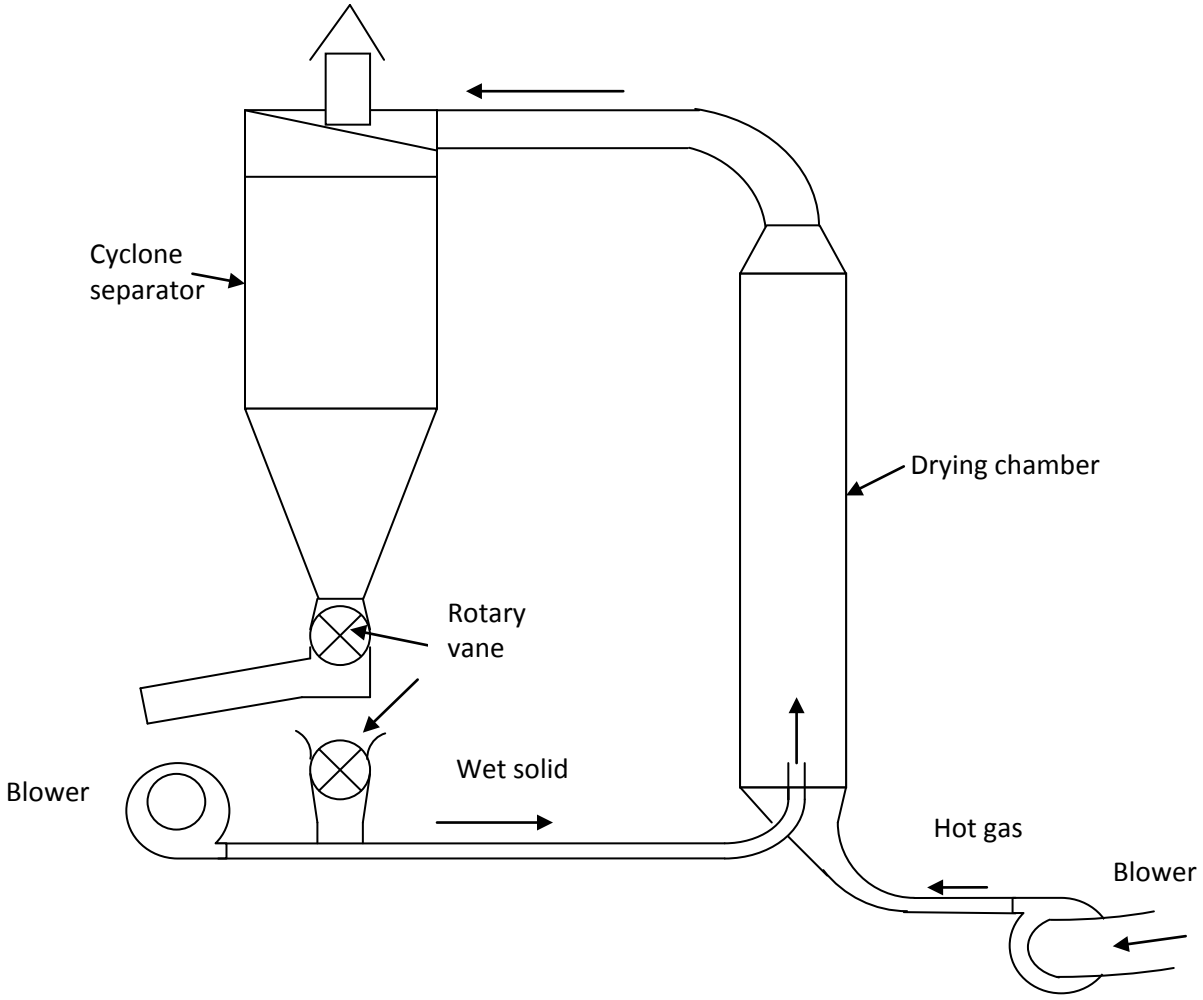

Figure 2.15: Schematic of a pneumatic drier system

A PTC can be incorporated in the design to generate hot air. These driers are suitable for drying of biomass but they have higher capital and operating cost. An economic analysis will have to be done putting in mind the opportunities to recover process heat in an industry.

CHAPTER 3

PERFORMANCE OF A PARABOLIC TROUGH CONCENTRATOR

3.0 Introduction

Parabolic trough concentrator performance is defined by heat transferred from the absorber to the fluid, the efficiency and heat losses. These depend on concentration ratio, aperture area, material properties and the accuracy of construction. In this chapter, performance parameters of the PTC are defined and discussed.

3.1 Definition of terms and PTC geometry

The collector is basically composed of a parabolic-trough-shaped concentrator that reflects direct solar radiation onto a receiver tube located in the focal line of the parabola. A typical illustration of a PTC is shown in Figure 3.1;

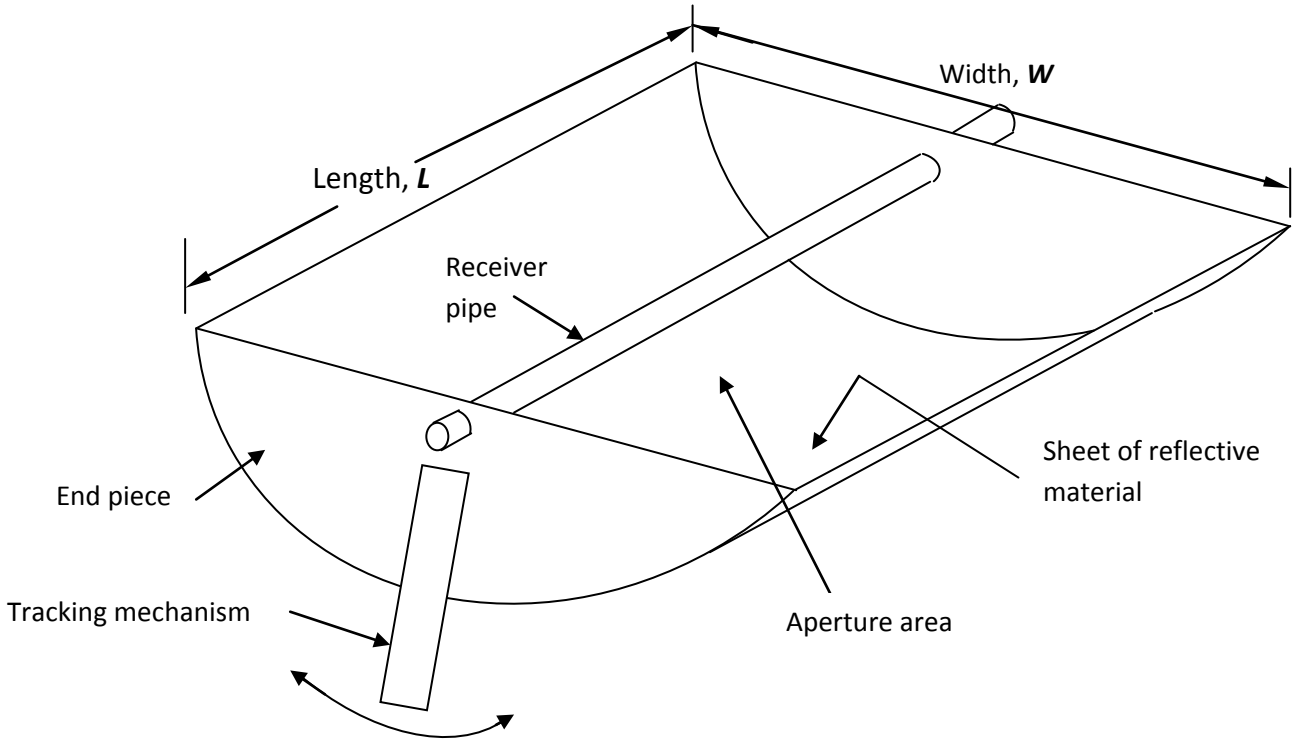

Figure 3.1: A typical parabolic trough concentrator

The following terms characterize the parabolic trough concentrator

Receiver area; It is the total area receiving the concentrated radiation. It is also the area through which useful energy is delivered to the system. It is the heart of the parabolic trough collector, because the overall efficiency of the collector depends on the optical and thermal properties of this element. The receiver tube is composed of an inner pipe which can be of copper, steel, galvanized iron etc, which is surrounded by a transparent glass pipe to reduce convective losses from the hot pipe.

Aperture area: The aperture area is the plane opening of the concentrator trough which the incident solar flux is accepted and is determined by multiplying the width ***W***, with the length ***L***, of the trough (Refer to Figure 3.1).

Concentration ratio: This is the ratio of the effective area of the aperture to the surface area of the receiver. Shown in Figure 3.2 is a cross section of a typical PTC;

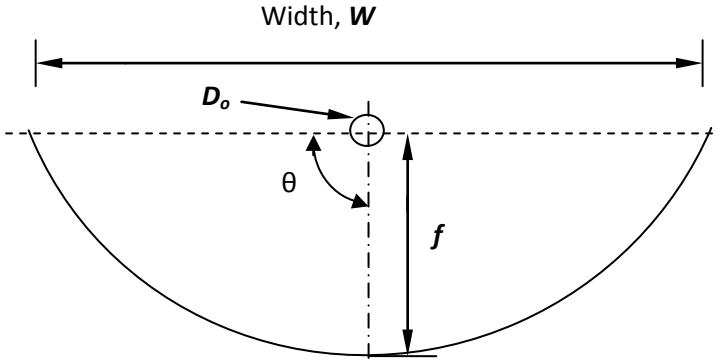

Figure 3.2: PTC cross-section

The concentration ratio is given by [**1**];

$$\boldsymbol{C = \frac{(W - D_o)L}{\pi D_o L} = \frac{(W - D_o)}{\pi D_o}} \quad \ldots \mathbf{3.1}$$

This ratio is always greater than 1. High concentration ratios results in higher working temperatures. However, high accuracy of the tracking mechanism and careful construction of the collector is required with increased concentration ratio. In practice, lower values of the concentration ratios than the theoretical ones are normally encountered.

Rim angle θ: it is the limiting angle over which incident ray path may deviate from normal to the aperture plane and still reach the absorber. Radiation is accepted over an angle 2θ because radiation incident within this angle reaches the receiver after passing through the aperture.

The equation adopted or generating a parabola is given as [**24**];

$$\boldsymbol{y = \frac{x^2}{4f}} \qquad \ldots \mathbf{3.2}$$

Where ***f*** is the focal length.

3.2 Solar time

It is necessary to convert standard time to solar time when taking solar radiation data with time of day. Solar time is the time based on the apparent angular motion of the sun across the sky, with solar noon being the time the sun crosses the meridian of the observer. The solar time can be obtained from the standard time by [**14**];

$$\boldsymbol{Solar\ time = Standard\ time + E + 4(L_{st} - L_{loc})} \qquad \ldots \mathbf{3.3}$$

Where $\boldsymbol{E}$ **=** the equation of time in minutes, $\boldsymbol{L_{st}}$ = the standard meridian for the local time zone, and $\boldsymbol{L_{loc}}$ = the longitude of the location in question, in degrees West.

The equation of time, **E** is obtained by [**14**];

$$\boldsymbol{E = 229.2(0.000075 + 0.001868CosB - 0.032077SinB - 0.014615Cos2B - 0.04089Sin2B)} \qquad \ldots \mathbf{3.4}$$

Where, $\boldsymbol{B = (n-1)\frac{360}{365}}$, **n**= day of the year. Thus $\boldsymbol{1 \leq n \leq 365}$

3.3 Optical analysis

The instantaneous optical performance of a trough can be measured by the optical efficiency. This is defined as the ratio of the energy absorbed by the receiver to the energy incident on the collector aperture area. The optical efficiency depends on the optical properties of the PTC materials, the geometry of the collector, and the various imperfections arising from the construction of the collector. Optical efficiency is obtained from [**9**];

$$\boldsymbol{\eta_o = \rho\alpha\tau} \qquad \ldots \mathbf{3.5}$$

Where, $\boldsymbol{\rho}$ is reflectivity of the reflecting material, $\boldsymbol{\alpha}$ is the absorptivity of the receiver material, and $\boldsymbol{\tau}$ is the transmissivity of the glass cover.

3.4 Thermal analysis

3.4.1 Energy absorbed by the receiver pipe

The energy absorbed by the receiver pipe depends on the incident solar radiation ($\boldsymbol{I}$ in W/m^2), the aperture area (***W*X*L***), the transmissivity ($\boldsymbol{\tau}$) of the glass cover, the reflectivity ($\boldsymbol{\rho}$) of the reflective material and the absorptivity ($\boldsymbol{\alpha}$) of the receiver material . Thus the energy absorbed by the receiver is given by [**16**];

$$\boldsymbol{Q_{absorbed} = \alpha\rho\tau I_b(W - D_o)L} \quad \ldots \mathbf{3.6}$$

3.4.2 Theoretical energy delivered by the collector

The theoretical energy delivered by the collector is expressed by [**18**];

$$\boldsymbol{Q_{th} = A_{ap}F_R\left(I_b\eta_0 - \frac{A_o}{A_{ap}}U_l(T_i - T_a)\right)} \quad \ldots \mathbf{3.7}$$

Where; $\boldsymbol{A_{ap}}$**=** Aperture area

$\boldsymbol{F_R}$**=** Heat removal factor

$\boldsymbol{A_o}$**=** Outer receiver area

$\boldsymbol{U_l}$**=** Overall heat transfer coefficient

The heat removal factor $\boldsymbol{F_R}$ is the ratio of the heat actually delivered to that delivered if the receiver pipe were at uniform temperature equal to that of the inlet fluid. It is obtained by [**18**];

$$\boldsymbol{F_R = \frac{\dot{m}C_p}{A_oU_l}\left(1 - e^{\left(\frac{-A_oF'U_l}{\dot{m}C_p}\right)}\right)} \quad \ldots \mathbf{3.8}$$

$\boldsymbol{F'}$ is the collector efficiency factor and it represents the ratio of the actual useful heat gain that would result if the collector-absorbing surface had been at the local fluid temperature. For a tubular absorber having a heat transfer coefficient $\boldsymbol{h_f}$ between absorber and the fluid and absorber thermal conductivity ***k,*** the collector efficiency factor is obtained by [**18**];

$$F' = \frac{1/U_l}{\frac{1}{U_l} + \frac{D_o}{h_f D_i} + \left(\frac{D_o}{2k} ln \frac{D_o}{D_i}\right)} \quad \ldots 3.9$$

3.4.3 Correlations for convective heat transfer coefficient in pipes

Convective heat transfer takes place wherever a fluid is in contact with a solid surface that is at a different temperature than that of the fluid. In a PTC, air is blown by a fan through a pipe and therefore forced convection results. Three important parameters which are very important in the analysis are Reynolds Number $\left(Re = \frac{VD_i}{\nu}\right)$, Prandtl Number $\left(Pr = \frac{\nu}{\alpha}\right)$ and Nusselt Number ($Nu_D = \frac{hD_i}{k}$) .

For forced convection in turbulent pipe flow, Equation 3.10 was proposed by Petukhov as a correlation for turbulent flow in tubes [**14**];

$$Nu_D = \frac{\frac{f}{8} RePr}{1.07 + 12.7\sqrt{\frac{f}{8}} x \left(Pr^{\frac{2}{3}} - 1\right)} \; valid\ for\ 0.5 \leq Pr \leq 2000$$

$$and\ 2200 \leq Re \leq 1.25x10^5 \quad \ldots 3.10$$

Where ***f*** is the Darcy friction factor and can be obtained from the Moody diagram**.** Turbulent pipe flow is expected for this study.

The temperature of the receiver surface can be obtained from [**25**];

$$T_r = T_b + \frac{\dot{m} C_p (T_o - T_i)}{h_i \pi D_o L} \quad \ldots 3.11$$

3.4.4 PTC Actual energy

The actual energy obtained from a parabolic trough solar collector is obtained by [**18**];

$$Q_{actual} = \dot{m} C_p (T_o - T_i) \quad \ldots 3.12$$

The energy supplied to the heat transfer fluid is the difference between absorbed solar energy and the losses due to radiation and convection. This is illustrated below [**9**];

$$\boldsymbol{Q_{actual} = Q_{absorbed} - Q_{loss}}$$

$$\boldsymbol{\dot{m}C_p(T_o - T_i) = \alpha\tau\rho I_b(W - D_o)L - U_l A_o(T_r - T_a)} \quad \ldots \mathbf{3.13}$$

Mass flow rate and specific heat of air are evaluated using the mean film temperature which is [**25**];

$$\boldsymbol{T_{m,f} = \frac{T_r + \frac{T_i + T_o}{2}}{2}} \quad \ldots \mathbf{3.14}$$

3.4.5 Overall heat loss coefficient, U_l

Energy loss in parabolic trough concentrators occurs in two ways, through radiation$\boldsymbol{Q_{rad}}$ and convection$\boldsymbol{Q_{conv}}$ [**14**];

$$\boldsymbol{Q_{loss} = Q_{conv} + Q_{rad}} \quad \ldots \mathbf{3.15}$$

This loss occurs at the receiver. $\boldsymbol{Q_{rad}}$ is proportional to the receiver-ambient temperature difference while $\boldsymbol{Q_{conv}}$ is due to free convection or wind effect. The overall heat loss coefficient is related to $\boldsymbol{Q_{loss}}$ [**14**];

$$\boldsymbol{Q_{loss} = U_l A_o(T_r - T_a)} \quad \ldots \mathbf{3.16}$$

Where the overall heat loss coefficient $\boldsymbol{U_l}$ is got from [**18**];

$$\boldsymbol{U_l = h_{conv} + h_{rad}} \quad \ldots \mathbf{3.17}$$

3.4.5.1 Radiation heat transfer coefficient h_{rad}

Radiation heat loss is a function of the receiver surface temperature and the ambient temperature. Radiation heat loss coefficient is obtained from [**18**];

$$\boldsymbol{h_{rad} = \epsilon\sigma(T_r + T_s)\left(T_r^{\,2} + T_s^{\,2}\right)} \quad \ldots . \mathbf{3.18}$$

Where T_s is the sky temperature and is obtained from [14];

$$T_s = T_a\left(0.711 + 0.0056T_{dp} + 0.000073{T_{dp}}^2 + 0.013Cos(15t)\right)^{\frac{1}{4}} \quad \ldots 3.19$$

Where T_{dp} is the dew point temperature in degrees Celsius, T_a and T_s are in degrees Kelvin.

The range of temperature difference between the sky and air temperature is from 5^0C in a hot moist climate to 30^0C in a cold, dry climate. It is fortunate that the sky temperature does not make much difference in evaluating the collector performance [**14**].

3.4.5.2 Convection heat transfer coefficient h_{conv}

Heat loss by convection occurs through natural convection and due to the wind. The heat transfer coefficient due to free convection can be obtained by the expression according to Churchill and Chu [14];

$$Ra = GrPr = \frac{g\beta(T_r - T_a)L^3}{\nu^2}Pr \quad 3.20$$

$$for\ 10^{-6} \leq Ra \leq 10^{12}$$

Also the Nusselt number is expressed as [**27**];

$$Nu_D = \left(0.6 + \frac{0.387Ra^{\frac{1}{6}}}{\left[1 + \left(\frac{0.559}{Pr}\right)^{\frac{9}{16}}\right]^{\frac{8}{27}}}\right)^2 \quad \ldots . 3.21$$

The free convection heat transfer coefficient is expressed as [**14**];

$$h_{free\ conv} = \frac{k}{D_o}Nu_D \quad \ldots 3.22$$

Heat loss by forced convection is due to wind. Hence the loss will be a function of wind velocity. The forced convection heat transfer coefficient is obtained from [**14**];

$$h_{wind} = \frac{Nu_D\, k_{air}}{D_o} \quad \ldots 3.23$$

Where k_{air} is the thermal conductivity of air.

The Reynolds number is obtained by [**18**];

$$\boldsymbol{Re = \frac{VD_o}{\nu}} \qquad \ldots \mathbf{3.24}$$

Correlations for Nusselt number in laminar and turbulent regimes are shown below [**18**];

$$\boldsymbol{Nu_D = 0.4 + 0.54Re^{0.53}} \qquad \boldsymbol{for\ 0.1 < Re < 1000} \qquad \ldots \mathbf{3.25}$$

$$\boldsymbol{Nu_D = 0.3Re^{0.6}} \qquad \boldsymbol{for\ 1000 < Re < 50{,}000} \qquad \ldots \mathbf{3.26}$$

3.4.6 Efficiency of PTC

The theoretical thermal efficiency is given by [**18**];

$$\boldsymbol{\eta_{th} = \frac{Q_{th}}{I_b A_{ap}}} \qquad \ldots . \mathbf{3.27}$$

The efficiency of the receiver based on the concentration ratio is given by [**16**];

$$\boldsymbol{\eta_{receiver} = \frac{Q_{absorbed} - Q_{loss}}{Q_{Solar}}} \qquad \ldots . \mathbf{3.28}$$

The overall thermal efficiency based on both the beam and ground reflected radiation is given by [**18**];

$$\boldsymbol{\eta_{overall} = \frac{Q_{actual}}{(I_b + I_d)A_{ap}}} \qquad \ldots \ldots \mathbf{3.29}$$

CHAPTER 4

CONSTRUCTION AND TESTING PROCEDURES

4.0 Introduction

In this Chapter, the design and fabrication of a parabolic trough concentrator (PTC), experimentation, and analysis procedure are presented. The PTC was designed and fabricated in the Mechanical Engineering Workshop. It begins with design, then construction, experimentation, data collection and finally analysis of data.

4.1 Design of the collector

4.1.1 Mass flow rate of hot drying air

The collector was intended to supply hot air at a temperature 100^0C-130^0. This heated air should be sufficient to dry 1kg of biomass having moisture content of about 50%. Energy required to evaporate the moisture in 1kg of bagasse will be determined by;

$$\boldsymbol{Q_{Drying} = 0.5C_{P(Biomass)}(100℃ - T_i) + 0.5C_{P(Water)}(100℃ - T_i) + 0.5h_{fg(Water)}} \quad \ldots \mathbf{4.1}$$

Where $\boldsymbol{C_P}$ is the specific heat, $\boldsymbol{T_i}$ is the initial temperature before drying and $\boldsymbol{h_{fg(Water)}}$ is the latent heat of vaporization of water at 100^0C.

Taking bagasse having moisture content of 50% as is produced in the sugar mills as an example, it has a specific heat of 2.968kJ/kg K [**28**]. The energy required to evaporate this moisture will be calculated using Equation 4.1 as;

$$\boldsymbol{Q_{Drying} = 1x2.968(100 - 25) + 0.5x2256 = 1350.6kJ} \quad .. \qquad \ldots \mathbf{4.2}$$

The mass of drying air required is obtained from;

$$\boldsymbol{M_{air} = \frac{Q_{drying}}{C_{P(air)}(130℃ - 105℃)}\ kgs = \frac{1350.6x10^3}{1.012398x10^3(130 - 105)} = 53.3624kg\ of\ air}$$

This mass flow rate of air ($\dot{m}_{air}$) in kg/s required to dry 1kg of biomass for 4 hours is got from;

$$\frac{kg}{s} = \frac{53.3624}{4x3600} = 3.706x10^{-3}kg/s \quad \ldots(4.3)$$

The energy required to heat air with a mass flow rate of $3.706x10^{-3}Kg/s$ from 25^0C to 130^0C under steady state conditions will be obtained using Equation 3.12 in Chapter 3 as;

$$3.706x10^{-3}x\ 1.0082x10^3x(130-25) = 392.32W$$

4.1.2 Sizing the collector

The actual energy obtained from a parabolic trough concentrator is dependent on the reflective and the receiver material under steady state conditions.

Assuming an average solar radiation of ***I*** W/m^2 on a clear day that is incident on the aperture area A is concentrated C times on a receiver of absorptivity α. The actual useful energy required to heat $\dot{m}_{air}$ from ambient to 130^0C is obtained from Equation 3.10. A theoretical analysis of heat losses is done so as to get the length of the collector required for this duty.

The average daily solar irradiation in more than 106000 km^2 of land in Kenya including Nairobi is about 6kWh/m^2 per day [4]. A solar radiation value of 850W/m^2 is used in this analysis. Aluminum foil is to be used as the reflective material and is to be glued on the inside of the trough. A 1 inch Class B galvanized water pipe was proposed to be the receiver pipe. Reflectivity ρ of aluminum foil is taken as 0.86 [14], absorptivity α of galvanized water pipe is taken as 0.65[25].

The length of the pipe required to heat the air from 25^0C to 130^0C under steady state condition will be obtained by assuming that the all energy absorbed using Equation 3.8 will be transferred to the air. To start with, a length is obtained using Equation 3.12 by neglecting the heat loss component;

$$392.32W = 0.86x0.65x850x(1.026-.0334)xl$$

$$l = 0.832m$$

Where $\boldsymbol{C_p}$ is evaluated at the mean bulk temperature.

This length will now be used to estimate losses due to radiation and convection. Thus the heat transfer coefficient is to be approximated. The Nusselt number will be obtained from Equation 3.10;

$$\boldsymbol{Nu_D = \frac{\frac{0.0405}{8} x7676.83x0.697}{1.07 + 12.7\sqrt{\frac{0.0405}{8}}x\left(0.697^{\frac{2}{3}} - 1\right)} = 30.9}$$

Where Reynolds Number is obtained from Equation 3.21, the friction factor $\boldsymbol{f}$ of the galvanized pipe is obtained from the Moody Chart as **0.0405** (**Appendix 3**).

The heat transfer coefficient is obtained from;

$$\boldsymbol{h_i = \frac{30.9x0.03003}{0.0254} = 36.53\ W/m^2{}^{\circ}\mathrm{C}}$$

Now an estimate of receiver surface temperature is for that length is obtained from Equation 3.11;

$$\boldsymbol{T_r = 77.5 + \frac{392.32}{36.53x\pi x.0334x0.832} = 200.5^0 C}$$

Assuming that heat loss occurs through natural convection then, the Rayleigh Number will be obtained using Equation 3.19;

$$\boldsymbol{Ra = GrPr = \frac{\frac{9.81}{385.25}x(200.5 - 24)x0.0334^3x0.69136}{(2.43837x10^{-5})^2} = 194722}$$

The Nusselt number is obtained from Equation 3.20;

$$\boldsymbol{Nu_D = \left(0.6 + \frac{0.387x(194722)^{\frac{1}{6}}}{\left[1 + \left(\frac{0.559}{0.69136}\right)^{\frac{9}{16}}\right]^{\frac{8}{27}}} \right)^2 = 9.247}$$

The convective heat transfer coefficient will be obtained from Equation 3.21;

$$\boldsymbol{h_{free\ conv} = \frac{0.0326x9.247}{0.0334} = 9.0255 W/m^2{}^\circ\text{C}}$$

The radiation heat transfer coefficient will be obtained from Equation 3.18;

$$\boldsymbol{h_{rad} = 0.28x5.67x10^{-8}(483.7 + 297)(483.7^2 + 297^2) = 4.0\ W/m^2{}^\circ\text{C}}$$

The overall Heat loss coefficient will be obtained from the sum of convective and radiation heat transfer coefficients;

$$\boldsymbol{U_L = 9.0255 + 4.0 = 13.14\ W/m^2{}^\circ\text{C}}$$

The total heat loss will be obtained from Equation 3.16;

$$\boldsymbol{Q_L = 13.14x\pi x0.0334x0.813(210.7 - 24) = 209.3W}$$

Thus the corrected length required will be obtained by adding the energy required to heat the air and the losses thus;

$$\boldsymbol{392.32 + 209.3 = 0.88x0.65x850x(1.026 - 0.0334)xl}$$

$$\boldsymbol{l = 1.25m}$$

The length obtained assumes that there is no dust on the reflective surface, there is no twisting of the trough, there are no tracking errors and that all the reflected radiation reaches the receiver. However, in practice this is not the case. Thus the length required might be longer. A

standard galvanized sheet with length of 2400mm was used for the trough. For the experiment, various mass flow rates would be used to determine the performance of the PTC.

4.1.3 Actual size of the collector

The theoretical length obtained from **Section 4.1.2** of **1.25m** is used as the basis of the actual size of the collector. A standard GI sheet of 8feet(2400mm) X 4 feet(1220mm) was proposed to be used by sticking kitchen aluminum foil on one side forming the inside of the trough. The long side formed the length of the trough and the shorter side became width of the trough. To have a trough having a rim angle of 90^0C and ensuring that the whole sheet was utilized, the focal length $\boldsymbol{f}$ was found to be 250mm using AutoCAD with the aid of Equation 3.2.

Table 4.1 was used to plot the parabola profile;

Table 4.1 Parabola curve coordinates

x(mm)	-500	-450	-400	-350	-300	-250	-200	-150	-100	-50
Y(mm)	250.0	202.5	160.0	122.5	90.0	62.5	40.0	22.5	10.0	2.5

0	50	100	150	200	250	300	350	400	450	500
0	2.5	10.0	22.5	40.0	62.5	90.0	122.5	160.0	202.5	250.0

The plot of the parabola is shown in Figure 4.1;

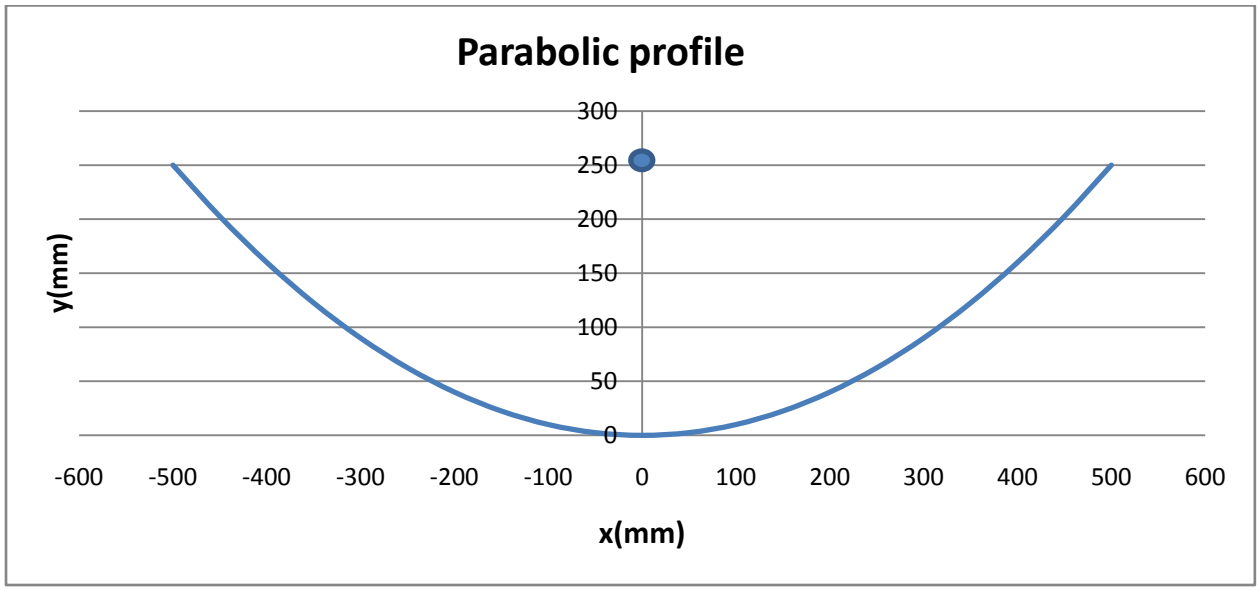

Figure 4.1: Parabola profile

Table 4.2 shows the summary of the collector specifications;

Table 4.2: Test parabolic trough concentrator specifications

Specification	**Values**
Collector aperture area (A_a=**L x W**)	2.4624m^2
Collector length (**L**)	2.4m (Refer Drawing No:007/PTC/2013)
Collector aperture (**W**)	1.026m (Refer Drawing No: 007/PTC/2013)
Concentration ratio (**C**)	9.34
Rim angle θ	90^0
Tracking mechanism	Manual
Reflector material	Kitchen aluminum foil
Receiver tube material	Galvanized water pipe
Reflectivity of aluminum foil (**ρ**)	0.86 [14]
Absorptivity of the receiver (**α**)	0.65 [**27**]
Emissivity of the receiver (**ε**)	0.28 [**27**]
Stefan Boltzmann constant (σ)	5.67X10^{-8} W/m^2 K^4 [**18**]
Transmittance of 3mm glass (τ)	0.85 [**29**]

4.2 Fabrication

4.2.1 Fabrication methodology

The parabolic trough collector air heating system has two main components. These are the parabolic trough concentrator and a blower. The parabolic trough concentrator provides the energy to heat the air while the blower provides the air to be heated. All drawings for this project were prepared. Then a bill of materials was prepared**.** Finally all the materials that cannot be obtained from the Mechanical Engineering Workshop were to be purchased.

The parabolic trough concentrator contains four main parts, the parabolic trough (Refer Drawing No: 007/PTC/2013), receiver pipe (Refer Drawing No: 005/PTC/2013), stands (Refer Drawing No: 002/PTC/2013, 003/PTC/2013, 003/PTC/2013) and the manual tracking system (Refer to Drawing No: 006/PTC/2013).

These four parts are reviewed in Sections 4.2.1.1 to 4.2.1.5.

4.2.1.1 The parabolic trough

The aim of the project was to fabricate two troughs. This is because it was anticipated that the troughs may be tested in series. Each trough was supposed to be composed of two end pieces and a reflective material. The end pieces were to be cut with one edge being straight and the other forming a parabolic shape. A hole was then to be drilled at the focal point of the parabola. This was to form the location of the receiver pipe.

When assembling the trough, a galvanized iron sheet was to be bent with the help of the parabolic-shaped edges of the two end plates. Self tapping screws were to be used to secure the sheet on the end pieces. A frame of 1 inch angle line was then to be secured on the top of the trough using a preformed channel that attaches the trough to the frame (Refer to Drawing No: 007/PTC/2013). This frame was to provide the area where glass cover will be put.

Finally, kitchen aluminum foil was to be glued using Conta glue on the inner side of the trough. This was to act as the reflective material.

4.2.1.2 Receiver pipe

This is the heart of the parabolic trough concentrator. In this project a galvanized steel water pipe is to be used as the receiver pipe. A 1 inch (25.4mm) diameter pipe was to be used to achieve one concentration ratio. Each trough had a receiver pipe prepared. The ends of the pipes were to be tapped so as to ensure connectivity when two troughs were being used in series and also to connect with the blower.

So as to ensure that temperature distribution is measured during experimentation, thermocouple wires were to be attached on the surface of the receiver pipes, using a heat resistant adhesive(gun gum), at equal distance with each other. A selector switch is then to be fabricated to make it easier to determine the temperature of any point on the pipe connected to the thermocouple wire. The selector switch is to be connected to the digital thermometer.

4.2.1.3 Stand

The stand holds the trough and the manual tracking system. It is to be made of 2 inch (50.8mm) mild steel square tubes. All the pieces are to be cut as indicated in the drawings and joined

using welding. Caster wheels will then be bolted on the stand so as to enable mobility of the parabolic trough concentrator.

4.2.1.4 Tracking system

Such tracking systems are of two types, automatic controlled and manual. A manual tracking system is to be adopted for the parabolic trough concentrator in this study as it is cheap and easy to fabricate. A shaft of 1 inch (0.0254m) diameter and length 1.09m is to be turned and threaded to 22.225mm diameter. The edges of the shaft are to be turned to 3/4 inch where a 3/4 inch pillow block bearing will be secured. The bearing together with the shaft will then be bolted to the edge of the stand together with preformed U-channels which is connected with the trough and nut and roller assembly(Refer to Drawing No: 006/PTC/2013).

This would ensure that as the shaft was turned, the nut and roller assembly would move along the U-channel attached on the side of the trough and thus the trough would turn (Refer Drawing No: 007/PTC/2013).

4.2.1.5 The blower

The blower used to be in the study is to be obtained from the foundry section of the Mechanical Engineering Workshop. The blower had a capacity of 120 cubic feet per minute. During the experimentation, a gate valve will be connected at the outlet of the blower so as to regulate the flow rate of air. A horse pipe will be connected between the blower and the valve so as to ensure flexibility during experimentation when turning the trough.

4.2.2 Actual construction of PTC

4.2.2.1 Preparation of components

The following 8 steps were used for the preparation of components.

1. **Making the ends**: The four end pieces were cut from one piece of 8feet X 4feet block board. The drawing of the parabola was fed into a computer CNC Shot Boot machine in CAD form. The machine then cut the pieces from the block boards. This machine is available in the Fablab workshop at the University of Nairobi. Shown in Figure 4.2 is the cutting process.

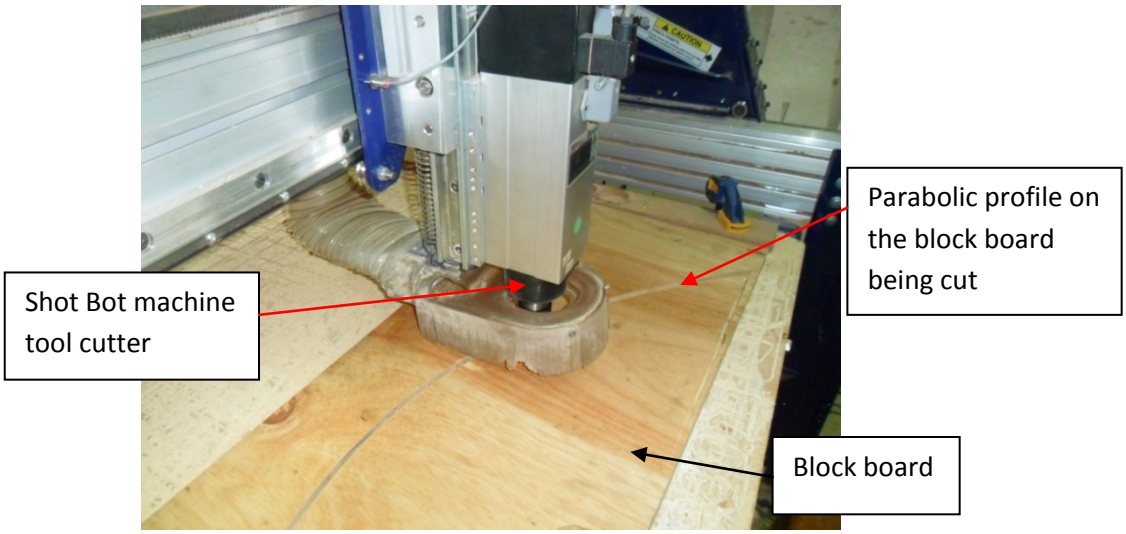

Figure 4.2: Making the end piece

2. **Making the stand**: The stand was fabricated using standard hollow sections of 2 inch X 2inch X 1/8 inches (50mmX50mmX3mm) thick. All the pieces are cut and joined together by welding. Three stands are fabricated (Drwg. No's: 003/PTC/2013, 004/PTC/2013, 005/PTC/2013 in Appendix 2.) One stand is fabricated to accommodate the tracking systems' shaft.
3. **Making the bearing housing**: 70mm ball bearings were used on the stands. The housing was fabricated using 2mm mild steel sheet with a 100mmX125mm steel plate of 4mm thickness welded below the housing so as to be attached on the stand using bolts. Figure 4.3 shows the ball bearing in the housing.

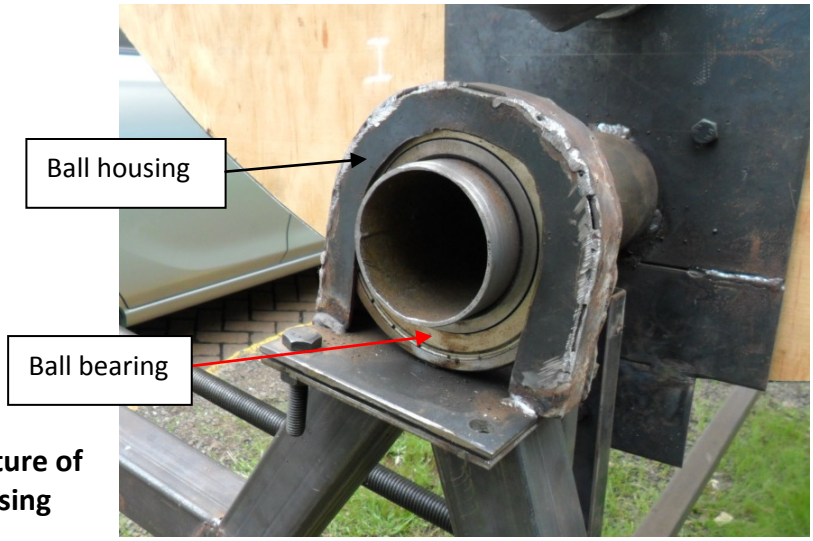

Figure 4.3: Picture of bearing housing

4. **Fabricating the tracking shaft**: A mild steel shaft, 1 inch diameter and 1110mm long was turned and threaded to a diameter of 22.225mm inch, 50mm from one end and 100mm on the opposite end. The ends were turned to ¾ inch diameter where ¾ pillow block bearings were fitted on the shaft. A handle was then welded on the 100mm free end (Drwg. No. 006/PTC/2013 in Appendix 2.). Figure 4.4 the tracking shaft attached to the stand and trough.

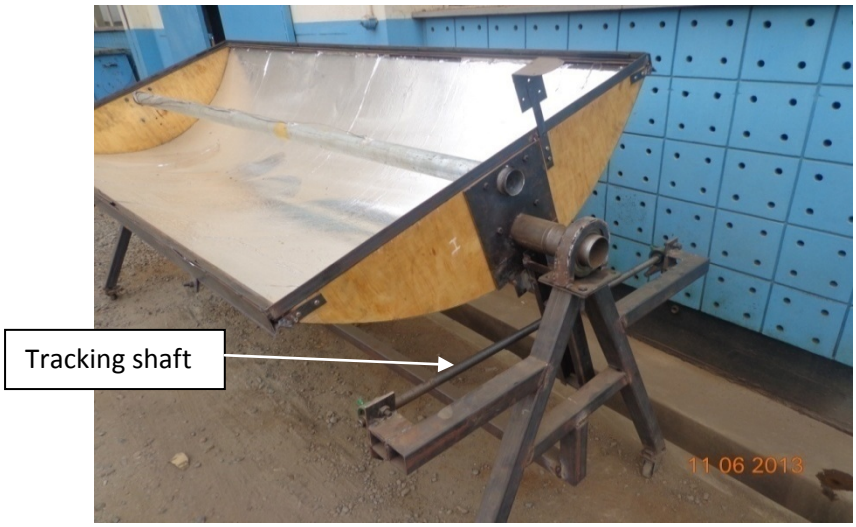

Figure 4.4: The tracking shaft on the concentrator

5. **Fabricating the manual tracking guide bracket**: Two mild steel plates 3mm thick having a length of 500mm and width of 88mm were prepared. They were then bent a right angles 20mm from both the longer sides to form a preformed U-channel. Two holes of diameter 3/8 inch were drilled 65mm apart, 10mm from the end (Drwg. No. 006/PTC/2013 in Appendix 2.). Shown in Figure 4.5 is the tracking system showing the preformed channels assembled in the trough.

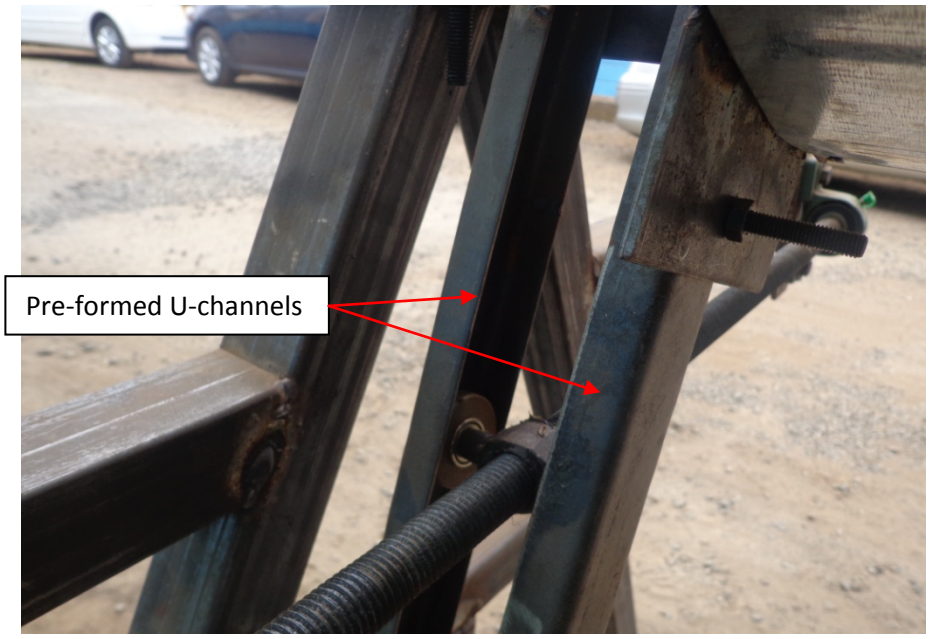

Figure 4.5: Tracking system on the concentrator

6. **Preparing the receiver pipes**: One size of pipe was used in the research. This was the 1inch (25.4mm) diameter pipe. One pipe section was cut to a length of 8feet, 2 inches long. Then it was threaded 1 inch from each end. The purpose of the threads was to ensure connection to the fan on one side and the second trough in case of when two troughs are used in the study. Thermocouple wires were then fixed on one 1 inch pipe. The pipes were divided into six sections. One inch from the inlet and outlet of the pipes had holes drilled and the thermocouple wires put in such a way that they were in contact with the air. In the middle sections thermocouple wires were fixed on the surface of the pipe using gun gum adhesive (Drwg. No. 005/PTC/2013 in Appendix 2).
7. **Preparing the selector switch**: All the thermocouple wires are connected to the digital thermometer through the selector switch. The switch assisted in the determination of temperature of the various locations of the pipe. The selector switch components were available in the thermodynamics laboratory and were assembled to suit the experiment. Shown in Figure 4.6 shows the switch which is used to select the position along the pipe where the temperature is to be determined and also shows the back of the selector having the wires attached to it.

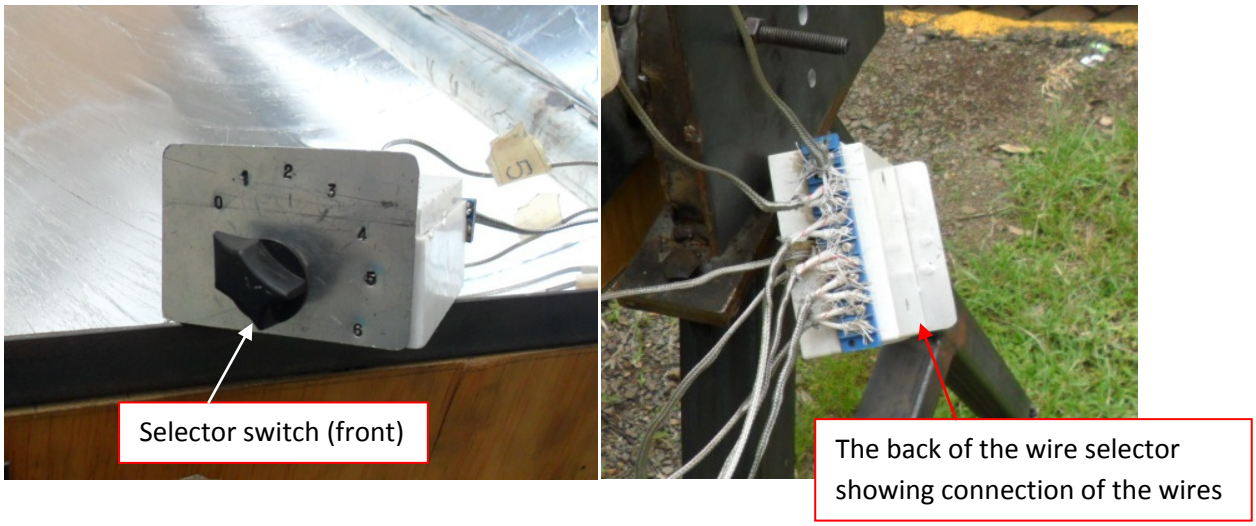

Figure 4.6: Selector switch

8. **Preparing glass cover**: A 3mm thick glass cover was required. This was to ensure that as much of the solar radiation was transmitted through and also to ensure that the trough doesn't become too heavy if a thicker glass plate was installed. The glass cover was put on the 25mmX25mmX3mm angle line frame secured on top of the trough (Drwg. 007/PTC/2013 on Appendix 2.). The dimensions where the glass could fit was measured and found to be 95½ inches (2426mm) X 42 inches (1067mm) from an allowance of half an inch (13mm) was considered from the edges of the angle iron frame. Since 3mm glass has a standard size of 72 inches by 48 inches, two pieces of 72 inch(1829mm) X 42 inches(1067mm) and two pieces of 23½ inches(597mm) X 42 inches(1067mm) were prepared by the supplier for the two troughs.

4.2.2.2 Assembly of the parabolic trough concentrator

The following 4 steps were used for the assembly of the PTC.

1. **Joining the trough**: Figure 4.7 shows the assembled trough. The back was made of galvanized iron sheet. The 4 feet long side formed the parabolic curved width of the trough while the 8 feet long side formed the length of the trough. A side angle was riveted on the edge of the length to reinforce the sheet on the end pieces. Then an angle iron frame of 25mmx25mmx3mm was made and secured on top of the trough by a flat that was welded

on the frame and bolted with the angle iron of the back. The frame minimized the twisting of the trough.

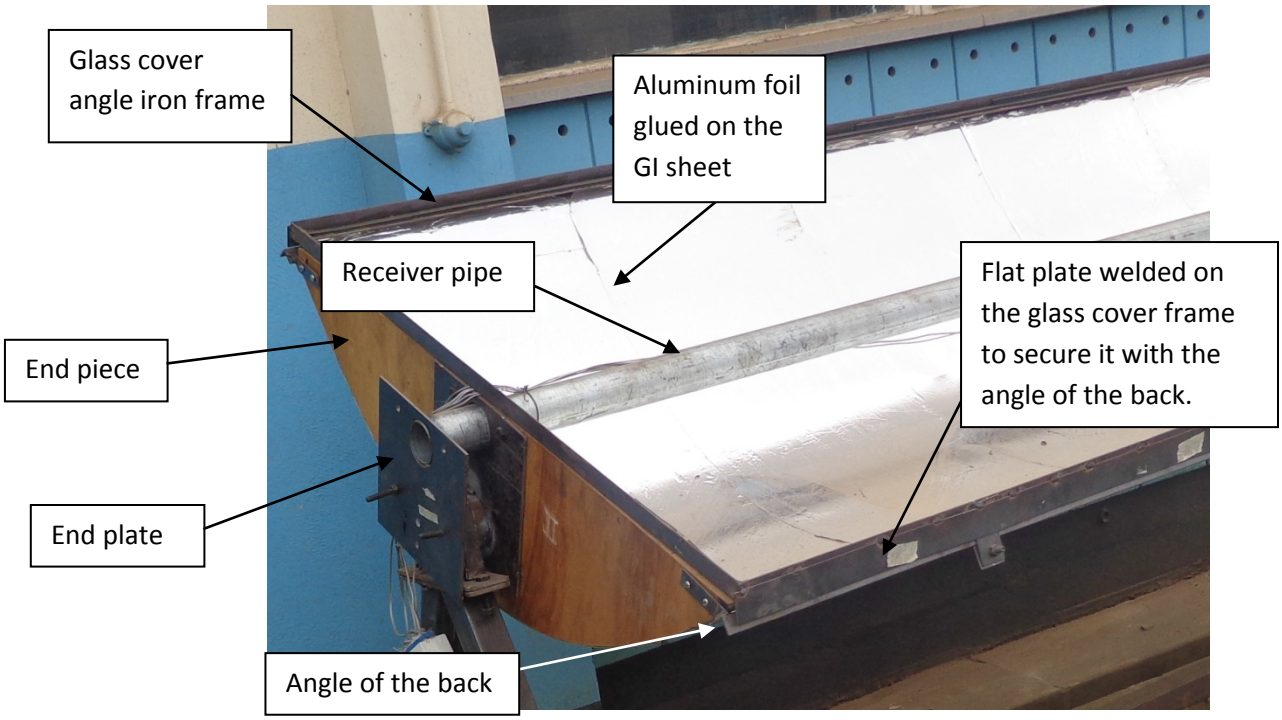

Figure 4.7: The assembled trough

2. **Forming the reflective surface**: After the end pieces were assembled with the galvanized iron sheet, the aluminum foil was then glued on the inside surface of the GI sheet using Contac glue (Figure 5.7).
3. **Assembling the tracking system**: The stands already fabricated were assembled with the trough. The shaft, complete with the nut and roller assembly and the pillow block bearing were assembled and bolted on the stand. Then the manual tracking guide bracket was fastened on the end plates by bolts. Care was taken so as to ensure that the nut and follower are secured properly on the guide.
4. **Attaching the thermocouple wires to the selector switch**: After the wires were attached on the pipe surface using gun gum, each wire was given a number and connected to the back of the selector switch to correspond to the number on the switch. For instance, No. 1 corresponded to the first point on the pipe surface from the inlet while No. 6 corresponded

to the outlet temperature of the heated air. The inlet temperature was determined with a separate thermocouple wire not connected with the selector switch.

4.3 Performance testing of the PTC

4.3.1 Experimental procedures

The main scope of the project was to heat air from ambient to at least a temperature of 100^0C. For the performance of the concentrator to be determined, measuring devices are required to measure temperature, flow rate and solar radiation. Figure 4.8 shows the experimental set-up.

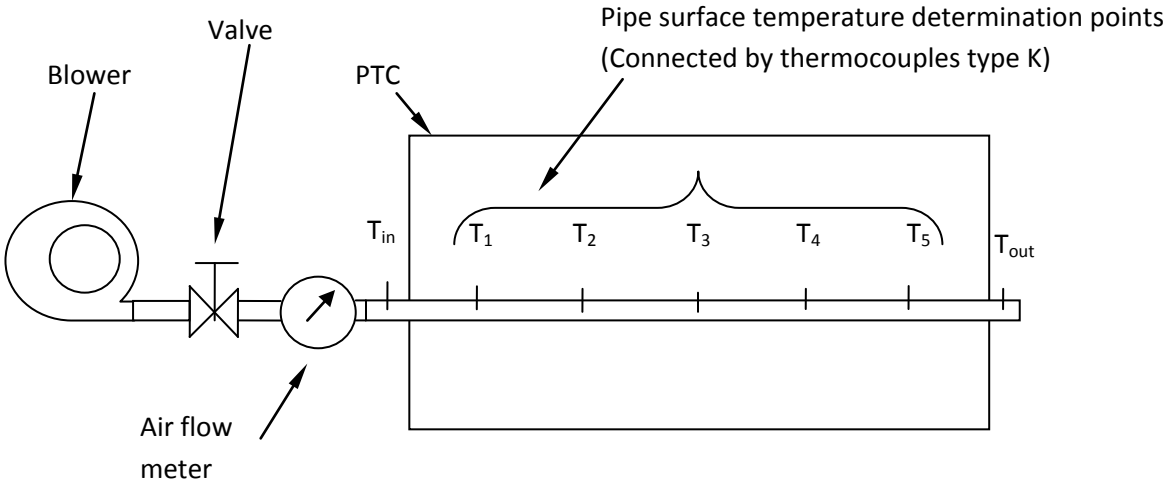

Figure 4.8: Experimental set-up

The experiment took place from 1100Hrs to 1500Hrs on the selected days. During the experimentation, the PTC was taken outside after setting the flow rate and aperture plane aligned to be perpendicular to the direction of the sun using the manual tracking system. This was made possible by ensuring that the image of the solar radiation covered one half of the receiver pipe. It was also ensured that the solar pyranometer sensor was secured properly on its bracket so as to ensure that it was parallel with the aperture plane. Care was taken not to interfere with the gate valve as it would have affected the flow rate

4.3.2 Data collection

The PTC was required to heat air using solar radiation at different mass flow rates to 100^0C and above. Thus data was collected so as to evaluate its performance. The data collected was on temperature, air flow rate and solar radiation.

4.3.2.1 Temperature

Since the duty of the collector was to heat air, the air inlet and outlet temperatures, surface temperature and the ambient temperature were measured and recorded on 5 minute intervals for every mass flow rate in the selected days of the study. Thermocouple wires, type K connected to a digital thermometer aided in the determination of inlet and outlet air temperatures together with the tube surface temperatures. A dry bulb thermometer was used to measure the ambient temperatures.

4.3.2.2 Flow rate

For every selected day, a single air mass flow rate was tested. A vane type wind anemometer was used to measure the velocity of the air in the pipe. The mass flow rate is then calculated using the cross section area of the pipe and density of air at room temperature. A valve was used to set the velocity at the beginning of the day. The wind anemometer was also used to measure the wind speed during experimentation. This was done by holding it against the direction of the wind.

4.3.2.3 Solar radiation

The instrument used to measure solar radiation was Henni Solarimeter. It measured both the direct and diffuse radiation. A bracket was bolted on the side of the trough where the Solarimeter sensor was attached as shown in Figure 4.9 in such a way that it does not obstruct solar radiation in the collector area but is close enough to receive the same solar irradiation;

Figure 4.9: Henni solarimeter sensor attached to the trough

4.3.3 Analysis of results

The data obtained by testing the already constructed PTC was to be analyzed so as to evaluate its performance. As the PTC was tested on a typical selected days, the following 5 phenomena were investigated;

1. The effects of solar variability on the collector.
2. The effect of mass flow rates on:
    - Temperature rise
    - Useful energy
    - Overall, receiver and theoretical efficiencies.
3. The effect of glass cover on PTC performance
4. The effect of collector length on:
    - Temperature rise
    - Useful energy
    - Overall, receiver and theoretical efficiencies.
    - Heat loss
5. Application in drying bagasse

CHAPTER 5

RESULTS AND DISCUSSION

5.0 Introduction

The fabricated PTC described in Chapter 4 was tested at the Department of Mechanical and Manufacturing Engineering, University of Nairobi (**S** 01^0 16' 34.5", **E** 036^0 49' 02.2", Elevation 1689m above sea level). The PTC was tested between 11.00am to 3.00pm standard time on selected days between 25th February to 22nd March 2013. The aim was to test the PTC when solar insolation is at maximum values, usually between 10.00am to 4.00pm. The tests were done for a selected number of days to assess the PTC performance.

Data on inlet and outlet temperature of air, the solar insolation and air mass flow rate was obtained. The data enabled the determination of the receiver efficiency, overall efficiency, useful energy and estimate the heat loss at each instant between the times of day. The data was averaged over a time of five (5) minutes and represented in intervals of ten (10) minutes. The graphs are plotted using local solar time. This Chapter presents the results from the tests.

5.1 Solar energy variability

The PTC was tested on selected days and the effect of solar variability on outlet temperature and useful energy was investigated. Figure 5.1 shows the variation of solar insolation, inlet and outlet temperatures with time, Figure 5.2 shows the variability of solar insolation with the useful energy obtained from the PTC with time while Figure 5.3 shows the variability of solar insolation with the overall efficiency with time taken on 28th February 2013 when the mass flow rate was kept at a constant value of 0.0054kg/s.

Figure 5.4 shows the variation of solar insolation, inlet and outlet temperatures with time, Figure 5.5 shows the variability of solar insolation with the useful energy obtained from the PTC with time while Figure 5.6 shows the variability of solar insolation with the overall efficiency with time taken on 15th March 2013 when the mass flow rate was kept at a constant value of 0.0006kg/s.

It can be seen from Figure 5.1 that solar insolation was fairly steady with an average value of 940W/m^2 between 1014hrs to 1319hrs solar time. There was then a cloud cover from 1319hrs to 1339hrs solar time. Thereafter, the solar insolation was steady but started dropping slowly from 1404hrs to 1414hrs solar time. The reason for the steady value of solar insolation is because Kenya lies along the equator. Thus the sun is directly above and the solar insolation value is expected to be above 900W/m^2 from 1000hrs to 1600hrs standard time on a clear day.

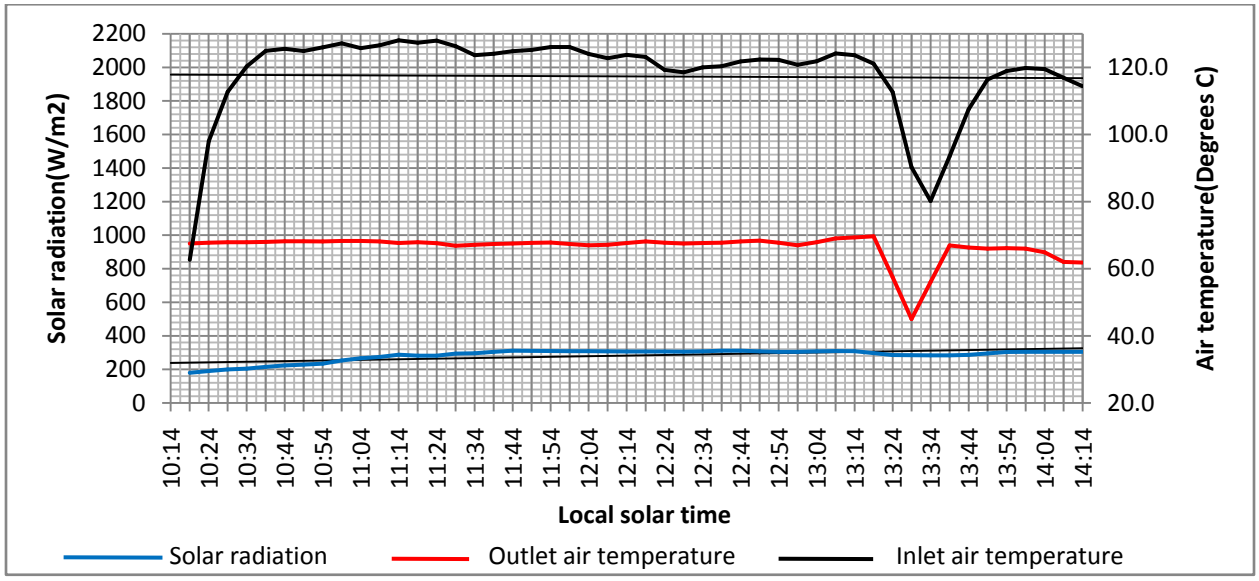

Figure 5.1: Variation of solar insolation, inlet and outlet temperatures with time taken on 28/2/2013 when the mass flow rate was kept at a constant value of 0.0054kg/s.

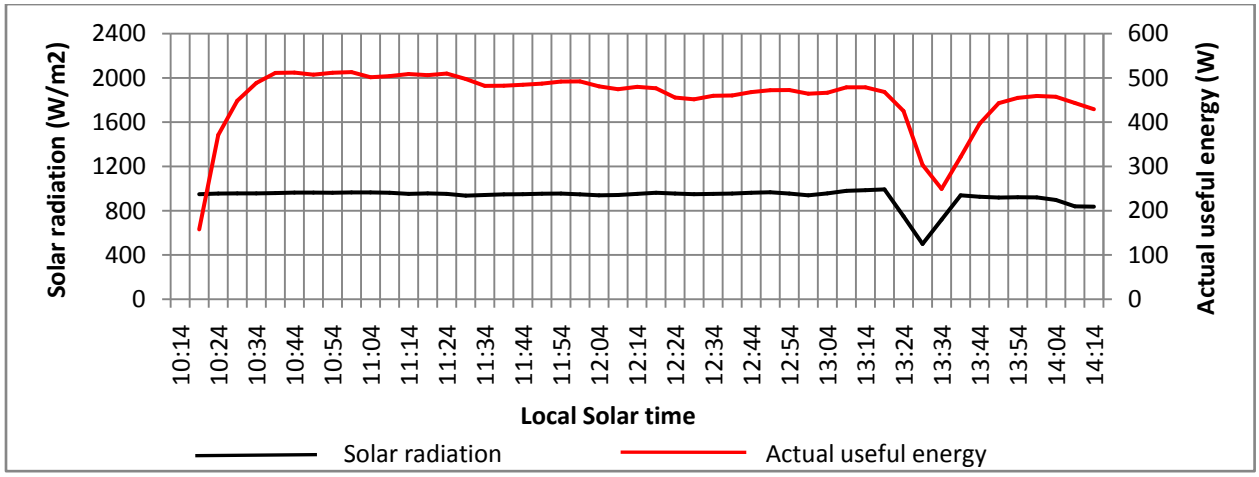

Figure 5.2: Variation of Solar insolation, useful energy with time when the mass flow rate was 0.0054kg/s taken on 28/2/13.

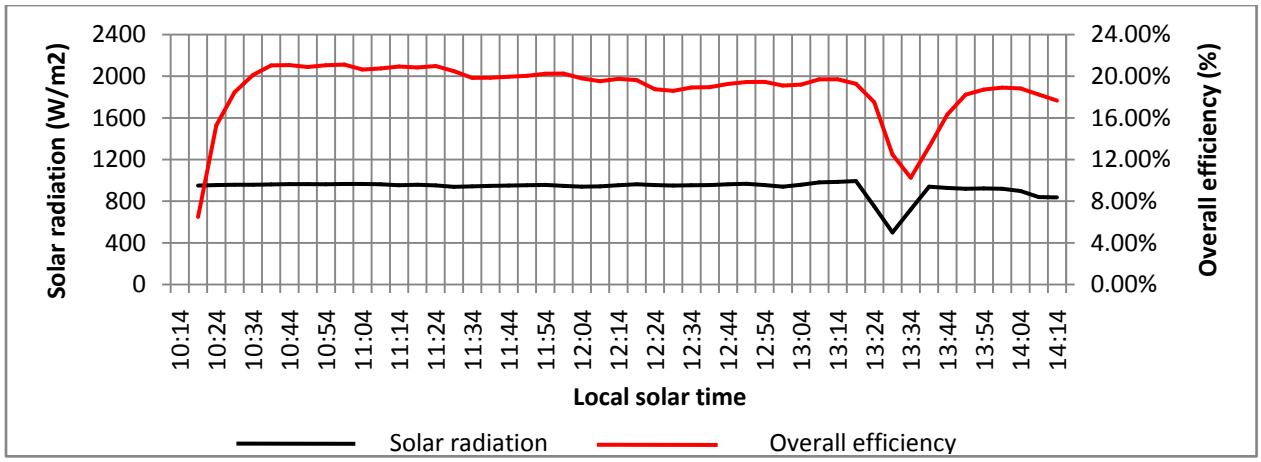

Figure 5.3: Variation of Solar insolation, overall efficiency with time with a mass flow rate of 0.0054kg/s taken on 28/2/13.

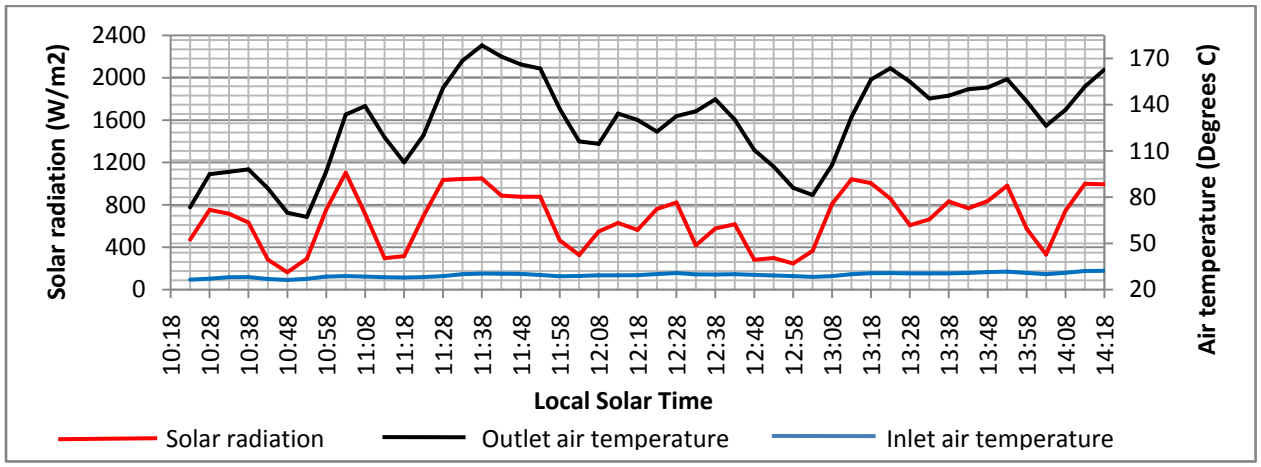

Figure 5.4: Variation of solar insolation, inlet and outlet temperatures with time taken on 15/3/2013 when the mass flow rate was kept at a constant value of 0.0006kg/s.

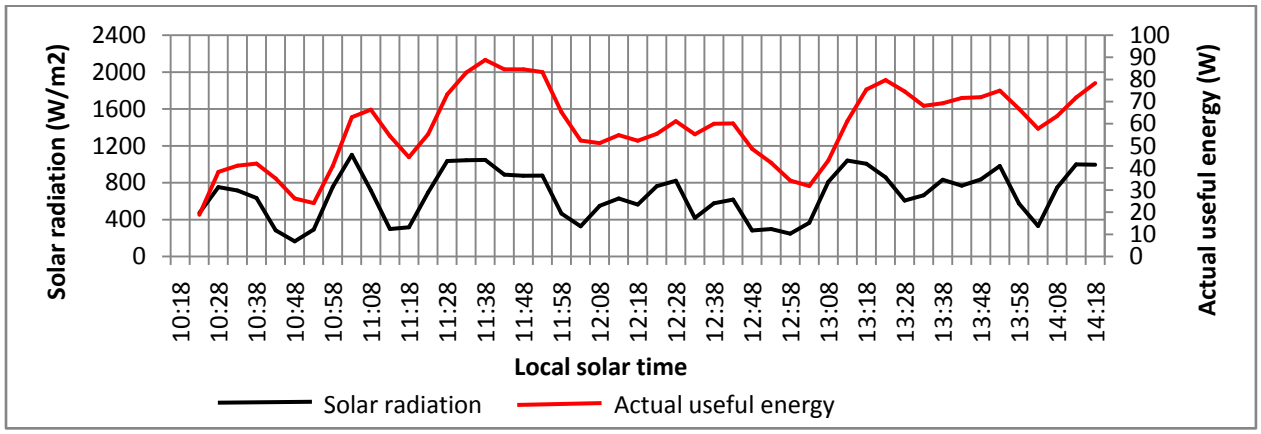

Figure 5.5: Variation of Solar insolation, useful energy with time when the mass flow rate was 0.0006kg/s taken on 15/3/13.

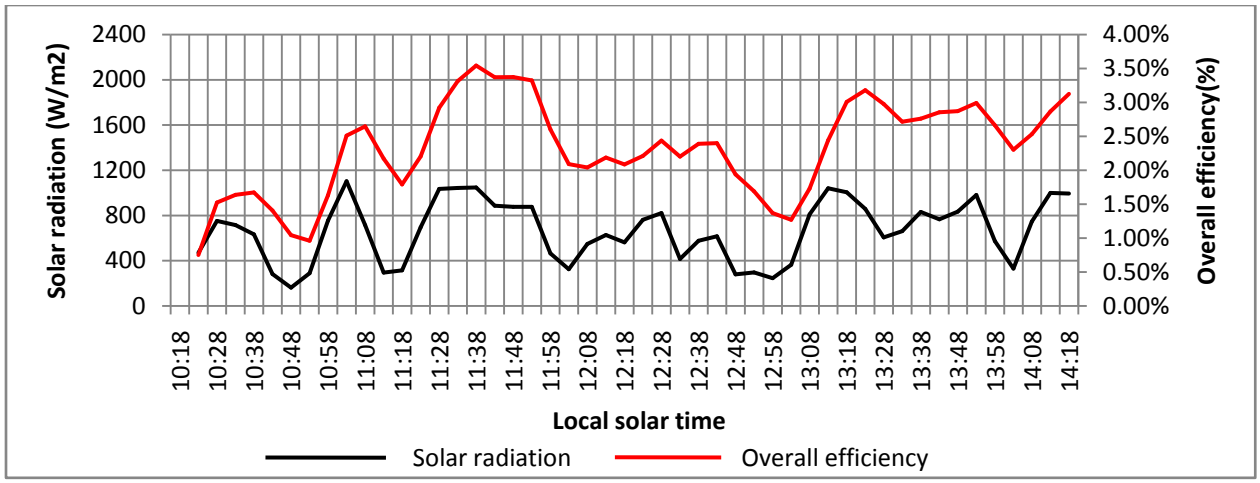

Figure 5.6: Variation of Solar insolation, Overall efficiency with time when the mass flow rate was 0.0006kg/s taken on 15/3/13.

It can be seen however that at 1319hrs solar time in Figure 5.1, the reduction of solar insolation due to cloud cover closely follows the reduction of outlet air temperature. From Figure 5.2 and Figure 5.3, it can be seen that the useful energy and overall efficiency closely follows the solar insolation. This is because they are a function of outlet air temperature and thus will exhibit a similar behavior.

The outlet temperature, useful energy and overall efficiency all have a near immediate response to changes of solar insolation. This is due to low heat capacity of air and the pipe and also high heat losses. Hence values of the temperature useful energy and overall efficiency may be directly related to the solar insolation. This can enable the comparison at different times and even different days.

5.2 Effect of mass flow rates

The PTC tests were repeated at 7 different varying mass flow rates between 0.0006kg/s to a maximum of 0.0078kg/s. The effect of mass flow rates on temperature rise, useful energy, overall efficiency, receiver efficiency and heat loss are presented.

5.2.1 Effect of mass flow rate on temperature rise (T_o-T_i)

Figure 5.7 shows the variation of solar radiation, inlet and outlet air temperature with time using the minimum mass flow rate of 0.0006kg/s while Figure 5.8 shows the variation of solar

radiation, inlet and outlet air temperature with time using the maximum mass flow rate of 0.0078kg/s.

For both the minimum and the maximum mass flow rates, the outlet air temperature closely follows the solar insolation. The temperature rise when the minimum flow rate is used is higher than when the maximum flow rate is used. The highest temperature obtained with the mass flow rate of 0.0006kg/s was 152^0C at 1221hrs solar time while for 0.0078kg/s was 108^0C at 1141hrs solar time. The reason is because less energy is required to heat a mass flow rate of 0.0006kg/s than is required to heat 0.0078kg/s with the solar insolation being almost constant at about 1000W/m^2.

Figure 5.9 shows the quantity $((T_o-T_i)/I)$ versus mass flow rate at an instant when the solar insolation was maximum. Clearly the temperature rise (T_o-T_i) and therefore outlet air temperature decreases with the increase in mass flow rate.

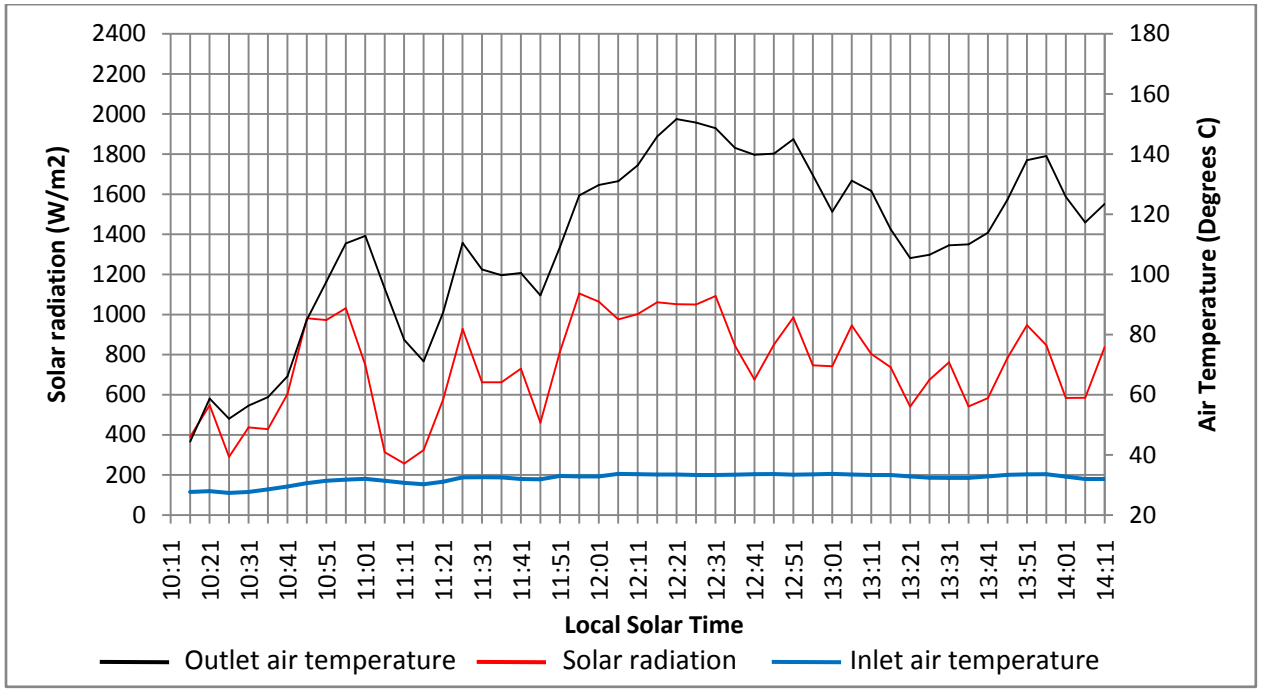

Figure 5.7: Variation of solar radiation with inlet and outlet air temperature and time taken on 12/03/13 with a mass flow rate of 0.0006kg/s.

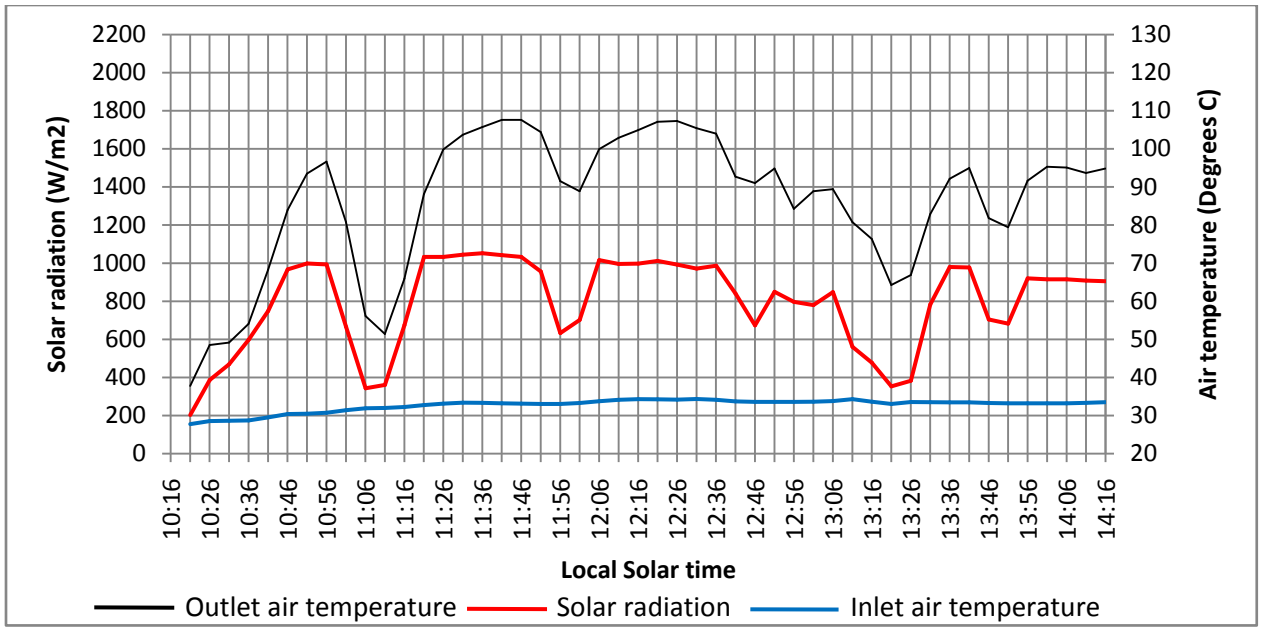

Figure 5.8: Variation of solar radiation with inlet and outlet air temperature and time taken on 11/03/13 with a mass flow rate of 0.0078kg/s.

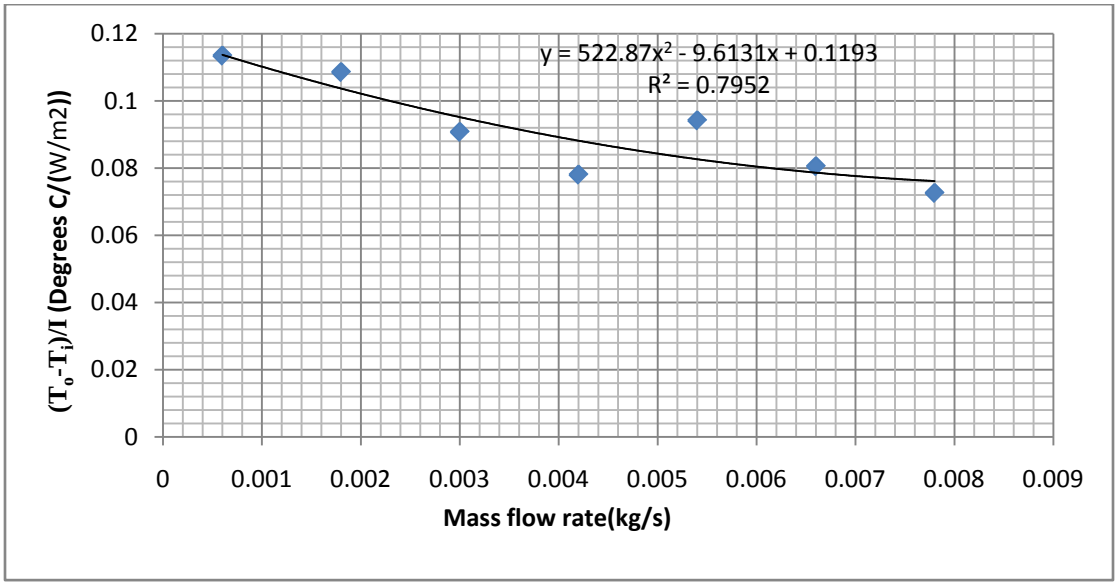

Figure 5.9: $((T_o-T_i)/I)$ versus air mass flow rate for uncovered collector

5.2.2 Effect of mass flow rate on useful energy

The corresponding useful energy variation with mass flow rate is presented. Shown in Figure 5.10 is the useful energy variation with air mass flow rate of 0.0006kg/s while Figure 5.11 shows the useful energy variation with air mass flow rate of 0.0078kg/s.

It is clear that useful energy increases with mass flow rate. The maximum useful energy obtained from the PTC with a mass flow rate of 0.0006kg/s was 71W while that got with the mass flow rate of 0.0078kg/s was 590W. This is because whereas low flow rates have high temperature rises as seen in Section 5.2.1, the heat transfer coefficients are lower. Higher flow rates results to higher heat transfer coefficients and thus more actual useful energy is obtained.

Figure 5.12 shows the quantity Q/I versus mass flow rate for the uncovered collector. Clearly the useful energy gain per unit solar radiation value and thus useful energy increases as the mass flow rate is increased. This means that the relative heat loss per unit solar radiation decreases with increase in mass flow rate.

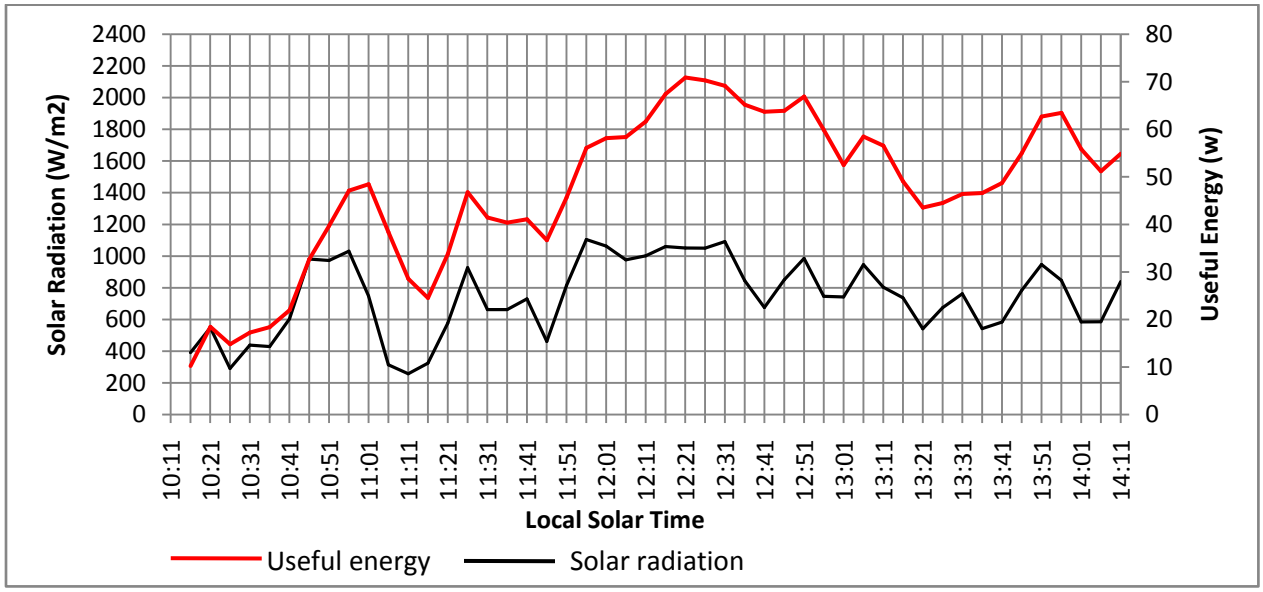

Figure 5.10: Variation of solar radiation with useful energy and time taken on 12/03/13 with a mass flow rate of 0.0006kg/s.

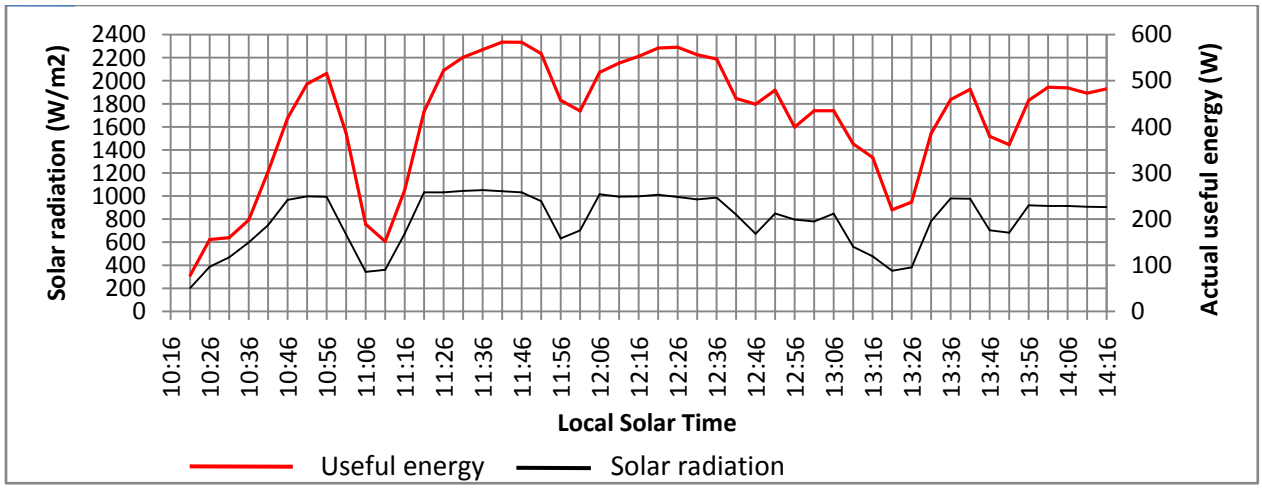

Figure 5.11: Variation of solar radiation with useful energy and time taken on 11/03/13 with a mass flow rate of 0.0078kg/s.

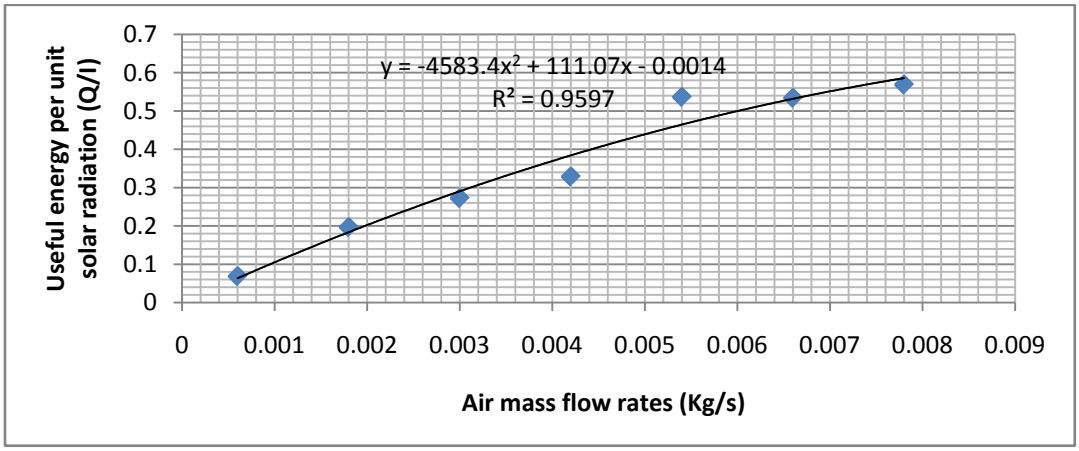

Figure 5.12: Variation of useful energy per unit solar radiation (Q/I) with mass flow rate

5.2.3 Effect of mass flow rate on overall efficiency and receiver efficiency

The overall efficiency as well as the receiver efficiency variation with mass flow rate of the uncovered PTC is shown in Figure 5.13.

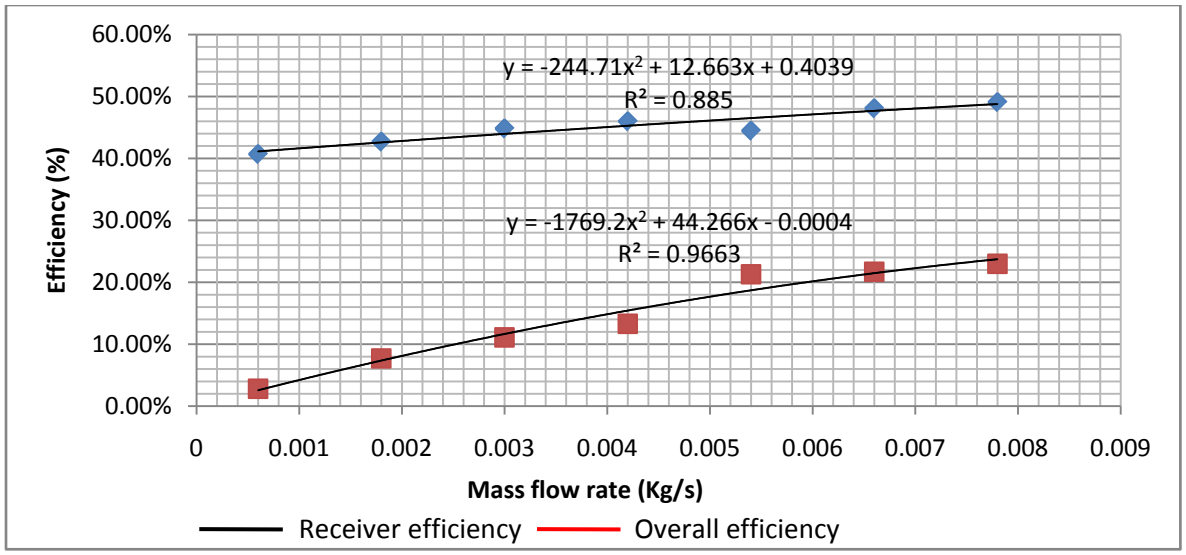

Figure 5.13: Overall and receiver efficiency variation with mass flow rate

The overall efficiency increases and approaches towards a maximum of 23%. The receiver efficiency increases and gets to a maximum of 49%.

5.2.4 Effect of mass flow rates on theoretical and experimental efficiency

The theoretical efficiency depends on the heat removal factor air heat transfer coefficient and the overall heat loss coefficient. Figure 5.14 shows the comparison between the experimental (Overall) efficiency and the theoretical efficiency.

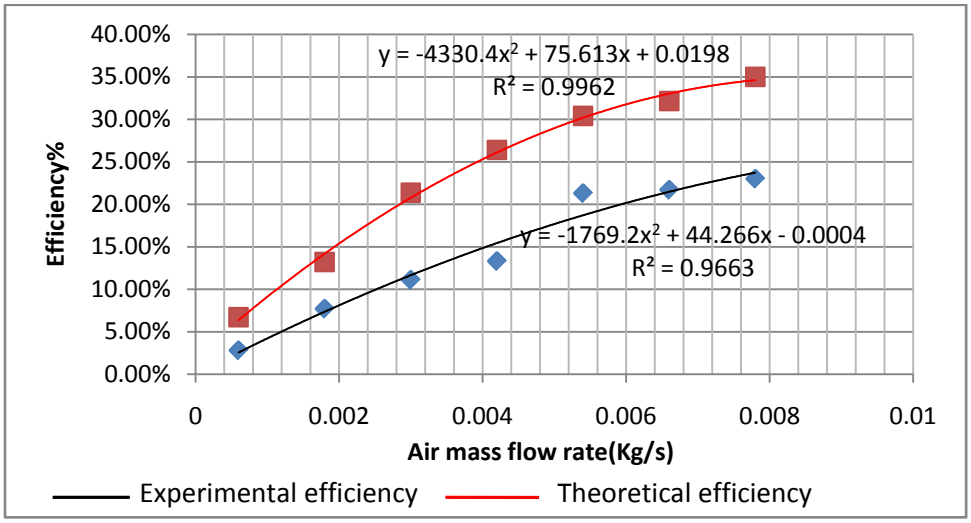

Figure 5.14: Variation of experimental and theoretical efficiency during selected days.

It is clear that the theoretical efficiency is higher than experimental efficiency by between 4-12%. Theoretical efficiency is higher since it takes into account the heat removal factor of the air at a particular flow rate. The figure shows there is agreement with this fact with Reference [**18**].

5.3 Effect of glass cover on PTC performance

The collector may need to be covered so as to avoid accumulation of dust on the reflective surface and also rain. Tests were carried out when the collector aperture area was covered with 3mm glass (ordinary glass). Three mass flow rates were tested 0.0006kg/s, 0.003kg/s, and 0.0078kg/s. Shown in Figure 5.15 is the PTC performance when not covered with a mass flow rate of 0.0078kg/s recorded on 11/3/13 while Figure 5.16 shows the performance when the PTC was covered with the same mass flow rate of 0.0078kg/s recorded on 19/3/13.

The outlet air temperature when the PTC was covered was found to be higher than when not covered. From Figure 5.15 the highest temperature attained was 108.5^0C at 1141hrs solar time when solar radiation value was 1040W/m^2 while from Figure 5.16, the highest temperature attained was 119.4^0C at 1254hrs solar time when the solar radiation value was 942W/m^2. This is expected since the glass cover would reduce heat losses by convection. It also prevents dust from settling on the reflecting surface which could affect the reflectivity.

Table 5.1 shows a summary of the performance for the three flow rates.

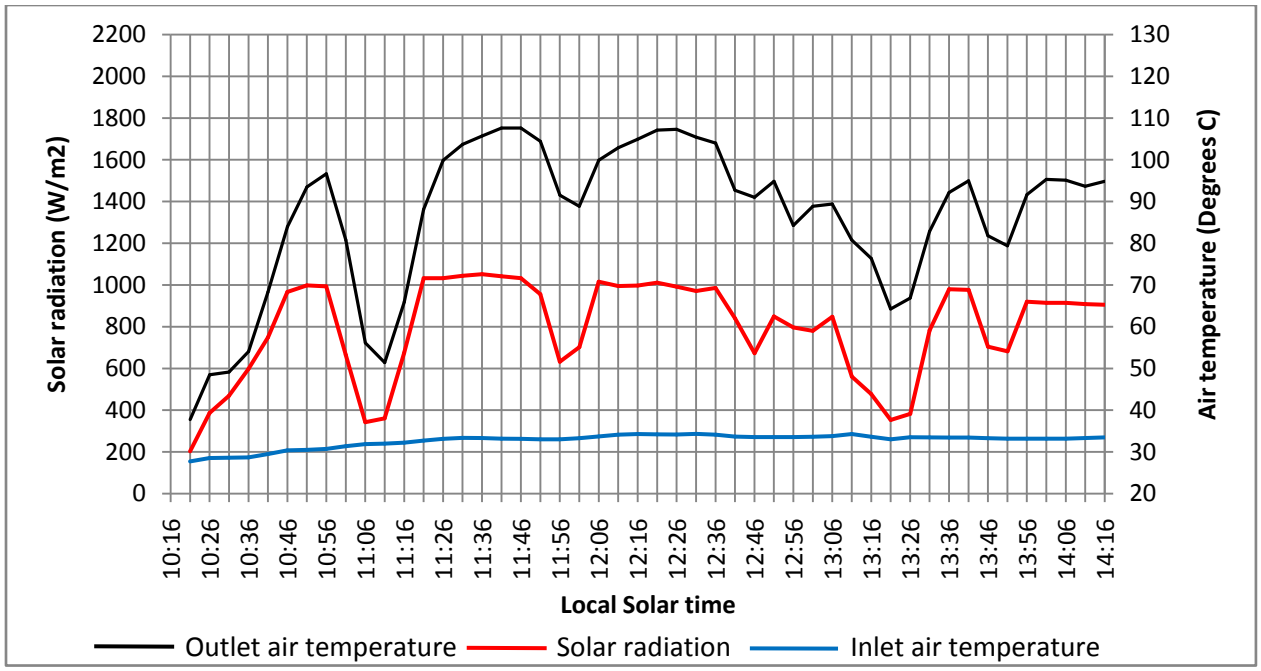

Figure 5.15: Variation of solar radiation with outlet air temperatures taken on 11/3/13 with a mass flow rate of 0.0078kg/s when the collector was uncovered.

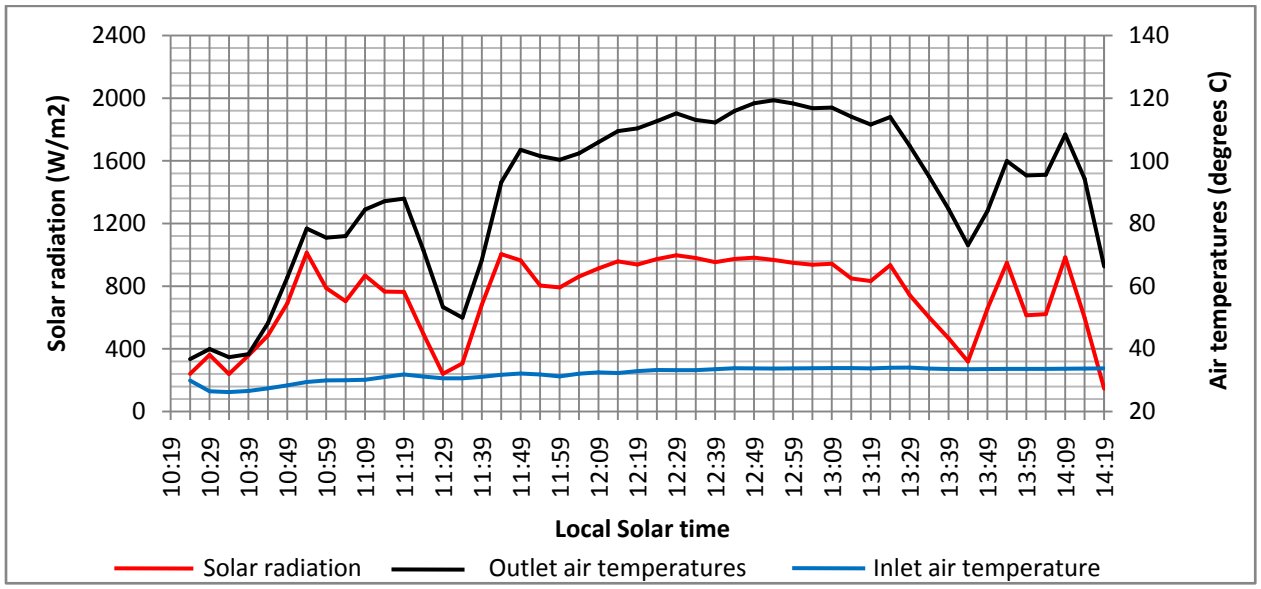

Figure 5.16: Variation of solar radiation with outlet air temperatures taken on 19/3/13 with a mass flow rate of 0.0078kg/s when the collector was covered.

Table 5.1: Comparison of temperature rise of a covered with an uncovered collector.

Mass flow rate (Kg/s)	Solar radiation for uncovered collector W/m2	(T_i-T_o) of uncovered collector (℃)	Solar radiation for covered collector W/m2	(T_i-T_o) of covered collector (℃)
0.0006	1040	118.8	1040	151.9
0.003	1050	95.3	960.6	116.9
0.0078	1037	75.3	977	87.5

5.4 Effect of collector length

The results obtained from tests of one collector can be used to estimate the effect of increasing the length of the PTC. Some studies have shown that increasing the collector length increases the outlet air temperatures and thus the useful energy. However the overall efficiency reduces as the length of the receiver pipe is increased.

During experimentation with one trough, pipe surface temperatures were recorded. These surface temperatures portrayed a linear relationship. An example is shown in Figure 5.17 where the temperature profile was taken on one inch diameter pipe with a mass flow rate of 0.0078kg/s. This was recorded on 11/03/2013 at 1225hrs standard time (1141hrs solar time) which was the highest efficiency point on that particular day.

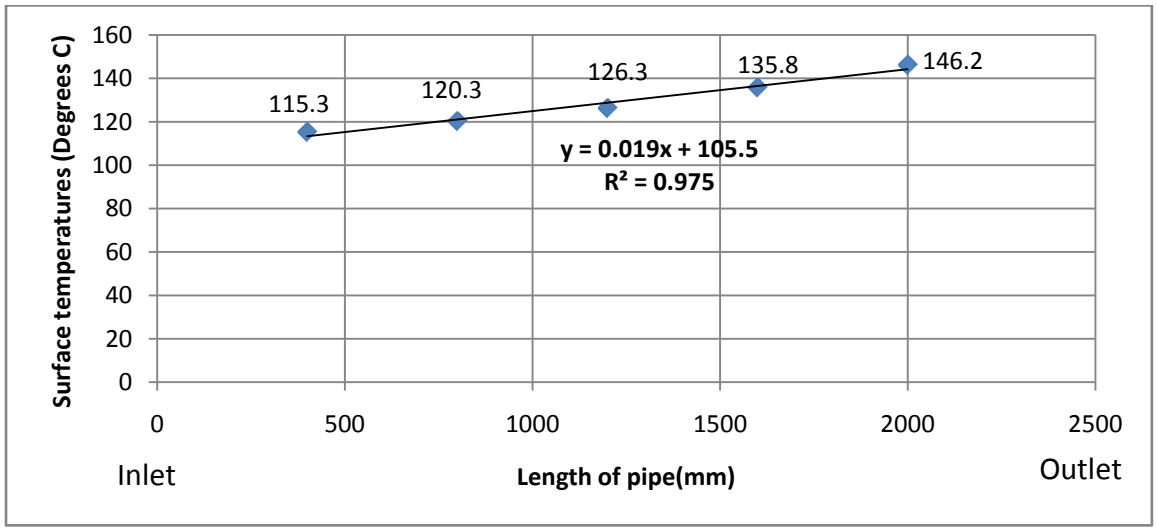

Figure 5.17: Surface temperature profile with pipe length with uncovered collector

From the equation displayed on the graph, the temperature of any point on the pipe can be determined. This is because there is uniform heat flux and the flow is fully developed as the length of the pipe is more than 10 times its diameter

5.4.1 Effect of collector length on temperature rise

The outlet temperature at the end of the second trough can be estimated. The outlet temperature of the first trough becomes the inlet temperature of the second trough. For instance, using the mass flow rate of 0.0078kg/s the surface temperature at the inlet of the receiver pipe of one trough is 108.5^0C and at the exit of the receiver pipe is 151.1^0C using the equation displayed on the graph. When the troughs are connected in series, the length of the trough doubles and becomes 4800mm. The surface temperature at the exit of the second trough can be estimated by the equation displayed on the graph as;

$$y = 0.019x4800 + 105.5 = 196.7^0C$$

Figure 5.18 shows the determination of the temperatures of the second trough with condition of uniform heat flux.

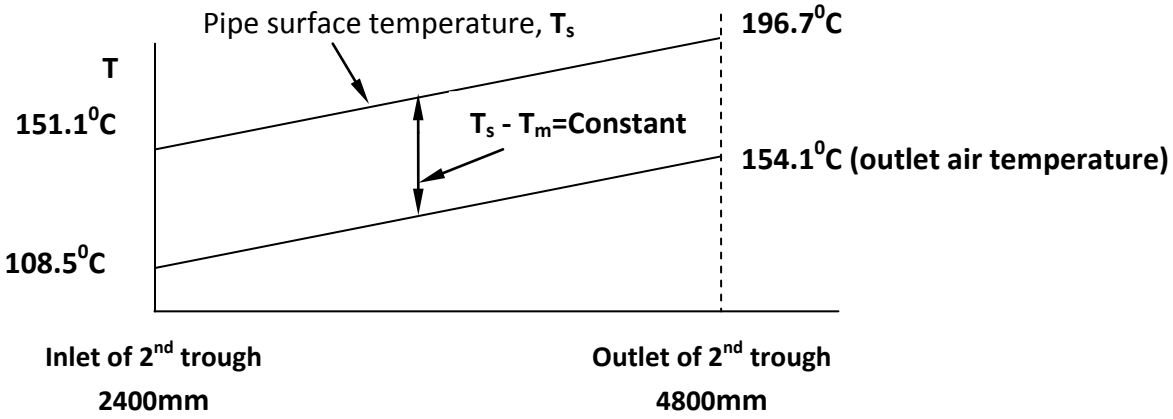

Figure 5.18: Theoretical surface and outlet air temperature profile distribution with pipe length for the second trough.

Using the same criteria, the outlet air temperature when the length of the PTC is doubled for different mass flow rates can be approximated. Table 5.2 shows the comparison between the outlet air temperature when one trough is used and when the length is doubled.

Table 5.2: Comparison between outlet air temperatures of one trough and two troughs connected in series.

Mass flow rate (Kg/s)	Inlet air temperature (T_i in ^0C)	Outlet air temperature with one trough (^0C)	Outlet air temperature with two troughs (^0C)
0.0006	33.4	152.2	190.6
0.0018	32.1	142.0	180.4
0.003	29	124.3	172.3
0.0042	33.5	109.2	140.4
0.0054	32	127.3	175.3
0.0066	32.9	110.2	163.0
0.0078	33.2	108.5	154.1

5.4.2 Effect of collector length on useful energy

As the collector length is increased, the outlet air temperature also increases because the aperture area is increased. Table 5.3 shows the comparison between the useful energy when one trough is used and when the length is doubled.

Table 5.3: Comparison between useful energy with one trough and when two troughs are connected in series

Mass flow rate (Kg/s)	Solar radiation W/m^2	Useful energy with one trough (W)	Useful energy with double the length (W)
0.0006	1040	71.3	95.4
0.0018	1029	119.2	270.0
0.003	1050	286.0	288.2
0.0042	970	318.7	453.1
0.0054	965	517.5	782.0
0.0066	960	512.5	867.4
0.0078	1038	590	952.3

It is clear that useful energy increases as the collector length is increased. This is because more solar energy is incident as the aperture area is increased.

5.4.3 Effect of collector length on overall and receiver efficiency

Though the outlet air temperatures are higher with increased length of PTC, the overall efficiency reduces. Shown in Figure 5.19 is the variation of overall efficiency with mass flow rates for one collector and when the collector length is doubled.

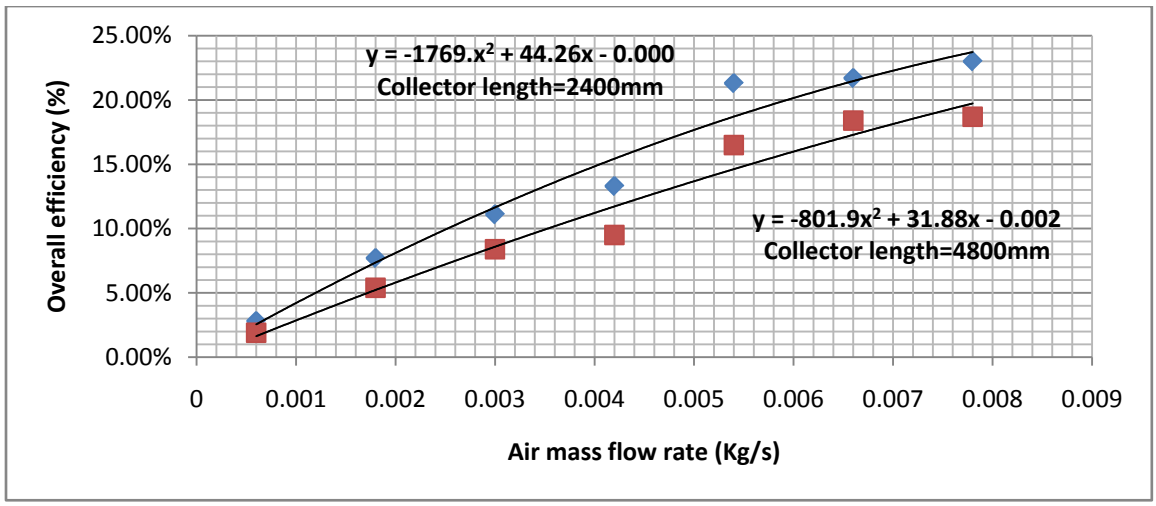

Figure 5.19: Overall efficiency variation with mass flow rates on collector length.

With the minimum flow rate of 0.0006kg/s the overall efficiency reduces from 2.8% to 1.9% while with the maximum flow rate of 0.0078kg/s, the overall efficiency reduces from 23% to 18%. This fact is in agreement with Reference [**15**]. The reason is because longer lengths result to greater heat losses to the surroundings since both the receiver temperature and the size of the collector are increased. Thus more than two troughs would result in very low efficiencies.

Now considering the receiver efficiency, Figure 5.20 shows the receiver efficiency with one trough length and with double the trough length. It is clear that the receiver efficiency decreases with the increase in the length of the collector provided the mass flow rate is kept constant. On the other hand the receiver efficiency increases with the increase of mass flow rate provided the collector length is kept constant.

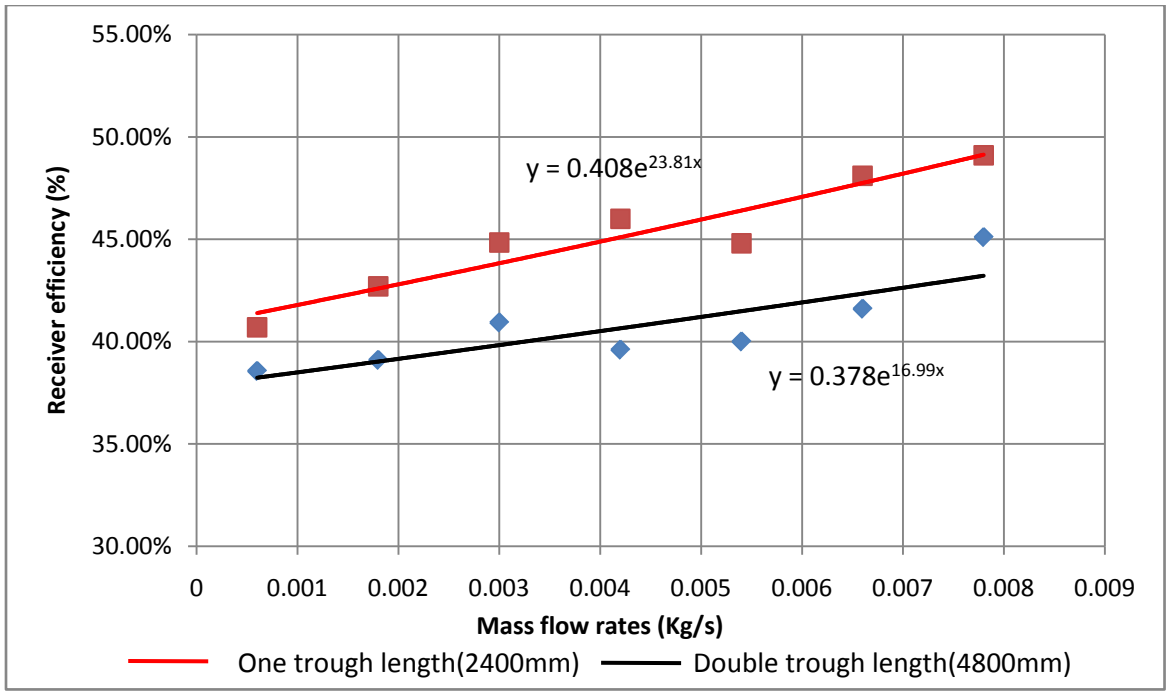

Figure 5.20: Receiver efficiency for one collector length and for double the collector length.

5.4.4 Effect of collector length on the heat loss

During experimentation, the effect of wind was noted. The wind was blowing mainly from North West to South East. The collector axis was aligned in the North- South direction. The wind speeds ranged between 0.1m/s to 1m/s as recorded in the wind meter. The best highest efficiency point of the PTC per mass flow rate was characterized by less wind speeds of 0.2m/s or less.

The overall heat loss coefficient was determined by using Equation 3.15 in Chapter 3. Shown in Figure 5.21 is the variation of overall heat losses with air mass flow rates at the highest efficiency points on the two collector lengths.

From the figure, it is clear that heat loss increases with increase in length of the collector. This is because as the length increases, the heat transfer area increases.

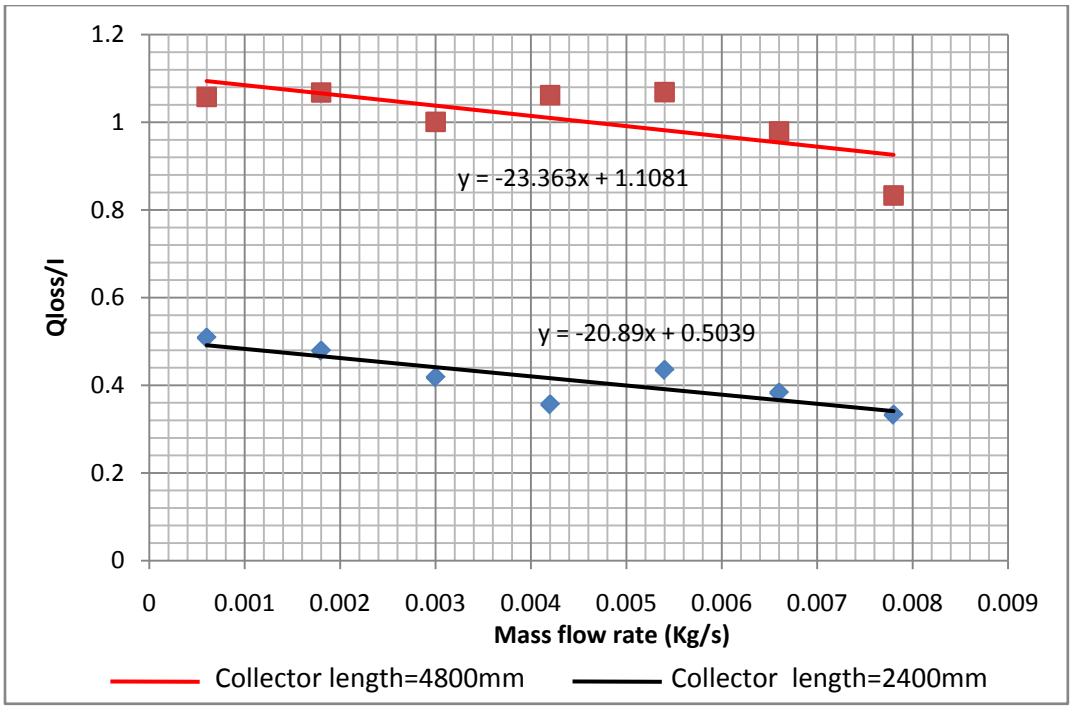

Figure 5.21: Variation of heat loss with mass flow rates on the collector length.

From the figure above, there was a higher heat loss per unit solar radiation with smaller mass flow rates than with higher mass flow rates. This can be attributed to the low heat transfer coefficients when using small flow rates.

5.5 Application in drying of bagasse

The parabolic trough concentrator is an ideal choice for the application in drying of bagasse. This is because it can generate hot air at temperatures of 100-130^{0}C and above. It is proposed that an active solar drier will be constructed where the PTC in the present study would be employed in the drying of bagasse. The drier will be fabricated using locally available materials. An illustration of the proposed setup is shown in Figure 5.22. It is assumed that theoretically the hot air generated by the collector would dry the bagasse in a drier.

From Section 4.1(a), the mass flow rate of air required to dry 1 kg of bagasse in four hours is $3.706\text{x}10^{-3}\text{kg/s}$ assuming the air inlet to the drier and outlet from the drier is 130^{0}C and 105^{0}C respectively. Thus theoretical can be done to ascertain the duty of the tested PTC. It was observed that the PTC would deliver more energy when covered with a glass cover as explained in Section 5.3.

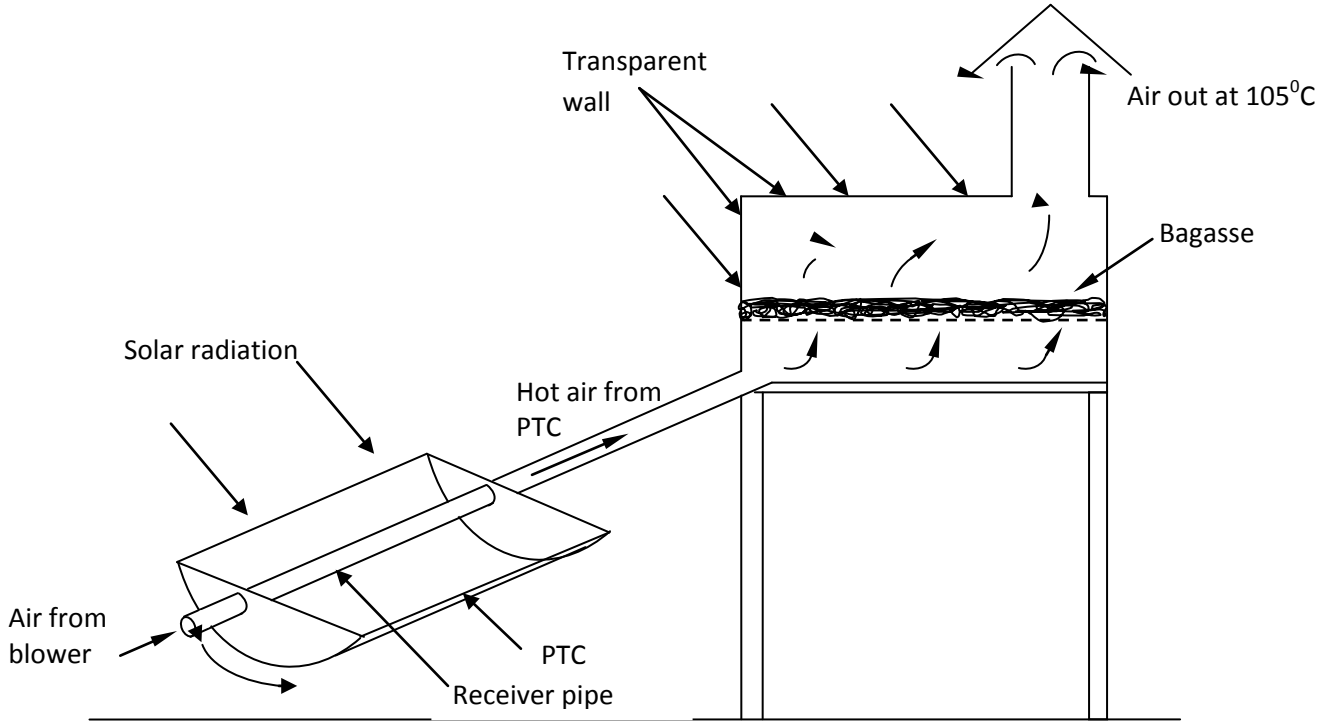

Figure 5.22: Proposed set-up of bagasse drying

5.5.1 Actual duty with one trough

The highest temperature attained with the maximum flow rate of 0.0078kg/s when the collector was covered was 119^{0}C and $\boldsymbol{I}$ was 977W/m^2. Assuming an air outlet temperature from the drier at 105^{0}C, then the energy delivered by the PTC in four (4) hours is;

$$\boldsymbol{Q_{actual} = 0.0078X1.0116875(119.4 - 105)X4X3600 = 1636.3kJ}$$

Where the value of $\boldsymbol{C_p}$ is calculated using the mean film temperature.

The energy required to completely remove the moisture content of 1 kg of bagasse is 1350.6kJ. Thus the amount of bagasse to be dried will be;

$$= \frac{\boldsymbol{1636.5\ kJ}}{\boldsymbol{1350.6\ kJ/kg}} = \boldsymbol{1.2kg}.$$

5.5.2 Actual duty with two troughs connected in series

The highest temperature attained with the maximum flow rate of 0.0078kg/s when the collector was covered was calculated as 167.4^{0}C and $\boldsymbol{I}$ was 977W/m^2. Assuming an air outlet temperature from the drier at 105^{0}C, then the energy delivered by the PTC in four (4) hours is;

$$\boldsymbol{Q_{actual} = 0.0078X1.01468925(167.4 - 105)X4X3600 = 7111.72kJ}$$

Where the value of $\boldsymbol{Cp}$ is calculated using the mean film temperature.

The energy required to completely remove the moisture content of 1 kg of bagasse is 1350.6kJ. Thus the amount of bagasse to be dried will be;

$$= \frac{\boldsymbol{7112.5\ kJ}}{\boldsymbol{1350.6\ kJ/kg}} = \boldsymbol{5.3kg}.$$

Thus two troughs connected in series would provide energy to dry more bagasse than when using one trough. When more than two troughs are used, the overall efficiency will reduce though temperature will occur until such a length is reached where the efficiency will be zero. Here the heat loss through radiation and convection will be equal to the useful energy into the fluid. Beyond this length, the temperature will drop until no temperature change of air takes place at the outlet of the receiver pipe.

CHAPTER 6

CONCLUSION AND RECCOMMENDATIONS

A parabolic trough concentrator (PTC) was fabricated in the Mechanical Engineering workshop, University of Nairobi. Testing of the PTC was done between 1100hrs to 1500hrs standard time on selected days between 28th February, 2013 to 22nd March, 2013.

It was found that during a clear sky day, the solar insolation was steady with little intermittence. During a cloudy day, the solar insolation had high intermittence which was associated with the cloud cover. Because of the low heat capacity of air and high conductivity of the receiver, the change in outlet air temperature followed closely or nearly immediately with the change in solar insolation. While outlet air temperature decreases with increase in mass flow rate; the useful energy, overall efficiency and receiver efficiency increases with increase in mass flow rate.

It was found that covering the collector led to increase in temperature rise, useful energy, overall efficiency and receiver efficiency. For instance, the efficiency got when the collector was not covered when the highest mass flow rate of 0.0078kg/s was tested was 23% while when covered was 27.94%. Thus it is recommended that the proposed future work of the biomass drier be done with the PTC covered with glass.

Finally, doubling the collector length was found to increase the temperature rise and useful energy. For example, with a mass flow rate of 0.0006kg/s the temperature rise was 118^{0}C with one collector length and it increased to 157^{0}C when the length was doubled. However, the overall efficiency and receiver efficiency were reduced. For instance when the mass flow rate was 0.0078kg/s, the overall efficiency for a collector length of 2400mm was experimentally determined as 23% while the efficiency of collector length of 4800mm was theoretically determined to be 18%.

Thus the collector was able to generate air at 100^0C and above which could be utilized to provide hot air for industries such as tea factories and also for drying of biomass.

The following recommendations are made which if applied would greatly improve the PTC for future studies;

- An automatic tracking system should be incorporated in the PTC so as to minimize tracking errors and thus improve the efficiency.
- The trough should be reinforced further so as to minimize twisting when turning during experimentation.
- Data loggers should be incorporated in the data collection to improve their accuracy.

References

1. Zarza E. (2011) "**Medium Temperatures Solar Concentrators**", Solar Energy Conversion and Photo energy systems-Vol 1
2. KPLC Annual Accounts Report of financial year 2011/2012.
3. Manikandan S.K., Kumaresan G., Velraj R., Iniyan S. (2012), "**Parametric Study of Solar Parabolic Trough Collector System**" Asian Journal of Applied Studies 5 (6): 384-393, 2012.
4. Ministry of Energy (2011-2031), "**Updated Least Cost Power Development Plan**" Government Printer.
5. Kalogirou S.A., (2004) **"Solar thermal collectors and applications"** Progress in Energy and Combustion Science 30(2004) 231-295
6. Akpinar K.E., Bicer Y., Cetinkaya F. (2006) **"Modeling of Thin Layer Drying of Parsley Leaves in a Convective Dryer and Under Open Sun"** Mechanical Engineering Department, Firat University, 23279 Elazig, Turkey.
7. Sankat C.K. and Mujaffar S (2004)" **Sun and Solar Cabinet Drying of Salted Shark Fillets**" Proceedings of the 14th International Drying Symposium (IDS 2004) São Paulo, Brazil, 22-25 August 2004, vol. C, pp. 1584-1591.
8. Laszlo Imre (2006) **"Handbook of Industrial Drying, Chapter 13: Solar drying"** Taylor & Francis Group, LLC.
9. Hii, C.L.; Law, C.L. (2012) **"Solar Drying of Major Commodity Products. In Solar drying: Fundamentals, Applications and Innovations, Ed. Hii, C.L., Ong, S.P., Jangam, S.V. and Mujumdar"**, A.S., ISBN - 978-981-07-3336-0, published in Singapore, pp. 73-94.
10. Weiss W, Buchinger J. (2004), **"Solar Drying"** Institute for Sustainable Technologies, Austria.
11. Visavale, G.L. (2012), **"Principles, Classification and Selection of Solar Dryers. In Solar Drying: Fundamentals, Applications and Innovations, Ed. Hii, C.L., Ong, S.P., Jangam, S.V. and Mujumdar, A.S., 2012"** ISBN - 978-981-07-3336-0, Published in Singapore, pp. 1-50.

12. Bhuiyan M. H. R., Alam M. M. and Islam M. N. (2011) "**The Construction and Testing of a Combined Solar and Mechanical Cabinet Dryer**" Journal of Environmental Science and Natural Resources, 4(2): 35-40, 2011.
13. Zeinab S. Abdel-Rehim, Zenat A. Nagib (2007), **"Solar drying of Bagasse Pulp"**Journal of Applied Sciences Research, 3(4): 300-306, 2007 © 2007, INSInet Publication.
14. Duffie J.A., Beckman W.A.(1980) **"Solar Energy of Thermal Processes"** John Wiley & Sons, New York.
15. Tchinda R. (2007), "**Thermal Behavior of Solar Air Heater with Compound Parabolic Concentrator**" Energy Conservation and Management 49 (2008) 526-540.
16. Fletcher E. A. (2001). "**Solar thermal processing: A review**". Journal of Solar Energy Engineering **123** (2): 63.
17. Mokhtari A., Yaghoubi M., Kanan P., Vadiee A.. Hessami R. (2007**) "Thermal and Optical Study of Parabolic Trough Collectors of Shiraz Solar Power Plant"** Proceedings of the Third International Conference on Thermal Engineering: Theory and Applications May 21-23, 2007, Amman, Jordan
18. Tadahmun A.Y. (2012),**"Experimental and Theoretical Study of a Parabolic Trough Solar Collector"** Anbar Journal for Engineering Sciences.
19. Sosa-Arnao J.H., Oliveira F.M, Corrêa J.L. G., Silva M.A. and Nebra S.A. **"Sugar Cane Bagasse Drying – A Review"** Proceedings of the 14th International Drying Symposium (IDS 2004) São Paulo, Brazil, 22-25 August 2004, vol. B, pp. 990-997
20. Shah S, Joshi M. (2010) **"Modeling Microwave Drying Kinetics of Sugarcane Bagasse"** International Journal of Electronics Engineering, 2(1), 2010, pp. 159-163.
21. Jefferson L.G.C, Daniel R.G., Maria A.S., Silvia A.N., (2004) **"Cyclone as a Sugarcane Drier"**, Chinese J. Chemical Engineering Vol. 12(6) pp 826-830.
22. Roos C.J. (2008) **"Biomass Drying and Dewatering for Clean Heat and Power"** WSU Extension Energy Program.
23. Negoi R.M, Ragazzi M, Apostol T, Rada E.C, Marculescu C. (2009) **"Bio-drying of Romanian municipal solid waste: An analysis of its viability"** U.P.B. Sci. Bull, Series C, Vol. 71, Iss. 4, 2009

24. Pidhuwan M., Teekasap S., Khedari J. (2004) **"The Effective Length of Solar Parabolic Concentrating Collector"** the Joint International Conference on "Sustainable Energy and Environment" Hua Hin, Thailand.
25. Yunus C., Robert T., John C. (2008) **"Fundamentals of Thermal Fluid Sciences"** Boston: McGraw-Hill 3rd Edition.
26. Pitts D.R., Sissom L.E. (1998) "**Schaum's Outline of Theory and Problems of Heat Transfer**" McGraw-Hill, 2nd Edition.
27. Incropera F.P., Dewitt D.P., Bergman T.L., Lavine A.S. (2007) "**Fundamentals of Heat and Mass Transfer**" 6th Edition, John Willey & Sons Inc.
28. Cortez L.A.B., Gomez E.O. (1998), **"A Method of Exergy Analysis of Sugarcane Bagasse Boilers"** Brazilian Journal of Chemical Engineering, Vol. 15 No. 1.
29. Arasteh D. (1995) "**Advances in Window Technology-1973-1993: In Advances in Solar Energy, an Annual Review of Research and Development Vol. 9**" American Solar Energy Society Inc., Boulder Co. 1994.

Appendix 1: Bill of materials

Item No.	Particulars	Quantity	Rate KShs.	Amount KShs.
1.	Galvanized iron sheet	1	4000	4000
2.	1 inch diameter Class B galvanized iron water pipe	1	2600	2600
3.	1 inch diameter PVC pipe Class D	1	400	400
4.	1 inch Galvanized sockets	4	65	260
5.	1 inch PVC metal adopter	1	100	200
6.	Hard Board 8feet long X 4 feet wide X 20mm thick	1	4674	4674
7.	Right angled section 1”X1”X1/8”	4	1350	5400
8.	3mm thick clear glass pieces: two pieces of 72”X48” and two pieces of 23 ½”X48”			2850
9.	Thermocouple wire type J	10m	400	4000
10.	Gun gum	1	250	250
11.	Kitchen aluminum foil 45cmX3000cm	1	510	510
12.	Pop rivets	30	3	90
13.	Selector switch	1	1000	1000
14.	1 inch gate valve	1	1000	1000
15.	2” inch air horse pipe	6m		4190
16.	Power extension cable	1	1100	1100
17.	Rubber sealing cord	8m	390	3120
18.	2 inch diameter class C pipe and 2 inch long	1	500	500
19.	3 inch diameter Class C pipe- 0.5m long	1	1000	1000
20.	RHS 2”X2”X1/8”	2.5	3577	8943
21.	70mm nominal diameter Ball bearing	3	1450	4350
22.	Castor wheels 2.5 inches	6	195	1170
23.	1 inch diameter by 1100mm long mild steel shaft	1	2000	2000
24.	7mm ball bearing	2	250	750
25.	¾” pillow block bearing	2	1450	2900
26.	4mm thick plate 4 feet long and 4 feet wide	1	6000	6000
27.	M10X25 Hex bolts and nuts	52	20	1040
28.	M6X20 Hex bolts and nuts	12	15	180
29.	M11X25 Hex bolts and nuts	4	45	180
30.	M22 Nut (rough thread)	1	120	120
31.	Self tapping screws	60	4	120
32.	Welding rods G10	1 Pkt	1100	1100
33.	Labour			20000
34.	Contac adhesive	4 liters	585	2340
	TOTAL			**89437**

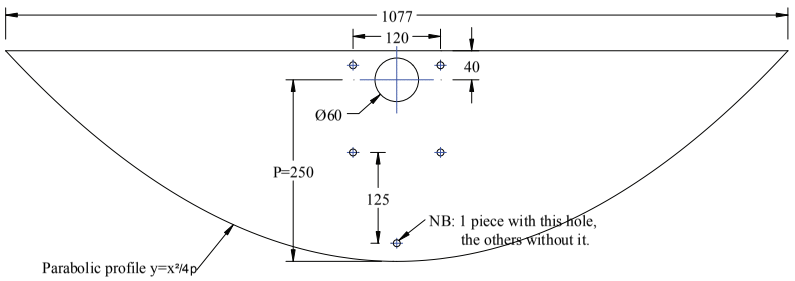

Part 1:End piece
Material: Hardboard
Quantity: 4 Required

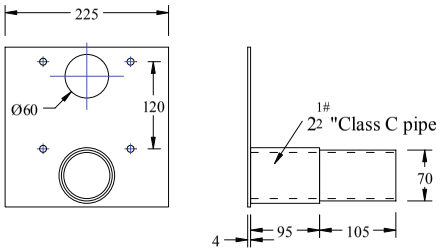

Part 2: End plate
Quantity: 1 Required
Material: M.S.

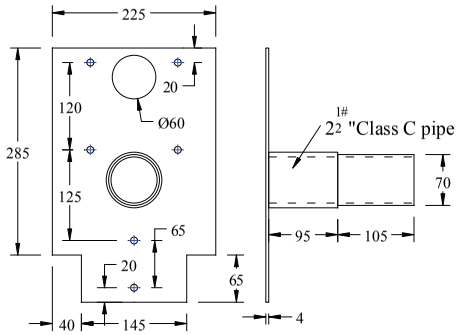

Part 3:End plate on the tracking side
Quantity: 1 Required
Material: M.S.

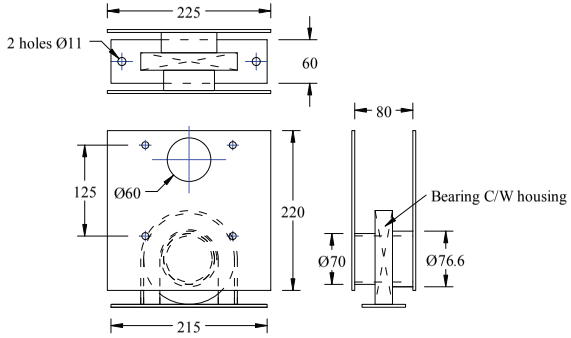

Part 5: Mid trough support bracket C/W bearing
Quantity: 1 Required
Material: M.S.

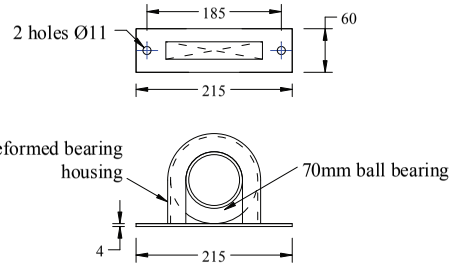

Part 6: Bearing C/W Housing
Quantity: 2 Nos Required

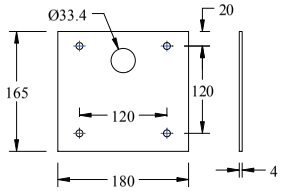

Part 4: End plate for 1" pipe
Quantity: 4 Required
Material: M.S.

NB: Unless stated Otherwise, all holes have a diameter of 9.5mm

Project: PTC air heater	
Title: End piece and support bracket details	
Drawn by: W.Kariuki.	
Checkd by: Dr. A.A. Aganda	
Approved by: Dr. A.A Aganda	
Drawing No: 001/PTC/2013	Date: 10/06/2013 Scale: 1:10

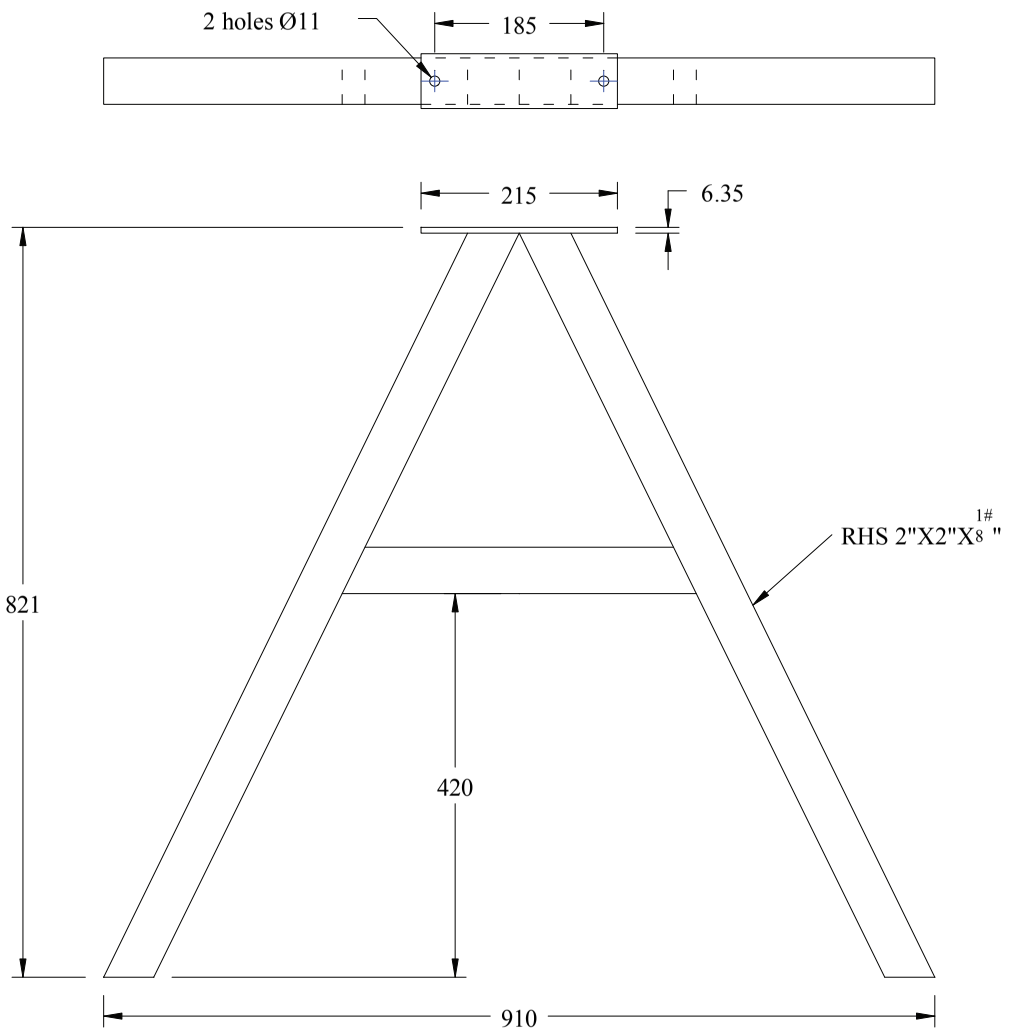

Project: PTC air heater	
Title: Mid stand	
Drawn by: W.Kariuki.	
Checkd by: Dr. A.A. Aganda	
Approved by: Dr. A.A. Aganda	
Drwg No: 002/PTC/2013	Date: 10/06/2013 Scale: 1:8

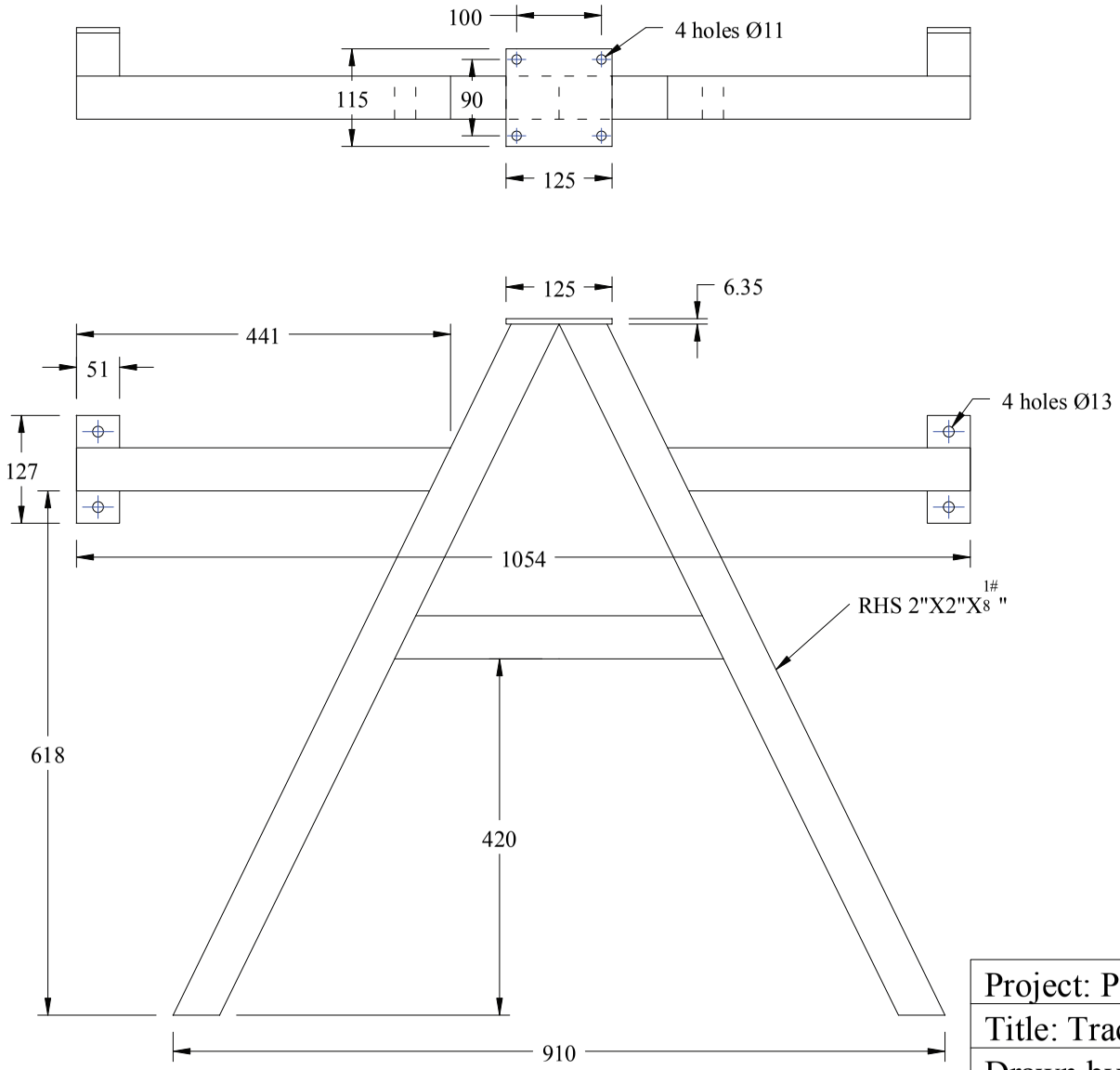

NB: All dimensions are in millimeters

Project: PTC air heater	
Title: Tracker side stand	
Drawn by: W.Kariuki.	
Checkd by: A.A. Aganda	
Approved by: A.A. Aganda	
Drwg No: 003/PTC/2013	Date: 10/6/13 Scale: 1:8

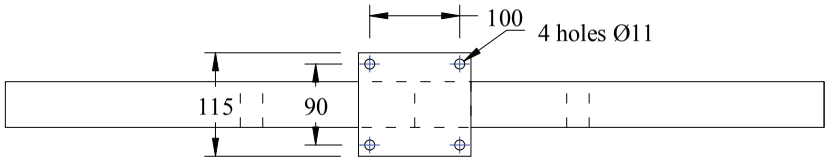

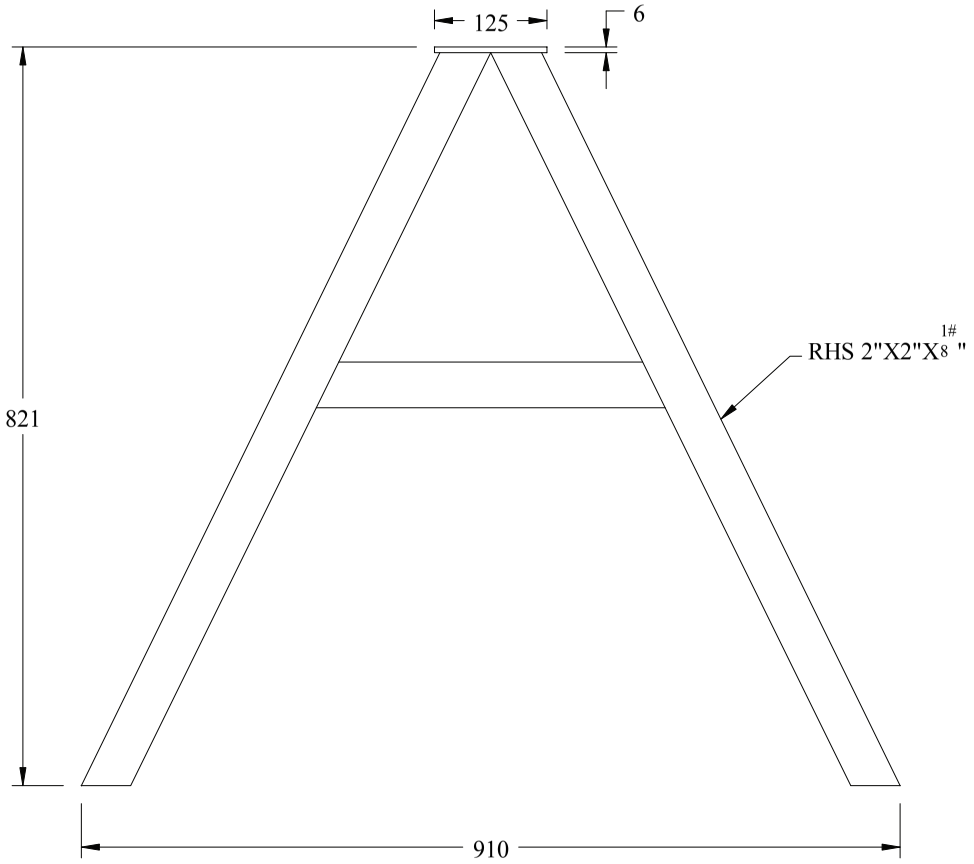

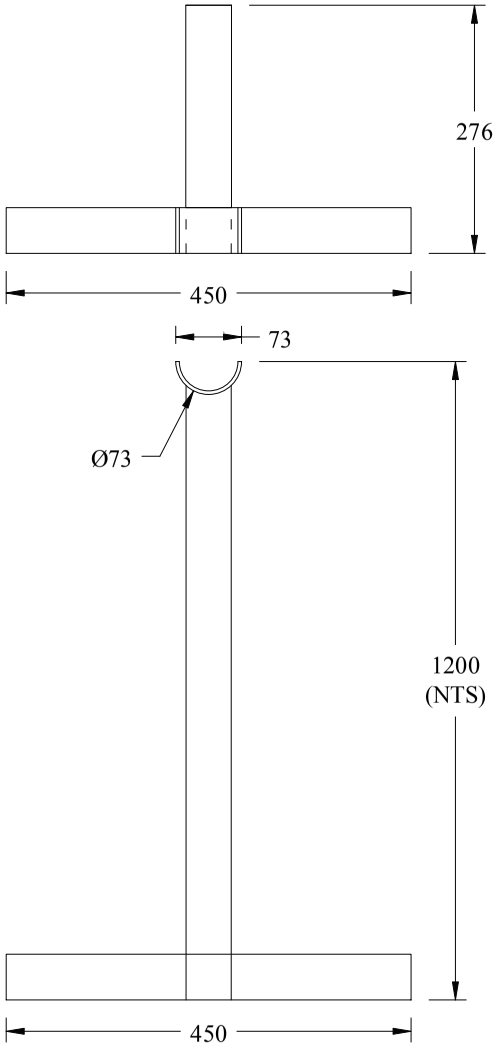

Project: PTC air heater	
Title: End side stand	
Drawn by: W.K.	
Checkd by: A.A. Aganda	
Approved by: A.A. Aganda	
Drwg No: 004/PTC/2013	Date: 10/6/13 Scale: 1:8

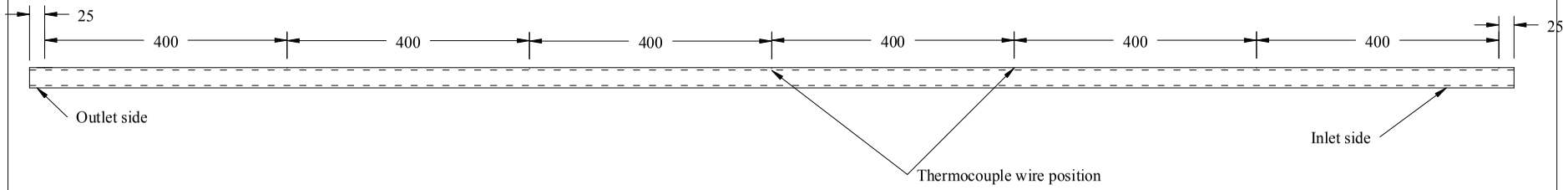

1 inch GI pipe

Quantity - 1 Required

	Project: Parabolic trough concentrator air heater
	Title: Receiver Pipe showing thermocouple wire positions
	Drawn by: W.Kariuki.
	Checked by: A.A. Aganda
	Approved by: A.A. Aganda
Drwg No: 005/PTC/2013	Date: 10/6/13 Scale: 1:10

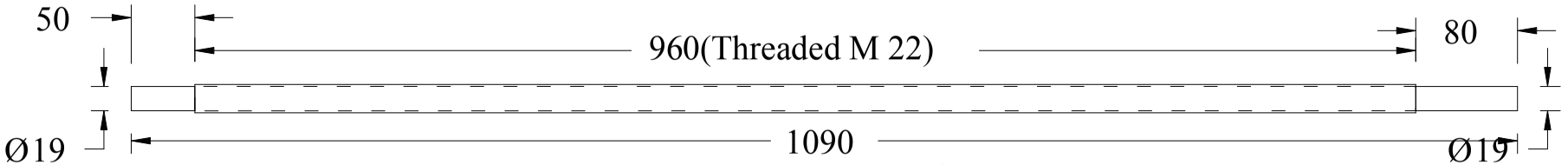

1. Tracking shaft

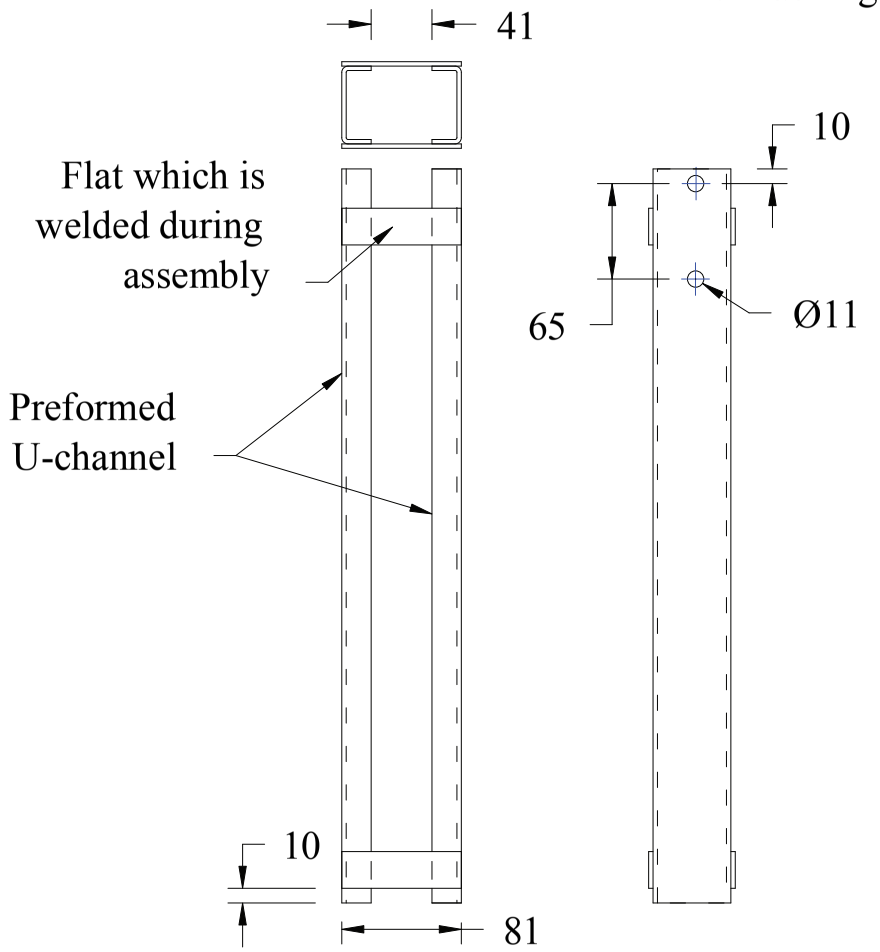

3. Nut and roller assembly bracket

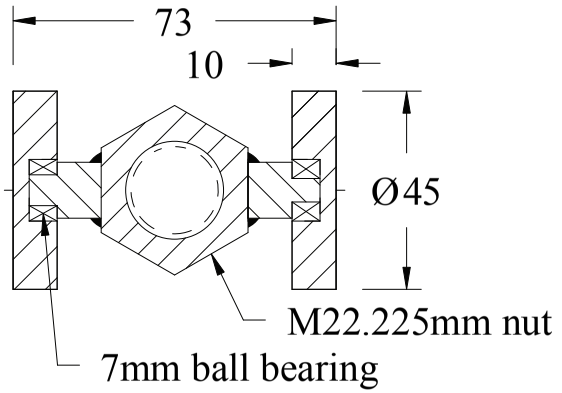

3. Nut and roller assembly
Scale: 3:1

80

NB: All dimensions in are millimeters

Project: PTC air heater	
Title: Tracking sysytem components	
Drawn by: Wilson K.	
Checked by: A.A. Aganda	
Approved by: A.A. Aganda	
Drwg No: 006/PTC/2013	Date: 10/6/13 Scale: 1:10

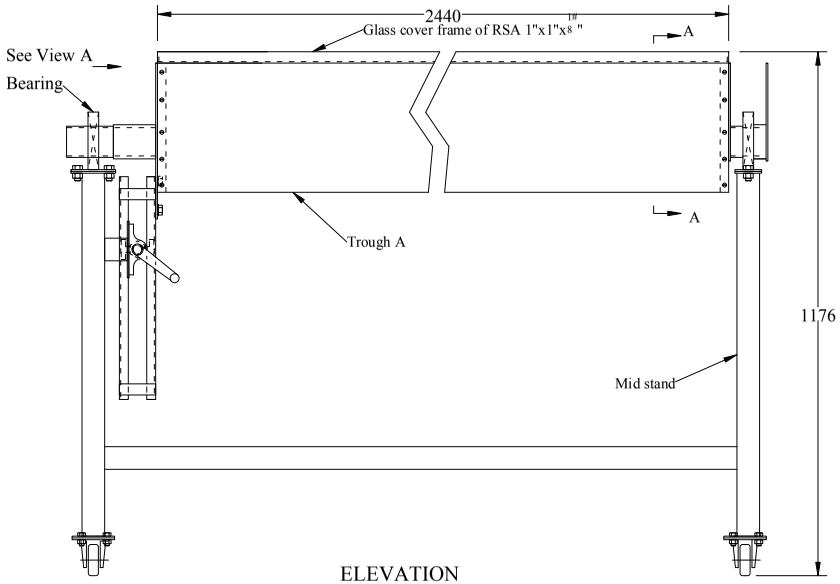

ELEVATION

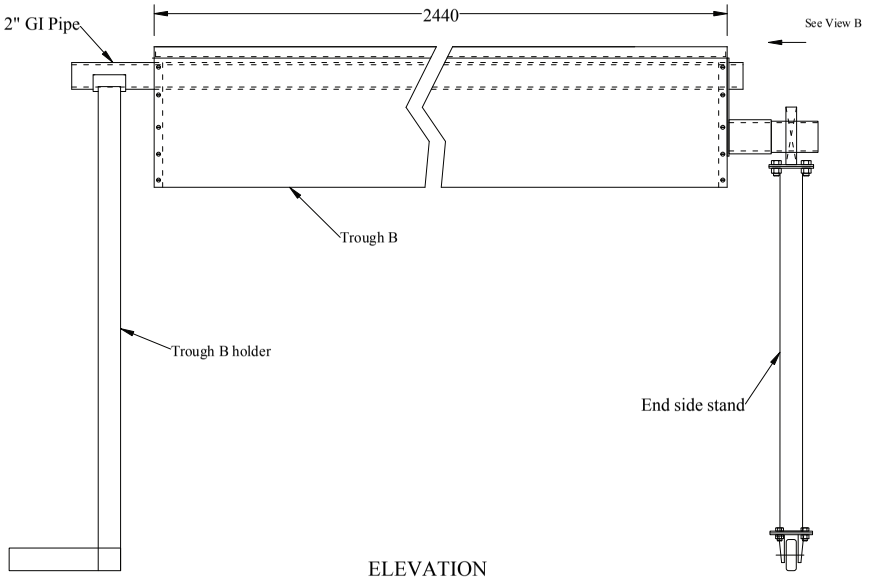

ELEVATION

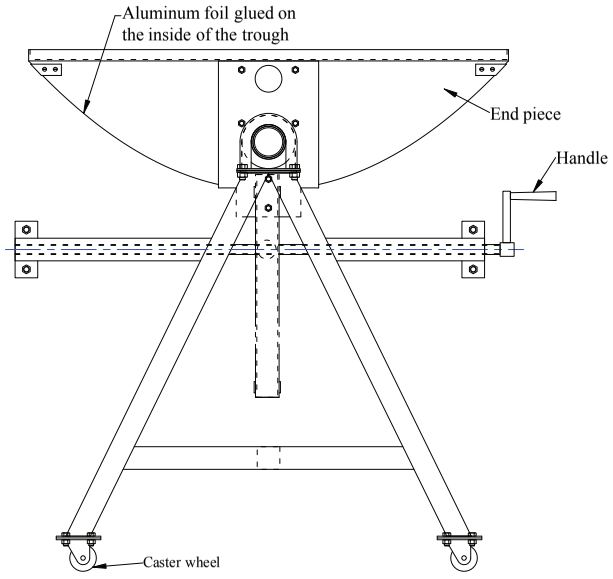

VIEW A

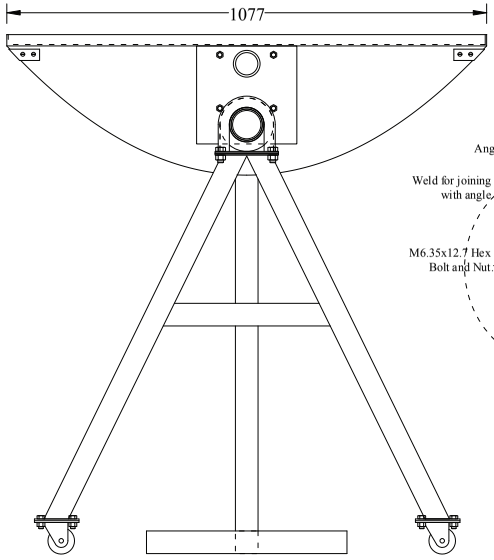

VIEW B

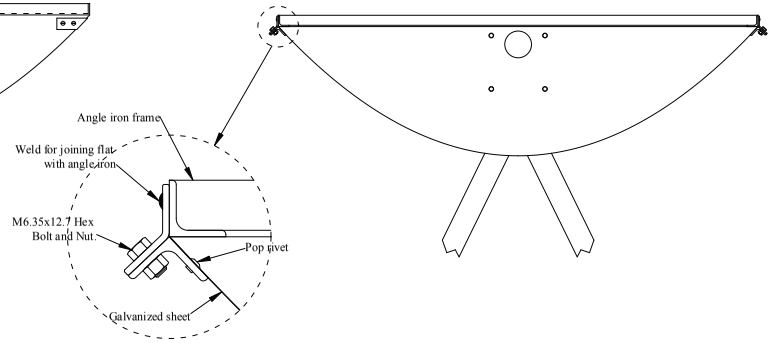

NB: All dimensions are in millimetres

Project: PTC Air heater	
Title: Assembled trough	
Drawn by: W.Kariuki	
Checkd by: A.A. Aganda	
Approved by: A.A. Aganda	
Drwg No: 007/PTC/2013	Date: 10/06/2013 Scale: 1:16

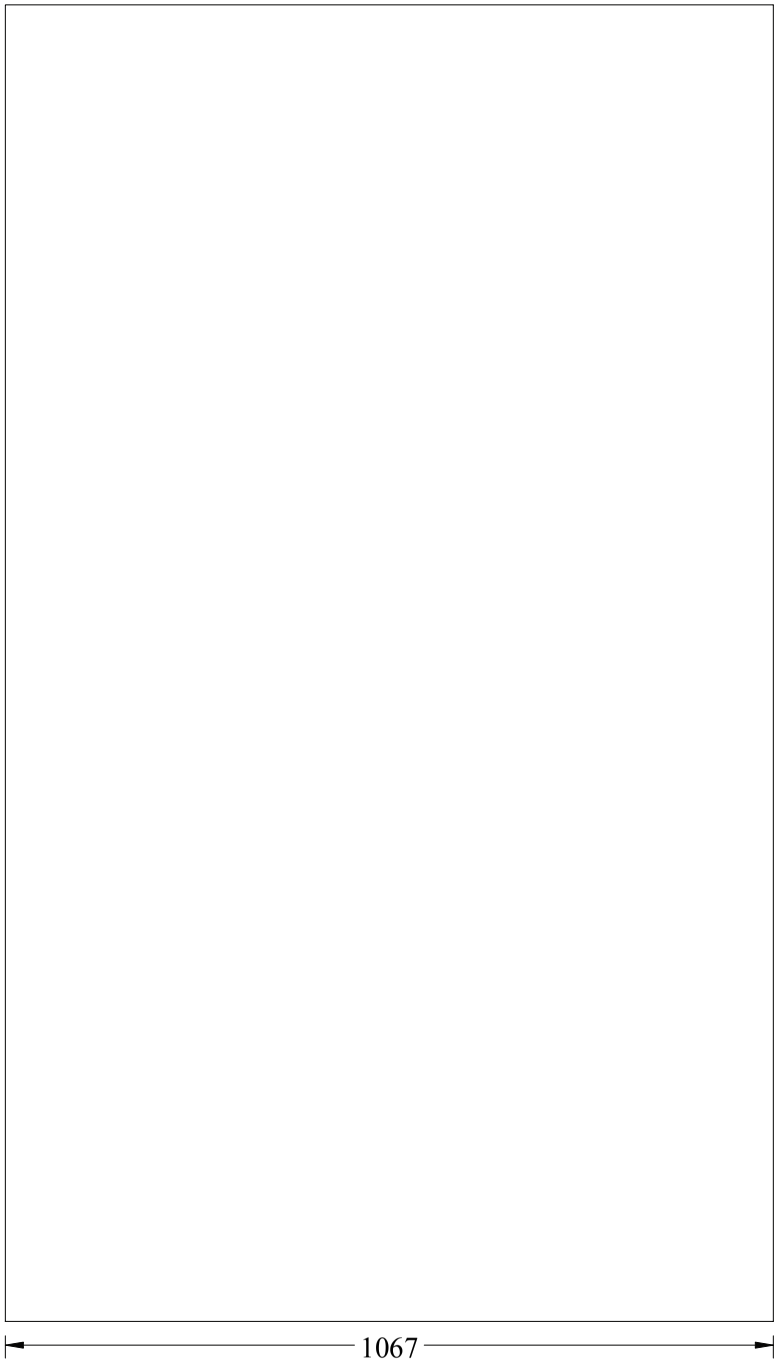

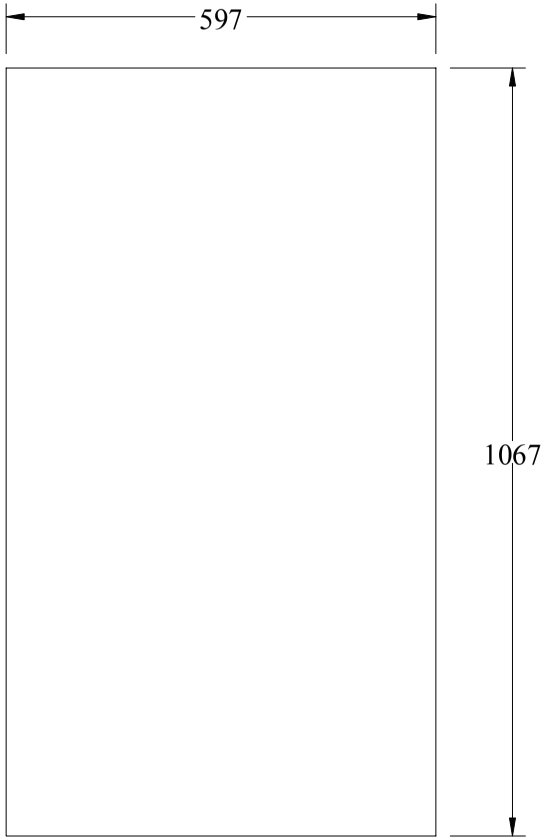

3mm thick clear glass pane
Quantity: 2 Nos Required

3mm thick clear glass pane
Quantity: 2 Nos Required

NB: All dimensions are in millimetres

Project: PTC Air heater	
Title: Glass panes for covering the collector	
Drawn by: W.Kariuki.	
Checkd by: A.A. Aganda	
Approved by: A.A. Aganda	
Drwg No: 008/PTC/2013	Date: 10/06/2013 Scale: 1:10

82

Appendix 3: Moody diagram